UNIVERSITY OF OKLAHOMA

GRADUATE COLLEGE

FORMATION AND DISSOLUTION OF SURFACTANT PRECIPITATES

A DISSERTATION

SUBMITTED TO THE GRADUATE FACULTY

in partial fulfillment of the requirements for the

Degree of

DOCTOR OF PHILOSOPHY

By

SUKHWAN SOONTRAVANICH
Norman, Oklahoma
2007

UMI Number: 3283863

UMI Microform 3283863

Copyright 2008 by ProQuest Information and Learning Company.
All rights reserved. This microform edition is protected against unauthorized copying under Title 17, United States Code.

ProQuest Information and Learning Company
300 North Zeeb Road
P.O. Box 1346
Ann Arbor, MI 48106-1346

FORMATION AND DISSOLUTION OF SURFACTANT PRECIPITATES

A DISSERTATION APPROVED FOR THE
SCHOOL OF CHEMICAL, BIOLOGICAL, AND MATERIALS ENGINEERING

BY

_____
Prof. John F. Scamehorn

_____
Prof. Jeffrey H. Harwell

_____
Prof. Edgar A. O'Rear

_____
Prof. David A. Sabatini

_____
Prof. Tohren C. G. Kibbey

© Copyright by SUKHWAN SOONTRAVANICH 2007
All Rights Reserved.

ACKNOWLEDGEMENTS

Firstly, I would like to express my deep gratitude to Dr. John F. Scamehorn for his guidance, enthusiastic support, and encouragement throughout my education. I gratefully acknowledge Dr. David A. Sabatini, Dr. Jeffrey H. Harwell, Dr. Edgar A. O' Rear, and Dr. Tohren C. G. Kibbey for valuable discussions and being on my committee. I would also like to give special thanks to all the people in the Surfactant Research Group, especially: Napaporn Komesvarakul, Prapas Lohatheeraparp Anuradee Wittayapanyanon, Edgar Acosta, Anand Upadhyaya, Lihn Do, Thu Nguyen, and Shahryar Gilani for all of those lab discussions and for being my great friends. Thanks go to all the undergraduate students who helped make this happen: Heyde Lopez, Sarah Walsh, Joline Munoz, Sarah Shobe, Grant Landrum, Damilare Oyesanya, Chase Waite, and Valerie Rivera. I would also like to thank the remaining faculty and staff, including, Sherry Childress, Terri Colliver, Donna King, and Alan Miles for their help.

Financial support for this work was provided by the industrial sponsors of the Institute for Applied Surfactant Research including Akzo Nobel, Clorox, Conoco/Phillips, Church and Dwight, Dow, Ecolab, Halliburton, Huntsman, Oxiteno, Proctor & Gamble, Sasol, Shell, and Unilever.

Finally, I would like to thank my family (mom, dad, sister, grandpa, and the rest of the family) and Wish Siripong for their constant supports. Without them this accomplishment would not have been possible.

TABLE OF CONTENTS

TABLE OF CONTENTS (Continued)

TABLE OF CONTENTS (Continued)

LIST OF TABLES

LIST OF TABLES (Continued)

Page

TABLE

LIST OF FIGURES

LIST OF FIGURES (Continued)

Page

FIGURE

LIST OF FIGURES (Continued)

LIST OF FIGURES (Continued)

Page

FIGURE

LIST OF FIGURES (Continued)

Page

FIGURE

ABSTRACT

Precipitation of surfactants is one of the most important considerations in surfactant applications. Understanding the formation and dissolution of surfactant precipitates provides more effective utilization of surfactants. In this study, firstly, the kinetics of precipitation of mixed anionic surfactants with calcium ion was studied and the relationship between the supersaturation ratios of precipitating surfactants and the rate of surfactant precipitation was established. The precipitation in mixed anionic surfactants is delayed substantially when the supersaturation ratios of precipitating surfactants are approximately the same, indicating the growth of each precipitating surfactant is interrupted by use of growing crystals as nucleation sites for the dissimilar surfactant to form crystals. Secondly, precipitation phase boundaries of an anionic surfactant and a pH sensitive amphoteric surfactant were measured and modeled at different pH levels. A hydrogen ion titration to obtain the pK_a of the amphoteric surfactant, regular solution theory to describe mixed micelle formation, and the solubility product of the precipitate were combined to predict the precipitation phase boundary. Lastly, the thermodynamics and kinetics of the dissolution of precipitate of calcium salt of a long chain fatty acid or soap scum using water-soluble surfactants and ligand were studied. Simultaneous removal of calcium from the soap scum molecule by ligand complexation and formation of mixed micelles of the alkyl carboxylate anion molecules and co-surfactants are responsible for high solubility and rapid dissolution of soap scum. The solution pH plays an important role in the dissolution in this system as pH affects the dissociation of calcium from soap scum

molecule and the release of calcium by affecting the effectiveness of the chelating agent used, as well as affecting the formation of mixed micelles by altering the charge on the surfactant head groups of a pH-sensitive amphoteric surfactant when used as an added surfactant.

CHAPTER 1

1.1 INTRODUCTION

The content in this dissertation can be divided into three major areas related to the formation and dissolution of surfactant precipitates. Chapter 2 is the study of mixed anionic surfactants (sodium dodecyl sulfate (SDS) and sodium octylbenzene sulfonate (SOBS)) precipitated with calcium ion. The supersaturation ratios of each precipitating surfactants were calculated and related to the delay in the precipitation reaction. The delay in the precipitation reaction in mixed anionic surfactant micelles occurs when the values of the supersaturation ratio of precipitating surfactants are almost the same. The interruption of crystal growth by another precipitating surfactant is responsible for the delay in the precipitation reaction as evidenced by image analysis done using several techniques including optical spectrophotometry, and scanning electron microscopy.

Chapters 3 and 4 discuss the interaction between anionic surfactant (SDS) and pH-sensitive amphoteric surfactant (dimethyldodecylamine oxide (DDAO)). In Chapter 3, the hydrogen ion titration combined with regular solution theory was used to obtain the concentration of each component at varying pH levels. Chapter 4 applied the method used in Chapter 3 to model the precipitation phase boundaries in a solution of SDS and DDAO at varying pH by incorporating the solubility product of precipitates of SDS and protonated DDAO. The prediction of precipitation phase boundaries agrees well with the experimental precipitation phase boundaries.

The last topic covered in this dissertation is the dissolution of soap scum, which is a calcium salt of long chain fatty acid. In this study, calcium stearate ($Ca(C_{18})_2$) was used as the model soap scum. Chapter 5 discusses the equilibrium solubility of $Ca(C_{18})_2$ in three different types of surfactants including anionic surfactant (SDS), amphoteric surfactant (DDAO), and nonionic surfactant (octyl polyglycoside (C_8APG)) in the presence of a chelating agent (disodium ethylenediaminetetraacetate (Na_2EDTA)) at varying pH levels. The kinetics of dissolution of $Ca(C_{18})_2$ in these surfactant solutions is discussed in Chapter 6. It was found that the removal of calcium and the synergism in formation of mixed micelles are responsible when high equilibrium solubility of soap scum is observed. Under these conditions used, the rate of soap scum dissolution is rate limited by an interaction at the solid surface.

CHAPTER 2

Relation of Supersaturation Ratio in Mixed Anionic Surfactants to Kinetics of Precipitation

Mixed surfactants have been widely used due to their cost-saving and synergistic properties. One of the benefits resulting from this synergism is the ability of mixed surfactants to reduce the equilibrium extent of and rate of precipitation. The overall time required for calcium-induced precipitation of mixed sodium dodecyl sulfate (SDS) and sodium octylbenzene sulfonate (SOBS) over a particular range of ratios has been found to increase dramatically when compared to single pure components. In this study, light transmission and isoperibol calorimetry were used to measure the delay in the precipitation reaction. Scanning electron and optical micrographs of crystals formed give insight into the mechanism of synergism of mixtures. The smaller the difference in the supersaturation ratio of the two precipitating surfactants, the longer the induction time is. The delay in the extent of precipitation is due to the interruption of crystal formation from dissimilar precipitating surfactants and the reduction in the supersaturation when mixtures of surfactants are used.

2.1 INTRODUCTION

Precipitation of anionic surfactants can be detrimental in several applications including surfactant-based separation processes, enhanced oil recovery, and detergency. Anionic surfactants tend to precipitate with cations such as Na^{+}, Ca^{2+}, and Mg^{2+} and other positively charged molecules such as cationic surfactants and polymers. Single anionic surfactants are generally found to precipitate with calcium within minutes [1-3]. The surface activity of the surfactants is reduced when precipitation of the surfactant occurs and the surfactant is removed from solution. Builders are often used in formulating detergents in order to avoid precipitation of surfactants with metal ions [4]. There are extensive studies on equilibrium precipitation in single anionic surfactants precipitating with monovalent and divalent ions and with cationic surfactants [5-27]. It is well known that mixtures of surfactants (anionic or anionic/cationic surfactant mixtures) inhibit their tendency to precipitate at equilibrium as characterized by decreasing Krafft temperatures, increasing hardness tolerance, and shrinking precipitation phase boundary concentration regimes as reviewed in detail by Scamehorn and Harwell [28].

Kinetics studies of precipitation in surfactant systems have received little attention in the scientific literature. This could be due to the difficulty in quantifying the rate of precipitation, especially in systems with complex surfactant mixtures. Clarke et al. first studied the effect of micelle formation related to the kinetics of precipitation of calcium dodecyl sulfate by stopped-flow spectrophotometry [1]. Lee and Robb followed the kinetics of precipitation of calcium dodecyl and tetradecyl

sulfate by stopped-flow spectrophotometry and conductance and were able to calculate the degree of reaction and chronomal analysis by using the Mie theory of light scattering. The precipitation rates from each method were in a good agreement. However, the analysis underestimated the precipitate mass due to several approximations involved [2]. Lee and Robb [29] showed that polymeric additives interact with precipitating species but were shown to have no specific effect on the rate of precipitation of surfactants, while nonionic surfactant affects mixed micelle formation and delays the precipitation reaction. Shifting of the precipitation phase boundary of alkylbenzenesulfonate surfactant and calcium ion as a function of time was observed by Peacock and Matijevic [10]. A calorimetric technique was developed to follow the rate of surfactant precipitation by measuring the heat dissipated from precipitation reaction in systems of single anionic surfactant and mixed anionic surfactant of sodium dodecyl sulfate (SDS) and sodium octylbenzene sulfonate (SOBS) precipitating with calcium chloride ($CaCl_2$) by Rodriguez et al. [3, 30, 31]. The delay in the precipitation reaction was found in this mixed anionic surfactant system at specific mole ratios of SDS to SOBS. Image analysis by atomic force microscope revealed the growth of one precipitating surfactant on another precipitating surfactant and the entrapment of nonprecipitating surfactant in the forming crystals to be key mechanisms in retarding the precipitation reaction [31].

The objectives of this work are to demonstrate the relationship between supersaturation ratio of each precipitating surfactant and precipitation induction time in a mixed surfactant solution and to further delineate how certain mole ratios of mixed anionic surfactants can delay the precipitation with calcium. In this work, the

induction time or the duration prior to the onset of precipitation was measured using calorimetry and light transmission techniques. Relationships between the induction times, and supersaturation ratios of each precipitating surfactants are discussed. The mechanisms that delay the precipitation reaction in these mixed surfactant systems were deduced from the kinetic data augmented by the image analysis done on the precipitate crystals by scanning electron microscopy (SEM) and optical microscopy techniques. The practical long-term goal of this research is development of guidelines for formulations with precipitation times exceeding processing times for applications such as laundry detergency in which equilibrium precipitation is not attained.

2.2 THEORY

2.2.1 Surfactant Precipitation

Precipitation of surfactant occurs when the product of the thermodynamic activity of the precipitating surfactant and precipitating counterion satisfies the solubility product equation. Below the critical micelle concentration (CMC) or in the absence of micelles, the solubility product relationship for the precipitation of anionic surfactants (SDS or SOBS) with calcium ion can be described as,

$$K_{SP} = \left[S^-\right]_{mon}{}^2 \left[Ca^{2+}\right]_{un} f_S^2 f_{Ca} \qquad (2.1)$$

where K_{SP} is the activity-based solubility product, $\left[S^-\right]_{mon}$ is the concentration of the precipitating anionic surfactant (SDS or SOBS) in monomer form, and $\left[Ca^{2+}\right]_{un}$ is the

unbound calcium ion concentration in the solution. Below the CMC, $\left[S^-\right]_{mon}$ and $\left[Ca^{2+}\right]_{un}$ are equal to the total concentrations of surfactant and calcium, respectively. Above the CMC, micelles form and there exists equilibrium between monomers and micelles and monomers and precipitates, if precipitation occurs. Dissolved calcium ions can stay unbound or bind to the micelles. The activities coefficients (f_i) of the surfactant and calcium, f_S and f_{Ca}, respectively, are calculated using an extended Debye-Huckel expression [32],

$$\log f_i = \frac{-A(z_i)^2 I^{0.5}}{1 + Ba_i I^{0.5}} - 0.3I \qquad (2.2)$$

where A and B are constants depending on the solvent and temperature of the solution. At 30 ^{o}C, the values of A and B for water are 0.5139 and 0.3297 x 10^8, respectively [33]. The ion valence, z_i, for both SDS and SOBS is equal to -1. For calcium, z_i is equal to +2. An empirical value, a_i, based on the diameter of the ion, is 6 x 10^{-8} cm^{-1} for calcium [10] and the a_i values of SDS and SOBS are approximated at 7 x 10^{-8} cm^{-1} [23, 33, 34]. Ionic strength, I, can be calculated from the following equation,

$$I = \sum 0.5 c_i (z_i)^2 = [SDS] + [SOBS] + 3[CaCl_2] \qquad (2.3)$$

where C_i is the total concentration of ion *i* in the solution and z_i is the valence of ion *i*, [SDS] is the total concentration of SDS, [SOBS] is the total concentration of SOBS, and [$CaCl_2$] is the total concentration of $CaCl_2$ in the solution, i.e. the parameters used, all concentration are in molar units (M).

Above the CMC, Eqs. 2.2 and 2.3 to calculate activity coefficient though the micellized anionic surfactant and bound calcium do not contribute as much to ionic strength as monomer surfactant and unbound calcium. However, accounting for the micelle shielding factors is extremely complex and the data to do so is unavailable for all but a very few systems [35]. So, Eqs. 2.2 and 2.3 are generally used above and below the CMC for lack of a better approach [23] and can be considered a convention in the surfactant field.

2.2.2 Calculation of Supersaturation Ratio

A supersaturation ratio (S_o) is defined as the ratio of excess concentration of the reactants (monomeric surfactant and unbound calcium) to the equivalent equilibrium product of reactant concentrations or the solubility product to the power of the inverse of the sum of the stoichiometric coefficients of the reactants [36],

$$S_o = \left(\frac{\left([S^-]_{mon} \right)^2 [Ca^{2+}]_{un} f_S^2 f_{Ca}}{K_{SP}} \right)^{1/3} \qquad (2.4)$$

The value of the supersaturation ratio is low when the initial surfactant or calcium concentration is increasingly close to the phase boundary. The solution

composition is in equilibrium with the precipitate when the supersaturation ratio is equal to 1. Since the driving force for the precipitation reaction increases with increasing supersaturation ratio, the higher S_0 is, the faster the rate of precipitation is in general.

In a mixed surfactant solution system, the supersaturation ratio of each precipitating surfactant can be calculated independently. Above the mixed CMC, mixed micelles are in equilibrium with monomers of each individual surfactant. Equilibrium monomer concentrations of single surfactants in the presence of both monovalent and multivalent counterions can be found from a model developed by Stellner and Scamehorn [23, 24]. To calculate the supersaturation ratio, firstly, the monomer concentration of each surfactant in the mixed surfactant solution was determined [23, 24] by assuming ideal mixing in the micelle for the similarly structured SDS and SOBS. The so-called simplified model is used in this study to predict single component monomer concentrations needed with ideal solution theory rather than the generalized model [23, 24] due to its simplicity and ease of use. The generalized model requires (generally unavailable) additional parameters to account for the effects of Ca^{2+} concentration on mixed micelle formation. The simplified model yields the surfactant monomer-micelle concentration and the fraction of bound and unbound Ca^{2+}. However, the simplified model ignores the effect of Ca^{2+} on the single anionic surfactant CMC values. The calcium causes a reduction in the CMC and a reduced concentration of surfactant monomer. The supersaturation ratio calculated based on the simplified model would be larger than the supersaturation ratio calculated based on the generalized model. The impact of the Ca^{2+} in lowering

the monomer concentration is assumed to be the same for both SDS and SOBS, so the relative difference in the supersaturation ratio of each surfactant calculated based on the two models would be comparable. The assumption made here is sensible since both surfactants have similar structure with the same valency and the depression of CMC by the cations is an electrostatic effect.

2.3 EXPERIMENTAL

2.3.1 Materials

Sodium dodecyl sulfate (SDS) (99+% purity), obtained from Fisher Scientific (Fair Lawn, NJ), was further purified by recrystallization from water and then from methanol, followed by drying under a vacuum at 30 ^{o}C. The 4-octyl benzenesulfonic acid, sodium salt (SOBS) (97%), obtained from Aldrich, was purified by recrystallization from methanol and then from water, followed by drying under a vacuum at 30 ^{o}C. The ACS grade calcium chloride ($CaCl_2$) was from Acros (NJ) and it was used as received. Double deionized water was used in all experiments.

2.3.2 Methods

2.3.2.1. Measurement of Induction Time by Calorimetry

The precipitation induction time was measured using an isoperibol calorimetric technique, which utilizes the temperature change due to the heat released from the exothermic precipitation reaction. The schematic diagram of the apparatus is shown in Fig. 2.1. A Tronac (Oreon, UT) model 458/558 calorimeter was used in an

isoperibol mode to measure the heat of reaction as a function of time. The isoperibol calorimeter operates in nearly an adiabatic mode. The temperature of the water bath was maintained at $30^{o}C \pm 0.025\ ^{o}C$ using a Tronac PTC-41 temperature controller. The procedure was modified from a method developed by Rodriguez et al. [30]. Approximately 48 g of surfactant solution was placed in the reaction vessel, which was then equilibrated to the temperature of the water bath. Approximately 2 g of a 0.25 M calcium chloride ($CaCl_2$) solution in a syringe was also equilibrated to the temperature of the water bath. The injection of the $CaCl_2$ solution was done quickly to allow instantaneous mixing of the reactants by a stirrer inside the reaction vessel. The temperature rise data in a temperature-time profile could be used to indicate the onset and the rate of precipitation.

2.3.2.2 Measurement of Induction Time by Turbidity

In the calorimetric technique, there is a substantial amount of heat loss in the system if the reaction runs for a long period of time, which cannot be accurately accounted for. Hence, turbidity was also used for slow reactions. A device that can measure the transmitted light through the solution was designed to detect the onset of precipitation in the system studied here as shown in Fig. 2.2. The device is composed of a a green light emitting diode (LED) with a DC power supply (HP E3612A) and a photo resistive, cadmium sulfide (CdS) type light detector, which has a variable resistance according to the amount of light it receives; resistance is high in darkness and low when illuminated. The resistance signal was measured by a digital

multimeter (METEX M3850D) interfaced with a computer and the signal was converted into a turbidity unit using the expression [37, 38],

$$\tau = \frac{1}{L}\ln\left(\frac{I_0}{I}\right) = \frac{1}{L}\ln\left(\frac{V}{V_0}\right) \qquad (2.5)$$

where τ is the turbidity, with units of inverse length, L is the light path length, I_0 is the light intensity detected for the isotropic solution, I is the light intensity measured by means of the voltage (V) drop of the phototransistor and V_0 is the voltage drop of the phototransistor corresponding to I_0. Since the resistance was actually measured in this experiment and $V \propto R$, where R is the resistance measured by the multimeter, Eq. 2.5 can be simply converted to

$$\tau = \frac{1}{L}\ln\left(\frac{R}{R_o}\right) \qquad (2.6)$$

where R_0 is the resistance corresponding to I_0.

The onset of the precipitation can be detected by a sharp increase in the resistance due to the turbidity as the precipitate forms. The solution was stirred at a constant rate to ensure homogeneous mixing. The temperature of solution was controlled at 30 ^{o}C by circulating water from a temperature-controlled water bath into a jacket outside the test tube cell. Prior to mixing solutions of surfactants and $CaCl_2$,

both solutions were equilibrated at 30 ^{o}C. A 1-mL solution of $CaCl_2$ was injected into the test tube containing 24-mL of surfactant solution with constant mixing.

2.4 RESULTS AND DISCUSSION

2.4.1 Onset of Precipitation and Induction Time

The induction time is defined as the duration of time prior to the onset of precipitation, which can be detected by the first sharp increase in the heat dissipated in the calorimetric method and the value of turbidity in the turbidity method. All experiments were at 30 ^{o}C. The induction time deduced from the calorimetry and the turbidity measurements are summarized in Fig. 2.3 for a system with a total surfactant concentration of 0.0192 M with 0.01 M $CaCl_2$. The two methods gave comparable results. The turbidity method is easier and faster to set up than calorimetry, but the turbidity alone, as set up here, cannot be used to quantify the amount of precipitates. However, since the onset of precipitation and induction time are the main focuses of this works, most results presented here are from the turbidity method.

A drastic change of temperature and turbidity was observed in the solutions that precipitate almost instantaneously such as the precipitation of pure anionic surfactants with Ca^{2+}. For example, as can be seen in Fig. 2.3, the induction time of pure SDS or SOBS system is very short compared that at a SDS mole fraction around 0.6. A similar trend was also observed by Rodriguez and Scamehorn for the same system at the same conditions using calorimetry where the slowest precipitation was observed at a SDS mole fraction of 0.6 [30]. In that work, only gross composition

effects were investigated (SDS mole fractions of 0, 0.2, 0.4, 0.6, 0.8, and 1.0). In this investigation, a much finer grid is used to probe behavior around this 0.6 SDS mole fraction where the remarkable synergism was observed. From Fig. 2.3, the longest induction is observed at an SDS mole fraction of 0.63 and substantial longest induction time is observed over a very narrow range of compositions (SDS mole fraction range of about 0.1 or only about 10% of the total composition range).

Figure 2.4 shows the induction time from Fig. 2.3 and that at two higher total surfactant concentrations of 0.0288 and 0.0384 M all with 0.01 M $CaCl_2$. The SDS mole fraction corresponding to the maximum induction time increases with increasing total surfactant concentration, occurring at 0.66 and 0.70 for the two higher concentrations in Fig. 2.4. The maximum observed induction time is also highly concentration dependent, increasing from 8 minutes for the lowest total surfactant concentration to 50 minutes and 80 minutes with increasing concentration. Although not very accurately determined, the range of SDS mole fractions over which synergism in induction time is observed appears to be about the same for the different concentrations. All these concentrations used are above the CMC.

2.4.2 Relation of the Onset of Precipitation to the Difference in Supersaturation Ratios

The supersaturation ratio of each precipitating surfactant was calculated from Eq. 2.4 and given in Tables 2.1-2.3 and Fig. 2.5. As shown in Figs. 2.6-2.9, the induction time and the absolute value of the difference in the supersaturation ratio of SDS and SOBS are shown for the three total surfactant concentrations studied.

From Figs. 2.6-2.8, it is remarkable how closely the surfactant composition at the maximum induction time corresponds to the minimum absolute value of the difference in supersaturation values for the two surfactants. There is little dependence of induction time on the actual values of S_o for each surfactant shown in Fig. 2.5, but their relative S_o is crucial. Figure 2.9 shows this $|S_o$ of SDS - S_o of SOBS| for the three systems and the magnitude for different total surfactant concentrations is quite similar (as are the actual values of S_o in Fig. 2.5), even though the maximum induction time is quite different for the three systems.

In general, the higher the supersaturation ratio, the higher the rate of precipitation [39]. If the supersaturation ratios of both surfactants in the mixed anionic surfactants solution are about the same, one might infer that each precipitating surfactant would start to precipitate out at the same time. The growing crystals can interrupt each other's growth while crystallizing using the dissimilar crystal as a nucleation site, interrupting the growth of the crystal of surfactant A, then precipitating A interrupting B, and so on, delaying creation of enough crystal to be detected. This might be valid only when the two precipitating surfactants have a similar rate of precipitation at the same supersaturation ratio. Rates of precipitation and induction time of pure calcium dodecyl sulfate ($Ca(DS)_2$) and calcium octyl benzenesulfonate ($Ca(OBS)_2$) at the same supersaturation ratio are only slightly different [30].

Figure 2.10 shows the turbidity as a function of time plotted for the precipitation of 0.0288 M of total surfactant at different SDS mole fractions precipitating with 0.01 M of $CaCl_2$. There appear to be two times at which onset of

precipitation occurs found at a mole fraction of SDS of 0.6, indicating there is one surfactant precipitating out first and followed by the second surfactant. On the other hand, at the mole fraction of SDS of 0.63 and 0.66, there is only one single step of precipitation observed and these ratios give longer induction time than at a SDS mole fraction of 0.6. It could be implied that at these ratios, in which the difference in the supersaturation ratio is at or close to minimum, the two precipitating surfactants start to precipitate at almost the same time so there appears to be a one-step change in the turbidity. Rodriguez et al. [31] also observed this two-step precipitation under some conditions.

The image analysis of crystals resulting from precipitation under different conditions was carried out using scanning electron microscopy (SEM) and optical microscopy. All the images taken in this study were taken after precipitation reaction began about 1 week unless otherwise stated. Figures 2.11-2.13 show the SEM micrographs of crystals precipitated from 0.0192 M of SDS, of SOBS, and of a mixed SDS/SOBS at a 60/40 mole ratio, respectively, with 0.01 M $CaCl_2$. Figure 2.14 shows the optical images of the crystal formed from supersaturated solutions of 0.0096 M of SDS, of SOBS, and of a mixed SDS/SOBS at a 60/40 mole ratio with 0.0038 M $CaCl_2$. The optical images of precipitates shown in Fig. 2.14 were taken at 5 minutes and 1 week after the precipitation reaction began. The $Ca(DS)_2$ crystals appear to have a different shape and size than the $Ca(OBS)_2$ crystals. The $Ca(OBS)_2$ crystals appear to have a more defined shape and have sharper, more jagged edges with an elongated flat crystals structure. The crystals precipitated from a mixed solution with a 0.0192 M total surfactant concentration of a 60/40 mole ratios of SDS to SOBS

have separate crystals characteristics of either $Ca(DS)_2$ or $Ca(OBS)_2$. The crystals from the mixed solutions are lumped together, not clearly separate from each other as the crystals formed in the pure solution of SDS and SOBS. It is also obvious that the $Ca(OBS)_2$ crystal structure precipitated from the mixed solution are not as well defined as the crystal from a pure SOBS solution. The 1-week optical images shown in Fig. 2.14 reveal similar characteristics of crystals as shown by the SEM images in Figs. 2.11-2.13. For the $Ca(DS)_2$ crystals from a pure surfactant solution taken at an early stage of crystal formation (5 minute after the precipitation detection), appear not to change over 1 week of ripening. In contrast, the $Ca(OBS)_2$ crystals from a pure surfactant solution at 5 minutes and 1 week after the precipitation detection are much different in size and shape, indicating how slow the precipitate of $Ca(OBS)_2$ take to fully develop or ripen into a well-defined structure. It appears that the crystals formed in mixed solutions develop into a well-defined structure slower than crystals formed in single surfactant solutions. After one week, there are mixed crystals of regular and irregular shapes in the precipitation system of mixed surfactant solutions. The AFM images of precipitates formed in a pure SDS, pure SOBS and mixed SDS/SOBS were reported by Rodriguez et al. [31] and the distinct characteristics of a crystal formed from a mixed SDS/SOBS were observed. Jagged edges of one crystal growing outwardly on the surface of a dissimilar crystal and the formation of holes are the features that were not observed in the AFM images of precipitates formed from either pure SDS or pure SOBS.

The optical, SEM and AFM results can help explain the greatest delay in precipitation corresponding to the minimum absolute value of the difference in the

supersaturation ratios of each precipitating surfactant. The non-well defined crystal habits found in the precipitates formed in a mixed solution is possibly due to the interruption of one crystal growing onto another forming crystal. The crystals precipitating from mixed surfactant solutions have different crystal habits from the pure crystals also observed by Rodriguez et al. Figure 2.15 shows the XRD patterns of Ca^{2+} precipitating with SDS (top), SOBS (middle) and mixed SDS-SOBS (bottom). As can be seen from this figure, the d-spacing of $Ca(DS)_2$ and $Ca(OBS)_2$ from pure solutions is different, indicating different lattice structure. The XRD patterns of crystals from mixed solution contain both of these crystal patterns from pure SDS and pure SOBS. This suggests that mixed solid crystal is not precipitating, but each of the individual surfactants is separately forming precipitate.

The adsorbing surfactant, which is different from that forming crystals, does not form mixed crystals, but adsorbed surfactant aggregates can cover the surface of a growing crystal, interrupting growth of one crystal and resulting in uneven edges observed in SEM micrographs and AFM images of crystals formed from a mixed surfactant solution. Crystals of both surfactants eventually separate out as can be seen in Fig. 2.13a. Possible reason for hole formation in precipitate from mixed surfactant systems observed in AFM studies is the entrapment of nonprecipitating surfactant in the forming crystal. It is not known how hole formation in precipitating crystals correlate to surfactant supersaturation ratios.

In conclusion, at the ratio where the supersaturation ratios of both precipitating surfactants are almost equal, precipitates start to form at the same time. Each precipitating surfactant tends to interact towards each other in several ways.

They might prefer to use other crystals as a seed for a heterogeneous nucleation, interrupting the crystal growth process or they may adsorb on dissimilar crystals or they may cause holes in the crystals, resulting in a slow rate of precipitation as observed.

2.5 REFERENCES

1. Clarke DE, Lee RS, Robb ID (1976) Precipitation of Calcium Salts of Surfactants. Faraday Disc. Chem. Soc. 61: 165-174
2. Lee RS, Robb ID (1979) Precipitation of Calcium Surfactants. Part 2. J. Chem. Soc. Faraday Trans. 1 75: 2116-2125
3. Rodriguez CH, Lowery LH, Scamehorn JF, Harwell JH (2001) Kinetics of Precipitation of Surfactants I. Anionic Surfactants with Calcium and with Cationic Surfactants. J. Surfact. Deterg. 4: 1-14
4. Tai LHT (2000) Formulating Detergents and Personal Care Products. A Complete Guide to Product Development. AOCS Press, Champaign, Illinois. pp. 49
5. Miyamoto S (1960) The Effect of Metallic Ions on Surface Chemical Phenomena. III. Solubility of Various Metal Dodecyl Sulfates in Water. Bull. Chem. Soc. Jpn. 33: 371-375
6. Hato M, Shinoda K (1973) Krafft Points of Calcium and Sodium Dodecylpoly(oxyethylene) Sulfates and Their Mixtures. J. Phys. Chem. 77: 378-381
7. Shinoda K, Tsuyoshi H (1977) Ionic Surfactants Applicable in the Presence of Multivalent Cations. Physicochemical Properties. J. Phys. Chem. 81: 1842-1845

8. Bozic J, Krznaric I, Kallay N (1979) Precipitation and Micellization of Silver, Copper, and Lanthanum Dodecyl Sulfates in Aqueous Media. Colloid Polym. Sci. 257: 201-205

9. Chiu Y (1982) Relationship of Oil Recovery Activity to Surfactant Aggregate Size in Petroleum Sulfonate Solutions. In: Mittal KL (ed) Solution Behav. Surfactants: Theor. Appl. Aspects, [Proc. Int. Symp.]. Plenum Press, New York. pp. 1415-1440

10. Peacock JM, Matijevic E (1980) Precipitation of Alkylbenzene Sulfonates with Metal Ions. J. Colloid Interface Sci. 77: 548-554

11. Celik MS, Manev ED, Somasundaran P (1982) Sulfonate Precipitation-Redissolution-Reprecipitation in Inorganic Electrolytes. AIChE Symp. Ser. 78: 86-96

12. Baviere M, Bazin B, Aude R (1983) Calcium Effect on the Solubility of Sodium Dodecyl Sulfate in Sodium Chloride Solutions. J. Colloid Interface Sci. 92: 580-583

13. Chou SI, Bae JH (1983) Surfactant Precipitation and Redissolution in Brine. J. Colloid Interface Sci. 96: 192-203

14. Gerbacia WEF (1983) Calcium Dodecyl Sulfate Precipitation from Solutions Containing Sodium Chloride. J. Colloid Interface Sci. 93: 556-559

15. Somasundaran P, Ananthapadmanabhan KP, Celik MS, Manev ED (1984) A Thermodynamic Model of Redissolution of Calcium Sulfonate Precipitates in Sodium Chloride Solutions. Soc. Pet. Eng. J. 24: 667-676

16. Kallay N, Pastuovic M, Matijevic E (1985) Solubility and Enthalpy of Precipitation of Magnesium, Calcium, Strontium, and Barium Dodecyl Sulfates. J. Colloid Interface Sci. 106: 452-458

17. Matheson KL (1985) Detergency Performance Comparison Between LAS and ABS Using Calcium Sulfonate Precipitation Boundary Diagrams. J. Am. Oil Chem. Soc. 62: 1269-1274

18. Matheson KL, Cox MF, Smith DL (1985) Interactions Between Linear Alkylbenzene Sulfonates and Water Hardness Ions. I. Effect of Calcium Ion on Surfactant Solubility and Implications for Detergency Performance. J. Am. Oil Chem. Soc. 62: 1391-1396

19. Cox MF, Matheson KL (1985) Interactions Between Linear Alkylbenzenesulfonates and Water Hardness Ions. II. Reducing Hardness Sensitivity by the Addition of Micelle Promotion Agents. J. Am. Oil Chem. Soc. 62: 1396-1399

20. Noik C, Baviere M, Defives D (1987) Anionic Surfactant Precipitation in Hard Water. J. Colloid Interface Sci. 115: 36-45

21. Fan XJ, Stenius P, Kallay N, Matijevic E (1988) Precipitation of Surfactant Salts II. The Effect of Nonionic Surfactants on Precipitation of Calcium Dodecyl Sulfate. J. Colloid Interface Sci. 121: 571-578

22. Hu PC, Tuvell ME (1988) Effect of Water Hardness Ions on the Solution Properties of an Anionic Surfactant. J. Am. Oil Chem. Soc. 65: 1340-1345

23. Stellner KL, Scamehorn JF (1989) Hardness Tolerance of Anionic Surfactant Solutions. 1. Anionic Surfactant with Added Monovalent Electrolyte. Langmuir 5: 70-77

24. Stellner KL, Scamehorn JF (1989) Hardness Tolerance of Anionic Surfactant Solutions. 2. Effect of Added Nonionic Surfactant. Langmuir 5: 77-84

25. Rodriguez CH, Chintanasathien C, Scamehorn JF, Saiwan C, Chavadej S (1998) Precipitation in Solutions Containing Mixtures of Synthetic Anionic Surfactant and Soap. I. Effect of Sodium Octanoate on Hardness Tolerance of Sodium Dodecyl Sulfate. J. Surfact. Deterg. 1: 321-328

26. Burckett St. Laurent J, Connor D, Cripe T, Kott K, Scheibel J, Stidham R, Reilman R (2000) Improved Alkyl Benzene Surfactants: Molecular Design and Solution Physical Chemical Properties. In: 5th World Surfactants Congress. Firenze, Italy Federchimica Assobase-P.I.T.I.O.

27. Kott KL, Gederle TW, Baillely, Scheibel JJ, Lawson RJ (2001) Proceedings of New Horizons: Detergents for the New Millennium. AOCS Press, Champaign, Illinois. Ch. 11

28. Scamehorn JF, Harwell JH (2004) Precipitation of Surfactant Mixtures. In: Abe M, Scamehorn JF (eds) Mixed Surfactant Systems. 2nd edn. Marcel Dekker, New York. pp. 601-655

29. Lee RS, Robb ID (1979) Precipitation of Calcium Surfactants. Part 3. J. Chem. Soc. Faraday Trans. 1 75: 2126-2136

30. Rodriguez CH, Scamehorn JF (2001) Kinetics of Precipitation of Surfactants. II. Anionic Surfactant Mixtures. J. Surfact. Deterg. 4: 15-26

31. Rodriguez CH, Yuan WL, Scamehorn JF, O'Rear EA (2002) Kinetics of Precipitation of Surfactants. III. Atomic Force Microscopy of Precipitate Crystals. J. Surfact. Deterg. 5: 269-280

32. Davies CW (1962) Ion Association. Butterworths, London. pp. 41

33. Klotz IR, Rosenberg RM (1991) Chemical Thermodynamics: Basic Theory and Methods, 4th edn. Krieger, Malabar. pp. 440

34. Robinson RA, Stokes RH (1959) Electrolyte Solutions. Butterworths, London. pp. 174

35. Burchfield TE, Woolley EM (1984) Model for Thermodynamics of Ionic Surfactant Solutions. J. Phys. Chem. 88: 2149-2155

36. Lieser KH (1969) Steps in Precipitation Reactions. Angew. Chem. Internat. Edit. 8: 188-202

37. Fletcher PDI, Morris JS (1995) Turbidity of Oil-in-Water Microemulsion Droplets Stabilized by Nonionic Surfactants. Colloids Surf. A 98: 147-154

38. Acosta EJ, Le MA, Harwell JH, Sabatini DA (2003) Coalescence and Solubilization Kinetics in Linker-Modified Microemulsions and Related Systems. Langmuir 19: 566-574

39. Walton AG (1967) The Formation and Properties of Precipitates. Interscience, New York. pp. 45

Table 2.1 Summary of the induction time, S_o for SDS and SOBS, and $|S_o$ of SDS-S_o of SOBS| for total surfactant concentration = 0.0192 M

Mole fraction of SDS in SDS-SOBS mixture	S_o of SDS	S_o of SOBS	$\|S_o$ of SDS-S_o of SOBS$\|$	Induction time (min)
0.2	2.16	6.40	4.24	< 1
0.5	3.54	4.95	1.41	< 1
0.6	3.92	4.20	0.28	5
0.63	4.03	3.98	0.05	9
0.65	4.10	3.82	0.28	8
0.7	4.27	3.43	0.84	5
0.8	4.59	2.58	2.01	< 1

Table 2.2 Summary of the induction time, S_o for SDS and SOBS, and $|S_o$ of SDS-S_o of SOBS| for total surfactant concentration = 0.0288 M

Mole fraction of SDS in SDS-SOBS mixture	S_o of SDS	S_o of SOBS	$\|S_o$ of SDS-S_o of SOBS$\|$	Induction time (min)
0.5	2.74	4.32	1.58	< 1
0.6	3.06	3.69	0.63	19
0.63	3.15	3.49	0.34	27
0.66	3.24	3.29	0.05	51
0.67	3.27	3.22	0.04	43
0.68	3.29	3.15	0.14	3

Table 2.3 Summary of the induction time, S_o for SDS and SOBS, and $|S_o$ of SDS-S_o of SOBS| for total surfactant concentration = 0.0384 M

Mole fraction of SDS in SDS-SOBS mixture	S_o of SDS	S_o of SOBS	$\|S_o$ of SDS-S_o of SOBS$\|$	Induction time (min)
0.5	2.23	3.73	1.50	2
0.6	2.49	3.19	0.70	22
0.65	2.62	2.91	0.29	33
0.70	2.74	2.61	0.13	80
0.72	2.79	2.49	0.30	43
0.75	2.86	2.30	0.56	4
0.8	2.97	1.98	0.99	1

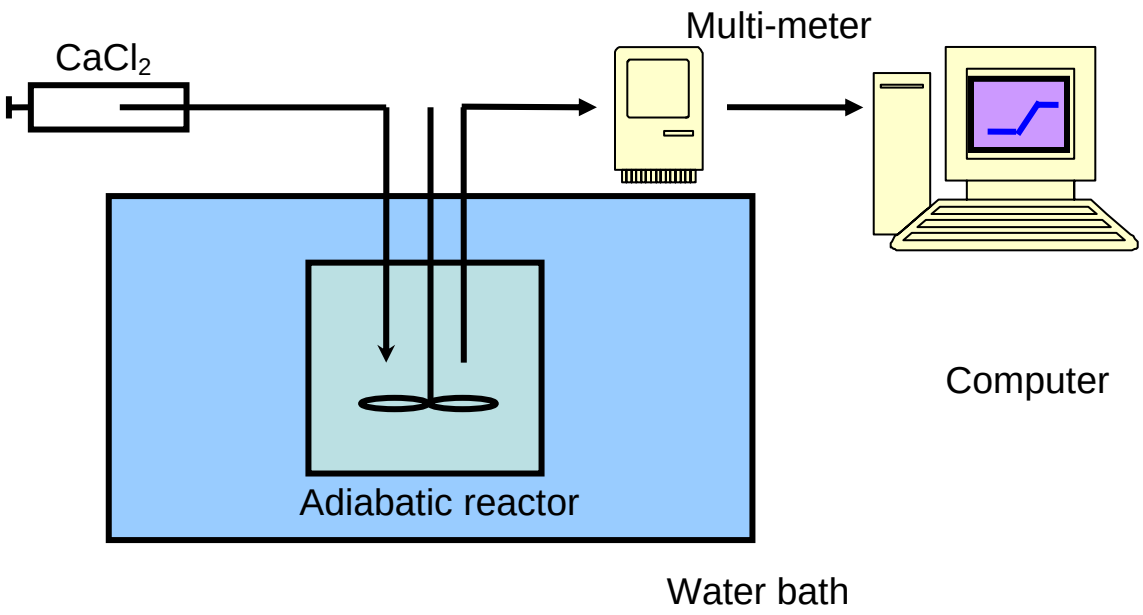

Fig. 2.1 Schematic diagram of the isoperibol calorimeter instrumentation

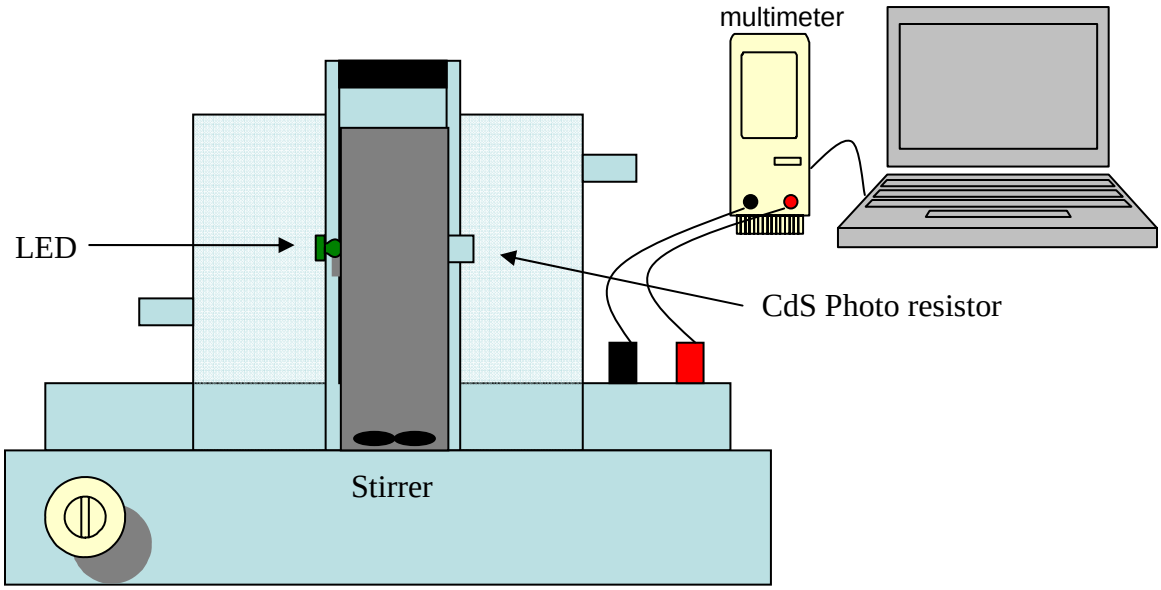

Fig. 2.2 Schematic diagram of turbidity meter used for surfactant precipitation kinetics study

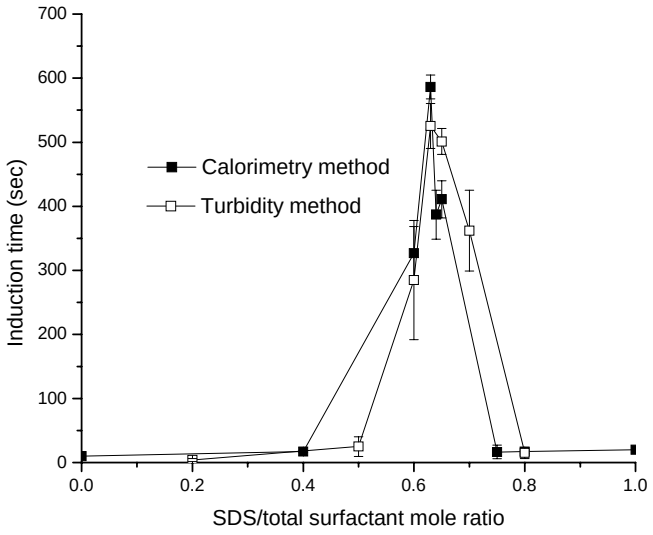

Fig. 2.3 Comparison of induction time from calorimetric and turbidity methods with a total surfactant concentration of 0.0192 M at different SDS mole fractions with SOBS and 0.01 M $CaCl_2$

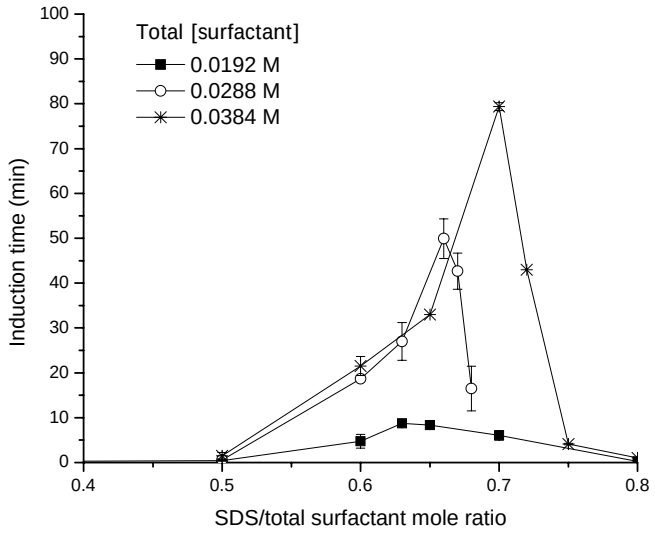

Fig. 2.4 Induction time of precipitation reaction in mixed SDS/SOBS solutions and 0.01 M $CaCl_2$

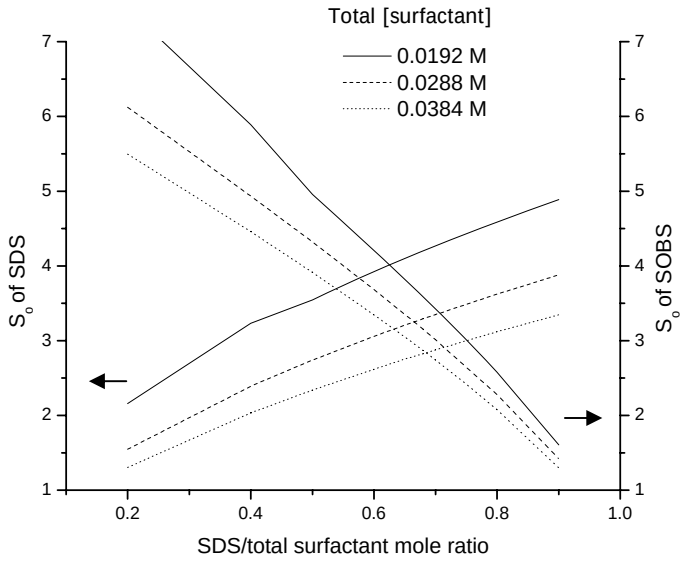

Fig. 2.5 Supersaturation ratios of SDS and SOBS in mixed SDS/SOBS solutions and 0.01 M $CaCl_2$

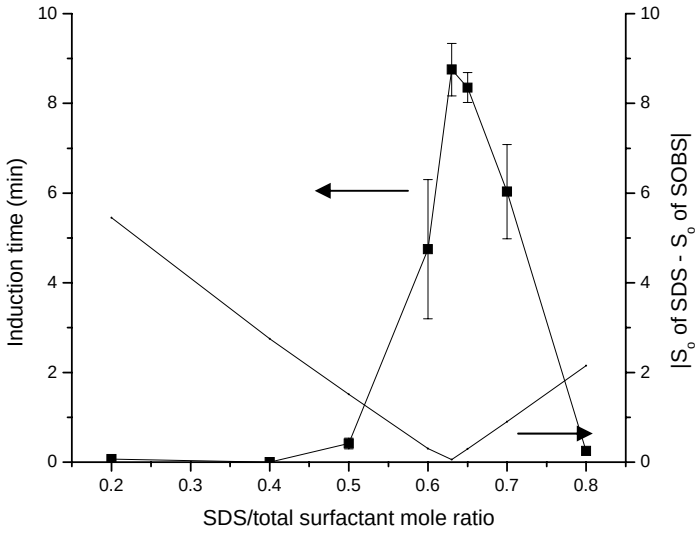

Fig. 2.6 Comparison of induction time and difference in supersaturation ratios of SDS and SOBS in the precipitation of a total surfactant concentration of 0.0192 M at different SDS mole fractions with SOBS and 0.01 M $CaCl_2$

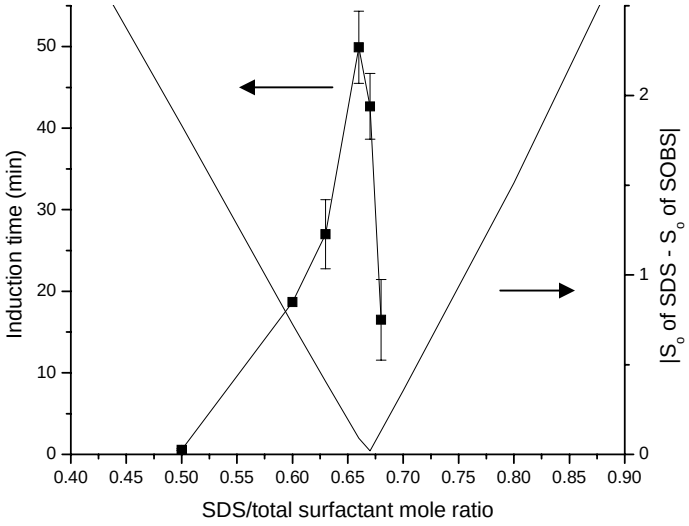

Fig. 2.7 Comparison of induction time and difference in supersaturation ratios of SDS and SOBS in the precipitation of a total surfactant concentration of 0.0288 M at different SDS mole fractions with SOBS and 0.01 M $CaCl_2$

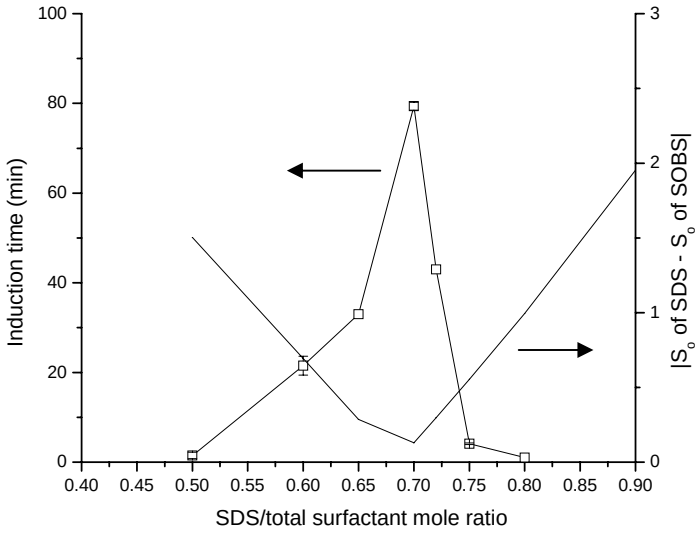

Fig. 2.8 Comparison of induction time and difference in supersaturation ratios of SDS and SOBS in the precipitation of a total surfactant concentration of 0.0384 M at different SDS mole fractions with SOBS and 0.01 M $CaCl_2$

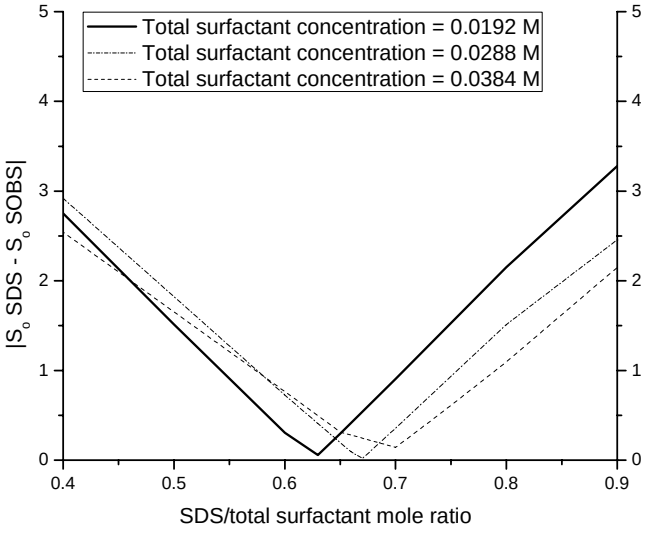

Fig. 2.9 The difference in the supersaturation ratios in the precipitation system of SDS/SOBS mixture solutions with 0.01 M $CaCl_2$

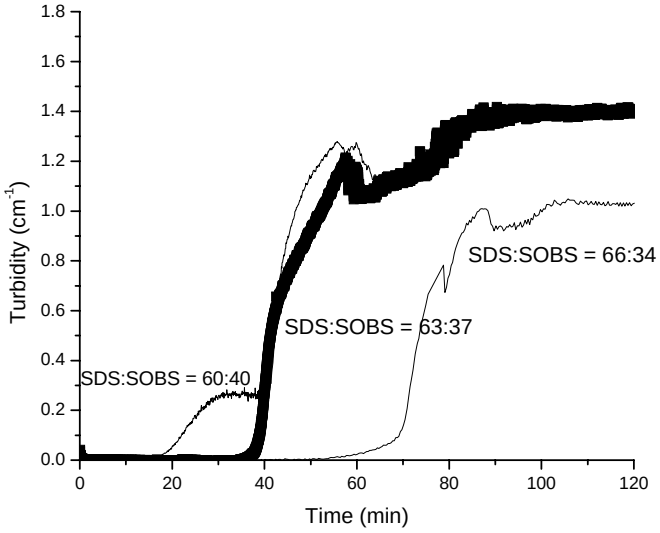

Fig. 2.10 Turbidity measurement of precipitation of mixed varying mole ratios of SDS and SOBS at a total surfactant concentration of 0.0288 M with 0.01 M $CaCl_2$

a. b.

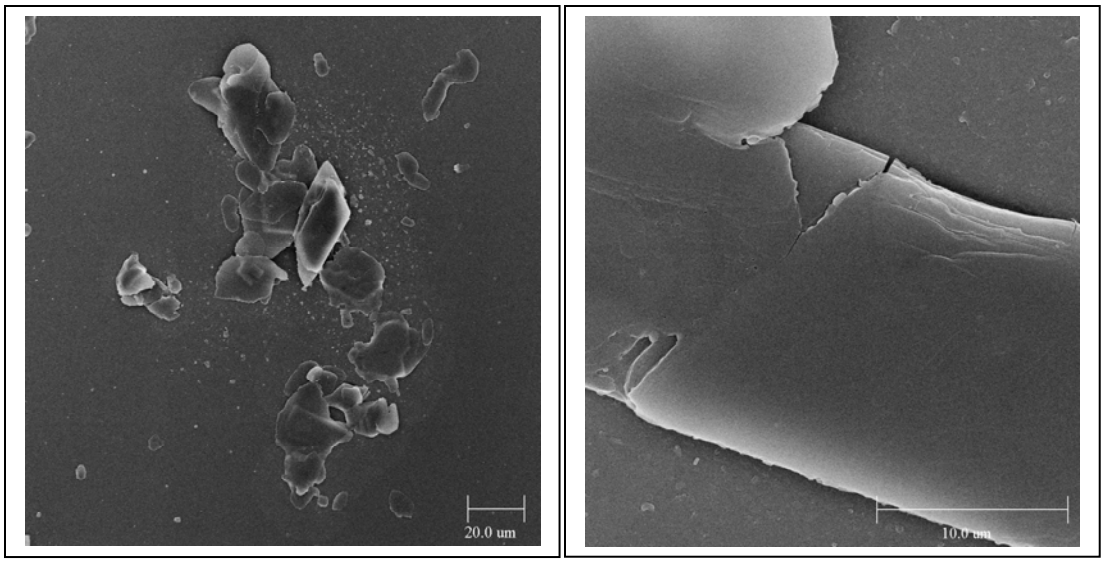

Fig. 2.11 SEM micrograph of crystal precipitated from a 0.0192 M SDS solution with 0.01 M $CaCl_2$

a. b.

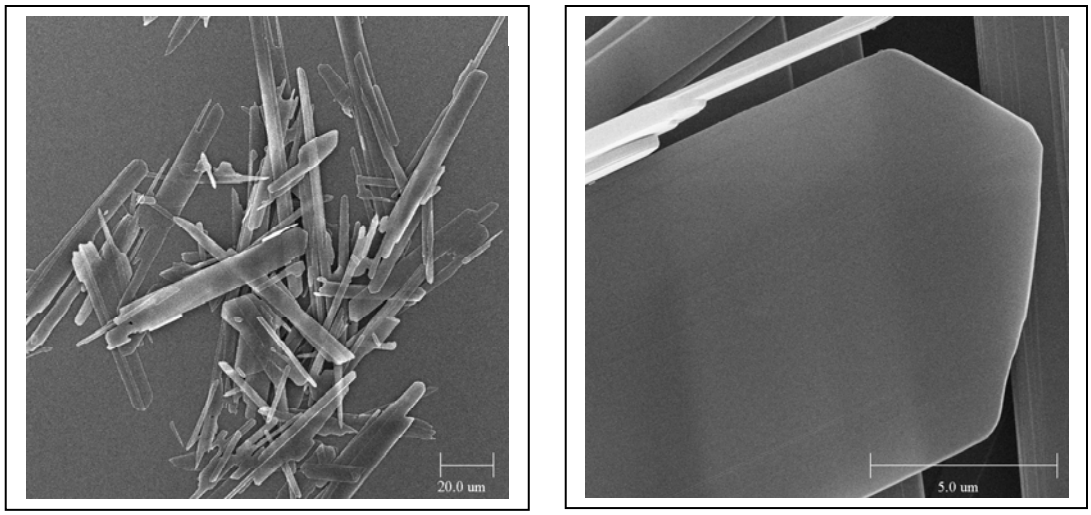

Fig. 2.12 SEM micrograph of crystal precipitated from a 0.0192 M SOBS solution with 0.01 M $CaCl_2$

a. b.

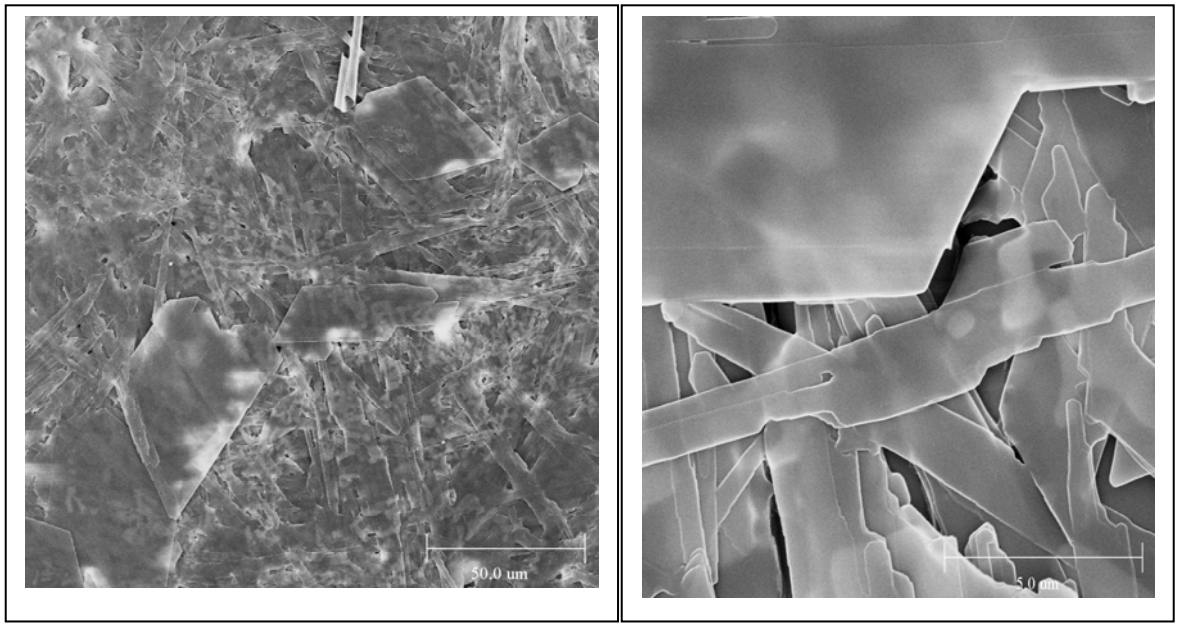

Fig. 2.13 SEM micrograph of crystal precipitated from a solution with a total surfactant concentration of 0.0192 M at SDS mole fraction of 0.60 with SOBS and 0.01 M $CaCl_2$

(a) 5-minute after precipitation detected

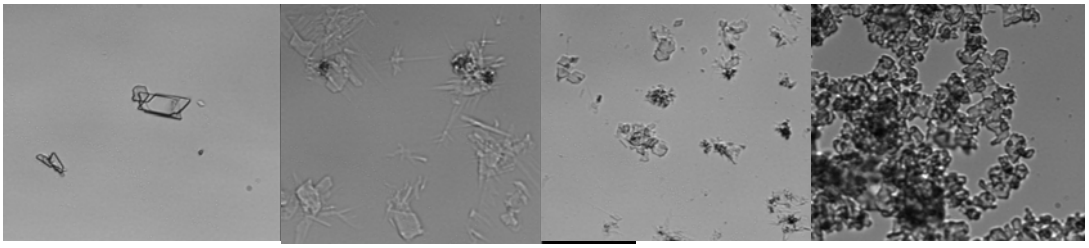

SDS/SOBS = 100/0 SDS/SOBS = 60/40 SDS/SOBS = 40/60 SDS/SOBS = 0/100

(b) 1-week after precipitation detected

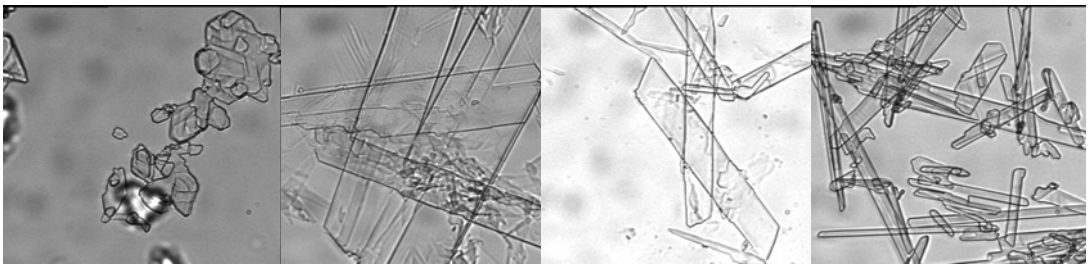

SDS/SOBS = 100/0 SDS/SOBS = 60/40 SDS/SOBS = 40/60 SDS/SOBS = 0/100

Fig. 2.14 Optical images of crystal precipitated from a solution with a total surfactant concentration of 0.0096 M and 0.0038 M $CaCl_2$ (400X)

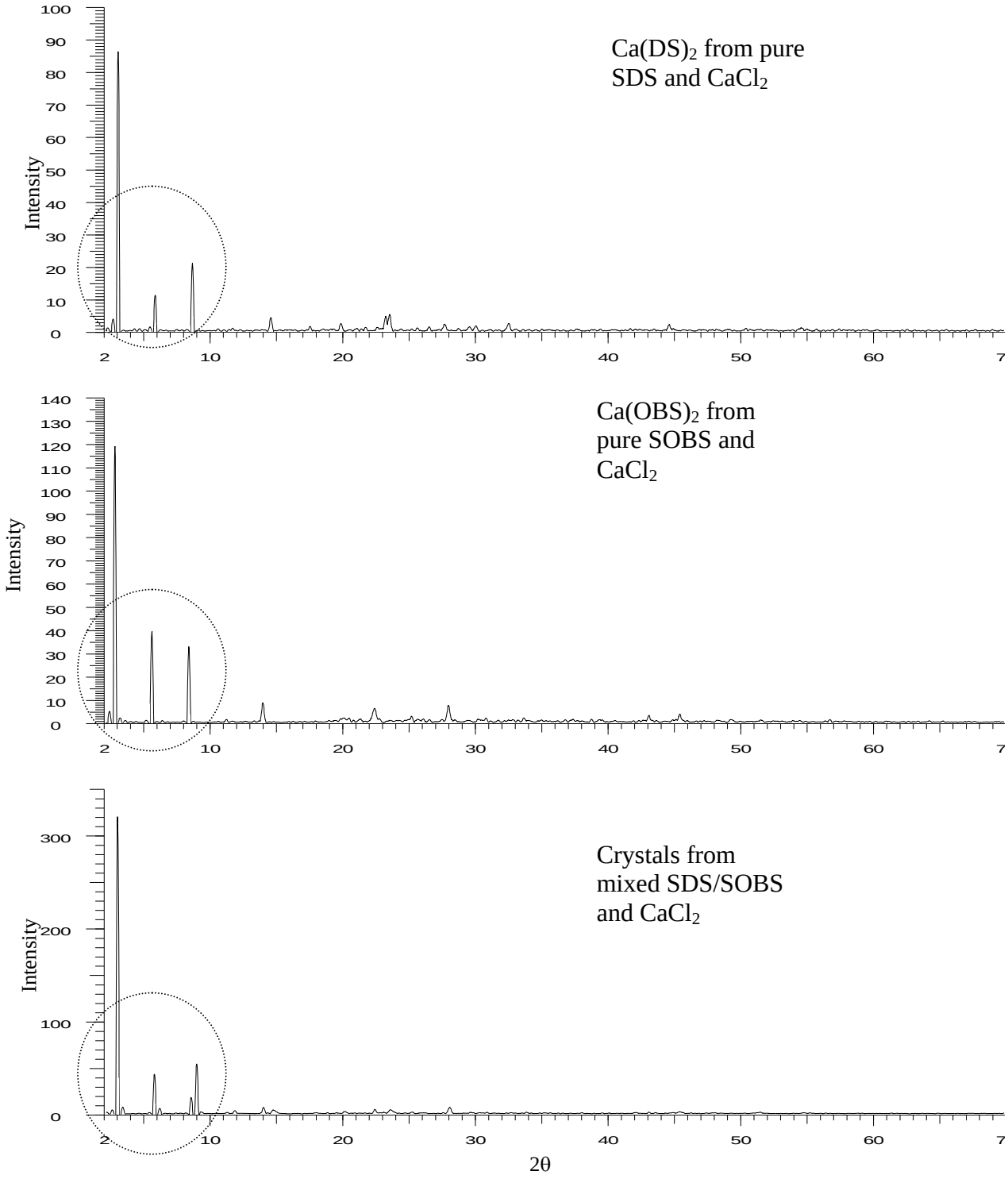

Fig. 2.15 X-ray diffraction patterns of crystals from pure and mixed solution of SDS and SOBS at total surfactant concentration of 0.0192 M with 0.01 M $CaCl_2$

CHAPTER 3

Interaction Between an Anionic and an Amphoteric Surfactant.

Part I. Monomer-Micelle Equilibrium

A mixture of anionic and amphoteric surfactants is composed of three components at intermediate pH levels: anionic, cationic (protonated amphoteric), and zwitterionic (unprotonated amphoteric). Knowledge of the composition of each surfactant in both monomer and micellar forms (monomer-micelle equilibrium) is important in applications using this mixture. Hydrogen ion titration of the mixed surfactant solution as a function of surfactant composition is combined with the pseudophase separation model and regular solution theory for the three-surfactant mixture to calculate the concentration of each surfactant in monomer and in micelle forms at different pH levels. The specific system studied here is sodium dodecyl sulfate (SDS) and dimethyldodecylamine oxide (DDAO), which are normally used in a wide range of consumer products. The degree of protonation of monomeric DDAO is not affected by the presence of SDS, indicating an insignificant formation of ion pairs between these monomers. However, the presence of SDS in micelles shifts the micellar pK_a of DDAO protonation significantly and the method used here allows the quantification of partial fugacities of each individual surfactant in micelle form. The composition in the monomer phase at each pH will aid in understanding and

predicting solution compositions corresponding to anionic/amphoteric surfactant precipitation, which is the focus of the subsequent paper in this series.

3.1 INTRODUCTION

In consumer product applications, surfactant mixtures are often used to obtain various specific beneficial properties simultaneously and to gain general benefits from synergistic effects. Mixtures of amphoteric and anionic surfactants are often used in shampoo, hand-dishwash, and other liquid formulations. Anionic surfactants are well known for cleaning properties, while amphoteric surfactants are often used for skin mildness and good foam properties [1, 2]. However, precipitation can be extremely detrimental to system performance if surfactants used have oppositely charged headgroups. Since precipitation is driven by monomer concentrations (i.e., thermodynamic activities) of each surfactant forming the precipitate, the activities of each surfactant must be known in order to determine whether precipitation occurs or not.

A mixture of amphoteric surfactant dimethyldodecylamine oxide (DDAO) and anionic surfactant sodium dodecyl sulfate (SDS) is studied here. Amphoteric surfactants may possess both positive and negative charges on its head group and the net charge is pH sensitive [1, 2]. The amine oxide surfactant exhibits properties of cationics at low pH values and zwitterionics at high pH values since it is protonated by hydrogen ions in a similar manner to weak acids. So the mixture of these two surfactants is essentially a ternary system containing anionic surfactant**,** cationic

surfactant (protonated amphoteric), and nonionic or zwitterionic surfactant (unprotonated amphoteric), resulting in synergism in micelle formation and depressed CMCs (relative to surfactants which form ideal mixed micelles).

Solution properties of the amine oxide surfactant have been shown to vary with pH and electrolyte concentration and type [3-8]. Rathman and Christian developed a method to determine monomer and micelle compositions of the amine oxide surfactant at various pH values and concentrations by a hydrogen ion titration method under a swamping electrolyte condition combined with use of the Gibbs-Duhem equation for analysis of the micellar phase activities [9]. Zimmerman and Schnaare extended this method for a non swamping electrolyte system by accounting for CMC changes due to counterions during hydrogen ion titration [10]. Both methods utilize regular solution theory (RST) to model the micellization of the amphoteric surfactant. Other models with different approaches have been developed to describe the micellization behavior of pH-sensitive surfactant, but these models are less convenient to use than RST [11-16].

The solution properties of amine oxide surfactants are also affected by the presence of other surfactants [17-25]. The absolute value of the surface potential of mixed micelles can increase when anionic surfactants are added to amine oxide [26]. A pseudophase approximation with the RST approach to model the hydrogen-ion titration of mixed micelles containing a pH-sensitive surfactant and any number of pH-insensitive surfactants has been developed and compared with experimental titration data of a pH-sensitive surfactant with cationic or nonionic surfactants [25].

In this research work, the thermodynamic activities of each surfactant at different pH levels are obtained by a hydrogen ion titration method combined with application of the pseudophase separation model and regular solution theory to describe mixed micellar thermodynamics for the three-surfactant mixture. A mixture of DDAO and SDS at intermediate pH is composed of three components (anionic, cationic, and zwitterionic), which are in different fractions at different solution pH values. The regular solution approximation is generally used to evaluate the synergism in multicomponent surfactant systems. We also address whether a soluble ion-pair between the SDS and protonated DDAO is present in significant concentrations that would affect the apparent pK_a of DDAO or protonation of DDAO in monomer form.

In Part II of this series [27], we utilize the model developed here to predict precipitation phase boundaries for this system and compare to experimental phase boundaries.

3.2 THEORY

Dimethyldodecylamine oxide (DDAO) is an amphoteric surfactant that can exist in the form of cationic or zwitterionic surfactant depending on solution pH. The amine group of DDAO surfactant can protonate in a similar manner to weak acids. Equilibrium of amine oxide protonation can be described by a dissociation constant, K_a;

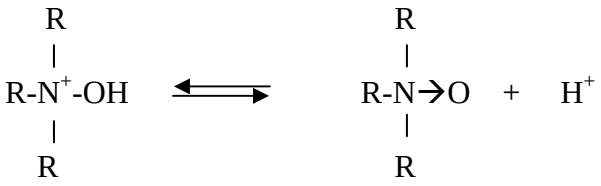

$$K_a = \frac{a_{H^+} a_{a^0}^m}{a_{a^+}^m} \qquad (3.1)$$

where a_{H^+}, $a_{a^0}^m$, and $a_{a^+}^m$ are the activities of the hydrogen ion, the zwitterionic amine oxide ($DDAO^0$), and the protonated amine oxide ($DDAO^+$) monomers, respectively. At the very low concentration at which monomer is present (< 10 mM), the monomer is assumed to behave as an ideal dilute solution following Henry's Law. In this work, we always have swamping electrolyte present, so ionic strength is approximately constant. This means that the added salt (NaCl) concentration is much higher than ionic surfactant and acid or base concentration. The extended Debye-Huckel equation can be used to calculate the activity coefficient of charged ions in solution:

$$\log \gamma_{\pm} = 0.5139 \mid i_i^2 \mid \left\{ \frac{\sqrt{I}}{1+\sqrt{I}} - 0.3I \right\} \qquad (3.2)$$

where $\gamma_{\pm}$ is the average activity coefficient of ionic surfactants given by the Debye-Huckel equation [28]; i_i is the valency number of the charged surfactant. The ionic strength, *I*, is calculated as follow;

$$I = \sum 0.5 C_i \left(i_i\right)^2 \qquad (3.3)$$

where C_i is the molar concentration of charged ions and the sum is overall charged species in solution.

For the two charged surfactants, where i is either a^+ for protonated DDAO or *ds* for anionic dodecyl sulfate:

$$\overline{f}_i^m = \gamma_{\pm} H_i C_i^m \qquad (3.4)$$

where $\overline{f}_i^m$ is the partial fugacity of surfactant i in the monomer phase; H_i is the Henry's law constant; C_i^m is the monomer concentration of surfactant *i*. When a hypothetical unit molarity solution (no added electrolyte) is chosen as the standard state for the monomeric surfactants:

$$f_i^{o,m} = H_i(1M) \qquad (3.5)$$

where $f_i^{o.m}$ is a standard state fugacity of surfactant i in the monomer phase. By definition, the activity of surfactant *i* in the monomer phase, a_i^m, is given by

$$a_i^m = \frac{\overline{f}_i^m}{f_i^{o,m}} \qquad (3.6)$$

By combining Eqs. 3.4-3.6,

$$a_i^m = \gamma_{\pm} C_i^m \qquad (3.7)$$

For hydrogen ion, the partial fugacity of H^+, $\overline{f}_{H^+}$, is defined as:

$$\overline{f}_{H^+} = \gamma_{\pm} H_{H^+} C_{H^+} \qquad (3.8)$$

where H_{H^+} and C_{H^+} are the Henry's law constant and hydrogen ion concentration in the solution. Hydrogen ion in the solution is also treated as an ideal dilute solution and its standard state is a hypothetical unit molarity with no added electrolyte. The standard state fugacity of H^+, $f_{H^+}^o$, is written as:

$$f_{H^+}^o = H_{H^+}(1M) \qquad (3.9)$$

The activity of hydrogen ion, a_{H^+}, is:

$$a_{H^+} = \frac{\overline{f}_{H^+}}{f_{H^+}^o} \qquad (3.10)$$

By combining Eqs. 3.8-3.10,

$$a_{H^+} = \gamma_{\pm} C_{H^+} \qquad (3.11)$$

For the uncharged amine oxide surfactant, $DDAO^0$, the partial fugacity of $DDAO^0$ in monomer, $\overline{f}_{a^0}^{m}$, can be written as:

$$\overline{f}_{a^0}^{m} = H_{a^0} C_{a^0}^{m} \qquad (3.12)$$

where H_{a^0} and $C_{a^0}^{m}$ are the Henry's law constant and $DDAO^0$ concentration in the monomer phase. The activity coefficient of $DDAO^0$ is equal to 1 according to Eq. 3.2. With a hypothetical unit molarity solution as a standard state, the standard state fugacity of $DDAO^0$ in monomer, $f_{a^0}^{o,m}$, is written as:

$$f_{a^0}^{o,m} = H_{a^0}(1M) \qquad (3.13)$$

The activity of $DDAO^0$, a_{a^0}, is:

$$a_{a^0} = \frac{\overline{f}_{a^0}^{m}}{f_{a^0}^{0,m}} \qquad (3.14)$$

By combining Eqs. 3.12-3.14,

$$a_{a^0} = C_{a^0}^{m} \qquad (3.15)$$

Substituting activities of $DDAO^+$, H^+, and $DDAO^0$ from Eqs. 3.7, 3.11, and 3.15 into Eq. 3.1, Eq. 3.1 becomes:

$$K_a = \frac{C_{H^+} C^m_{a^0}}{C^m_{a^+}} \qquad (3.16)$$

where $C^m_{a^+}$ is $DDAO^+$ concentration in the monomer phase. Since activity coefficients described by the Debye-Huckel equation are constant due to swamping electrolyte, they cancel out so they don't appear in Eq. 3.16. One could have defined standard states to avoid the Debye-Huckel correction factor. But in Part II of this series [27], we use the solubility product, K_{SP}, and unlike K_a, its value would depend on standard states, so we use the classically defined ones here so the numerical value of K_{SP} will have the same basis as is common in the literature.

The mole fraction of the amine oxide monomer that is protonated is defined as y_{a^+};

$$y_{a^+} = \frac{C^m_{a^+}}{\left(C^m_{a^+} + C^m_{a^0}\right)} \qquad (3.17)$$

By combining Eqs. 3.16 and 3.17,

$$pK_a = pH + \log\frac{y_{a^+}}{1 - y_{a^+}} \qquad (3.18)$$

The dissociation constant, K_a, is theoretically a true thermodynamic equilibrium constant so it is independent of the total surfactant concentration and pH. Any deviation of the observed pK_a from the thermodynamic pK_a of amine oxide surfactant solution below the CMC can indicate a significant formation of soluble premicellar aggregates (e.g., DDAO/SDS complexes) as observed with a titration of fatty acid at premicellar concentrations [29].

At higher concentration where micelles are present, the dissociation constant of the DDAO in the micelle, pK_{aM}, can be quantified once the composition of DDAO in both protonated and unprotonated forms is known. The calculation of pK_{aM} in Eq. 3.19 is done analogous to that of pK_a in Eq. 3.18 [30].

$$pK_{aM} = pH + \log \frac{x_{a^+}}{1 - x_{a^+}} \qquad (3.19)$$

where x_{a^+} is the mole fraction of $DDAO^+$ to total DDAO (DDAO-only) in the micellar phase.

$$x_{a^+} = \frac{C_{a^+}^M}{\left(C_{a^+}^M + C_{a^0}^M\right)} \qquad (3.20)$$

where $C_{a^+}^M$ and $C_{a^0}^M$ are the concentration of $DDAO^+$ and $DDAO^0$ in the micellar phase, respectively.

The use of the pK_{aM} term has been criticized as not being a true thermodynamic constant because it varies with the degree of protonation in the micelle [9]. However, we find the pK_{aM} to be useful as it indicates how the micellar environment affects the protonation of DDAO compared to that in the monomer [11, 25, 30, 31].

In a solution of an amphoteric surfactant, Rathman and Christian [9] have successfully applied the pseudophase separation model and the integrated form of the Gibbs-Duhem equation written for the surfactant components in the micelle pseudophase along with acid/base titration data to calculate the activities of the two amphoteric surfactant species at concentrations above the CMC. Results from an alternative calculation technique applying the pseudophase separation model and regular solution theory (RST) to describe nonideality in mixed micelle formation gave similar results as the use of the pseudophase separation model Gibbs-Duhem equation in the titration-based method.

Use of the Gibbs-Duhem equation to determine DDAO activities as applied by Rathman et al. [9] in the binary system does not give apparently useful relations for ternary systems as in the current study when SDS is present along with DDAO. So, for more than two surfactant components, it is necessary to assume the validity of a solution thermodynamic model such as RST to describe formation of mixed micelles.

The pseudophase separation model and RST to be applied to the mixed amphoteric-anionic surfactant system is described here. Above the CMC, there is an equilibrium of the surfactant between monomer and micelle forms. The degree of

protonation in the DDAO monomer can be different from that in the micelle. The mass balance of each component can be written as follow.

$$Z_{a^+} * C_t = Y_{a^+}(C^m_{a^+} + C^m_{a^0} + C^m_{ds}) + X_{a^+}(C_t - C^m_{a^+} - C^m_{a^0} - C^m_{ds}) = C^m_{a^+} + X_{a^+} * C_{mic} \quad (3.21)$$

$$Z_{a^0} * C_t = Y_{a^0}(C^m_{a^+} + C^m_{a^0} + C^m_{ds}) + X_{a^o}(C_t - C^m_{a^+} - C^m_{a^0} - C^m_{ds}) = C^m_{a^0} + X_{a^0} * C_{mic} \quad (3.22)$$

$$Z_{ds} * C_t = Y_{ds}(C^m_{a^+} + C^m_{a^0} + C^m_{ds}) + X_{ds}(C_t - C^m_{a^+} - C^m_{a^0} - C^m_{ds}) = C^m_{ds} + X_{ds} * C_{mic} \quad (3.23)$$

so that $Z_{ds} + Z_{a^0} + Z_{a^+} = 1$ (3.24)

where C_t is the total surfactant concentration; Z_{a^+}, Z_{a^0}, and Z_{ds} are the mole fraction of DDAO$^+$, DDAO^0, and SDS in the solution (includes both monomer and micelle forms); Y_{a^+}, Y_{a^0}, and Y_{ds} are the mole fraction of DDAO$^+$, DDAO^0, and SDS, respectively, in monomer form; X_{a^+}, X_{a^0}, and X_{ds} are the micellar mole fraction of DDAO$^+$, DDAO^0, and SDS; respectively. C^m_{ds} is the monomer concentration of SDS; C_{mic} is the total micellar surfactant concentration. Note that capitalized Y_i and X_i are mole fractions of monomers and micelles (surfactant-only basis) including all three surfactants which might be present. Lower case y_i and x_i are surfactant-only monomer and micelle mole fractions based only on DDAO^0 and DDAO$^+$ only since these are used to obtain pK_a and pK_{aM} in Eqs. 3.18 and 3.19.

The pseudophase separation model treats micelles as a separate thermodynamic phase that is in equilibrium with monomer in analogy to liquid in vapor-liquid equilibrium. Hence, the partial fugacities of each surfactant component are equal in the monomer and micellar phases.

$$\bar{f}_i^{\,m} = \bar{f}_i^{\,M} \qquad (3.25)$$

where $\bar{f}_i^{\,M}$ is the partial fugacity of surfactant *i* in the micelle pseudophase.

According to Eq. 3.4, Henry's law is applied to the monomer phase and so the partial fugacity is proportional to the surfactant monomer concentration with the activity coefficient described by the Debye-Huckel equation. For charged surfactant, SDS and $DDAO^+$,

$$\bar{f}_i^{\,m} = \gamma_{\pm} \mathrm{H}_i C_i^m = \gamma_{\pm} \mathrm{H}_i Y_i CMC_m \qquad (3.26)$$

where CMC_m is the mixed CMC at the mixture electrolyte concentration.

For surfactant in the micellar phase, the partial fugacity of surfactant *i*, $\bar{f}_i^{\,M}$, is described by,

$$\bar{f}_i^{\,M} = \gamma_i^M X_i f_i^{o,M} \qquad (3.27)$$

where $f_i^{o,M}$ is a standard state fugacity of surfactant *i* in the micellar phase, and γ_i^M is the activity coefficient of surfactant *i* in the micelle. The standard state in the micellar phase is a pure surfactant *i* micelle at the same temperature and electrolyte concentration as the mixture is at. This standard state micelle is in equilibrium with surfactant *i* monomer at a concentration equal to CMC_i (CMC of pure surfactant at the mixture electrolyte concentration).

$$f_i^{o,M} = \gamma_{\pm} \mathrm{H}_i CMC_i \qquad (3.28)$$

So, $$\bar{f}_i^M = \gamma_i^M X_i \gamma_{\pm} H_i CMC_i \qquad (3.29)$$

Combining Eqs. 3.25, 3.26, and 3.29;

$$C_i^m = Y_i^M CMC_m = \gamma_i^M X_i CMC_i \qquad (3.30)$$

For uncharged surfactant, $DDAO^0$, $\gamma_{\pm}$ is not valid. According to Eq. 3.12 the partial fugacity of $DDAO^0$ in monomer is,

$$\overline{f}_{a^0}^m = H_{a^0} C_{a^o}^m = H_{a^0} Y_{a^0} CMC_m \qquad (3.31)$$

For the fugacity of $DDAO^0$ in the micellar phase, Eq. 3.27 is applied here as well.

$$\bar{f}_{a^0}^{M} = \gamma_{a^0}^{M} X_{a^0} f_{a^0}^{o,M} \qquad (3.32)$$

The standard state of $DDAO^0$ in the micellar phase is a pure $DDAO^0$ micelle at the same temperature and electrolyte concentration as the mixture is at, which is in equilibrium with $DDAO^0$ monomer at a concentration equal to CMC of pure $DDAO^0$ at the mixture electrolyte concentration (CMC_{a^0}). The standard state fugacity of $DDAO^0$, $f_{a^0}^{o,M}$, can be written as:

$$f_{a^0}^{o,M} = H_{a^o} CMC_{a^0} \qquad (3.33)$$

$$\bar{f}_{a^0}^{M} = \gamma_{a^0}^{M} X_{a^0} H_{a^o} CMC_{a^0} \qquad (3.34)$$

Combining Eqs. 3.25, 3.33, and 3.34,

$$C_{a^0}^{m} = Y_{a^0} CMC_m = \gamma_{a^0}^{M} X_{a^0} CMC_{a^0} \qquad (3.35)$$

The monomeric concentration of SDS and $DDAO^+$ can be written according to Eq. 3.30.

$$C_{ds}^{m} = \gamma_{ds}^{M} X_{ds} CMC_{ds} \qquad (3.36)$$

$$C_{a^+}^{m} = \gamma_{a^+}^{M} X_{a^+} CMC_{a^+} \qquad (3.37)$$

where CMC_{a^+} and CMC_{ds} are the CMC values for the pure DDAO$^+$ and SDS (at the mixture electrolyte concentration), respectively; and γ_{ds}^{M}, $\gamma_{a^0}^{M}$, and $\gamma_{a^+}^{M}$ are activities coefficients of SDS, DDAO^0 and DDAO$^+$ in the micelle, respectively;

For the non-ideal mixed micelle, the RST activities coefficients are the same as from the one-parameter Margules equation, where each pairwise interaction between surfactants *i* and *j* is described by an interaction parameter, β_{ij}. In our system where mixture of 3 surfactants is present, RST can be formulated using the interaction parameters introduced by Holland and Rubingh (1983) for multicomponent system [32].

$$\gamma_{ds}^{M} = \exp\left(X_{a^+}^{2} * \beta_{a^+ds} + X_{a^0}^{2} * \beta_{a^0ds} + \left(\beta_{a^+ds} + \beta_{a^0ds} - \beta_{a^+a^0}\right) * X_{a^+} * X_{a^0}\right) \qquad (3.38)$$

$$\gamma_{a^+}^{M} = \exp\left(X_{a^o}^{2} * \beta_{a^+a^0} + X_{ds}^{2} * \beta_{a^+ds} + \left(\beta_{a^+a^0} + \beta_{a^+ds} - \beta_{a^0ds}\right) * X_{a^o} * X_{ds}\right) \qquad (3.39)$$

$$\gamma_{a^0}^{M} = \exp\left(X_{a^+}^{2} * \beta_{a^+a^0} + X_{ds}^{2} * \beta_{a^0ds} + \left(\beta_{a^+a^0} + \beta_{a^0ds} - \beta_{a^+ds}\right) * X_{a^+} * X_{ds}\right) \qquad (3.40)$$

where β_{a^+ds}, β_{a^0ds}, and $\beta_{a^+a^0}$ are binary molecular interaction parameters in the micellar phase for surfactant mixtures of DDAO$^+$-SDS, DDAO^0-SDS, and DDAO$^+$-DDAO^0, respectively.

The binary molecular interaction parameters, β_{ij}, are obtained from experimental CMC data for each pure surfactant and for mixed surfactant solution. For the binary surfactant 1 and surfactant 2 systems, molecular interaction parameter for mixed micelle formation can be found by solving Eqs. 3.41 and 3.42 simultaneously [33];

$$\frac{(X_1)^2 \ln\left(\alpha CMC_m / X_1 CMC_1\right)}{\left(1-X_1\right)^2 \ln\left[(1-\alpha)CMC_m / \left(1-X_1\right)CMC_2\right]} = 1 \qquad (3.41)$$

$$\beta_{12} = \frac{\ln\left(\alpha * CMC_m / X_1 CMC_1\right)}{\left(1-X_1\right)^2} \qquad (3.42)$$

where X_1 and X_2 are micellar mole fraction of surfactants 1 and 2; α is the mole fraction of surfactant 1 in the total surfactant in the solution phase; CMC_1 and CMC_2 are CMC of pure surfactants 1 and 2 at the mixture electrolyte concentration; CMC_m is the mixed CMC at a given value of α.

The β parameter for $DDAO^+$-$DDAO^0$ can also be approximated from a titration of DDAO (in the absence of SDS) using the Gibbs-Duhem equation for surfactant activities in micelles by using the following equation [14];

$$pK_{aM} = pK_M + \left(\frac{2\beta_{a^+a^0}}{\ln 10}\right) x_{a^+} \qquad (3.43)$$

where K_M is the intrinsic dissociation constant on the surface of the micelle. The $\beta_{a^+a^0}$ parameter can be found from a slope of a plot of pK_{aM} vs. x_{a^+}.

Experimental titration data for the ternary surfactant system yields the overall degree of protonation (z_{a^+}) by applying the charge balance equation,

$$z_{a^+} * (C_a) + \left[H^+\right] = \frac{K_W}{\left[H^+\right]} + \left[HCl\right] \qquad (3.44)$$

where z_{a^+} is the mole fraction of $DDAO^+$ in solution (both monomer and micelle) in DDAO-only mole fraction; C_a is the total DDAO-only concentration; $[H^+]$ is the parameter obtained from pH readings and [HCl] is the concentration of HCl added as a titrant in the solution; K_w is the dissociation constant of water (about 10^{-14} at the temperature of study). The concentration of SDS is not included in the equation because the added sulfate does not significantly protonate. Unlike Eq. 3.1, the weak acid dissociation constant calculated from z_{a^+} obtained from Eq. 3.44 is the apparent K_a, not the thermodynamic K_a.

$$pK_{app} = pH + \log \frac{z_{a^+}}{1 - z_{a^+}} \qquad (3.45)$$

where pK_{app} is the apparent pK_a.

If the CMC of each pure surfactant species, molecular interaction parameters in the micellar phase, and initial concentration of total DDAO and SDS are known,

the pH obtained from titration experiment along with the concentration change due to added titrant would yield mole fractions or concentrations of each species in both monomer and micelle forms by solving Eqs. 3.17, 3.18, 3.21-3.23, 3.35-3.40, and 3.44 simultaneously. In part II of this series of papers [27], this information will be combined with solubility product relationships to generate precipitation phase diagrams for DDAO/SDS mixtures, the practical result which is the incentive behind this line of inquiry.

3.3 Experimental

3.3.1 Materials

Dimethyldodecylamine oxide (DDAO) was obtained from Sigma-Aldrich (St. Louis, MO) and used as received. Its purity is greater than 99 %. Sodium dodecyl sulfate (SDS) was obtained from Fisher Scientific (Fair Lawn, NJ) and was subsequently purified by recrystallization with water and ethanol. The NaCl and HCl were from Fisher Scientific (Fair Lawn, NJ) and were used as received. All the solutions were prepared by using deionized water. The pH was measured by using Accumet AR20 pH meter with an Orion combination pH electrode with Ag/AgCl references electrode with dry nitrogen bubbled through the solution at a constant rate.

3.3.2 Methods

3.3.2.1 Critical Micelle Concentration (CMC)

CMC values were determined by using a Wilhelmy plate type tensiometer (Kruss). In all experiments, 0.15 M of NaCl was used as a swamping electrolyte to minimize changes in the ionic strength of the solution. All experiments were controlled at 30 ^{o}C by circulating water through the jacket of the sample holder for the tensiometer.

3.3.2.2 Titration Experiment

All solutions for titration experiments also contained 0.15 M NaCl as a swamping electrolyte. Solutions were prepared and equilibrated at 30 ^{o}C and maintained at this temperature throughout the titration experiment. A known amount of HCl was added to the solution that was moderately stirred with dry nitrogen bubbled through the solution.

3.4 RESULTS AND DISCUSSION

3.4.1 Critical Micelle Concentration and Interaction Parameter

CMC values of DDAO (SDS-free system) at various pH levels were obtained by titration of DDAO above the CMC with application of an integrated form of the Gibbs-Duhem equation [9] and by direct measurement using surface tensions below and above the CMC as shown in Table 3.1. The two methods yield similar CMC values.

At extremely low pH (pH 2-3), the DDAO is fully protonated ($DDAO^+$), while at high pH (pH 10), it is zwitterionic ($DDAO^0$). In the presence of 0.15 M NaCl, the CMC of the $DDAO^+$ and the CMC of $DDAO^0$ were found to be 1.3 and 1.2 mM, respectively. Rathman et al. reported the CMC_+ and CMC_0 to be 2.0 and 1.9 mM at 25 ^oC with 0.06 M of NaBr [9]. The values reported here are smaller because of the higher electrolyte concentration used (0.15 M NaCl).

The CMC values of mixtures of DDAO and SDS at different ratios and pH values were also measured. The CMC of DDAO at intermediate pH is a mixed CMC of $DDAO^+$ and $DDAO^0$. At extreme pH, a mixture of DDAO and SDS would give a binary surfactant system rather than a ternary system. So, the CMC of mixed $DDAO^+$ and SDS was measured at pH 3 to ensure all DDAO is fully protonated; while the CMC of mixed $DDAO^0$ and SDS was measured at pH 9, at which all DDAO is in its zwitterionic form. Ratios of DDAO to SDS were chosen to give isotropic solutions (avoid precipitation) in the pH range studied here. The absence of precipitate was confirmed by the comparison to experimental precipitation phase boundaries [27] and also by direct visual observation. The CMC values of pure and binary surfactant systems were subsequently used in regular solution theory to calculate binary interaction parameters according to Eqs. 3.41 and 3.42. The CMC values of mixed DDAO and SDS at different pH are shown in Table 3.2 and the resulting β_{ij} parameters are shown in Table 3.3.

An increasingly negative β value indicates that the two surfactants have a stronger attractive interaction upon mixing. The smallest β in this solution system is found for the mixture of $DDAO^+$ and $DDAO^0$. The $\beta_{a^+a^0}$ obtained from the measured

CMC is -2.6, which has an absolute value slightly higher than the values reported in other studies [9, 10, 14, 25]. The $\beta_{a^+a^0}$ derived from Eq. 3.43 gives the value of -2.0. In applying the latter method, the CMC of DDAO at intermediate pH levels is not needed.

The β parameters of mixed SDS and DDAO (β_{a^+ds} and β_{a^0ds}) are obtained by measuring the surface tension of mixed SDS and DDAO, pure SDS, and pure DDAO at different pHs. From experimental surface tension of mixed SDS and DDAO at high pH, β_{a^0ds} is -6.61, which is comparable to -7 as reported by Goloub et al. [34]. The values of β for SDS and other zwitterionic surfactants have varied from -2 to -14 [32, 34, 35]. This could be due to the specific interaction between head groups of SDS and zwitterionic surfactants. The β_{a^+ds} was found in a similar manner to β_{a^0ds}, but at low pH so DDAO was fully protonated. The absolute β value is highest in the mixed SDS and $DDAO^+$ due to strong electrostatic attraction between anionic and cationic molecules. The anionic/cationic surfactant β of -12.8 is similar in magnitude to a β of -8.62 for an SDS/dodecylpyridinium chloride micelle also at a 0.15 M NaCl swamping electrolyte condition [36].

3.4.2 Titration Below CMC

For DDAO in the presence of 0.15 M NaCl and no SDS below its CMC, by combining the titration curve with a charge balance equation according to Eq. 3.44 for the fraction of protonated DDAO, a least-squares regression on Eq. 3.18 yields the average pK_a. The pK_a reported here, shown in Fig. 3.1, was 4.9 and independent of

DDAO concentration, which is in good agreement with the values reported elsewhere [4, 5, 9, 17]. The concentration of cationic and zwitterionic DDAO at different pH values can be calculated from Eqs. 3.16-3.18 in the absence of SDS.

Premicellar aggregates of DDAO and SDS may affect the protonation of DDAO. The concentration of DDAO was prepared at 0.001 M and varying concentration of SDS between $1x10^{-7}$ to $5x10^{-5}$ M with 0.15 M NaCl swamping electrolyte. These concentrations are below the CMC of the surfactant mixture so there are no micelles present at the conditions studied here. Data analysis from a titration experiment and calculation were carried out in a similar manner as discussed in the previous paragraph. Figure 3.2 shows that the pK_a remains at around 4.9-5.0, suggesting that there is insignificant amount of premicellar aggregation between DDAO and SDS. The charge balance equation was used to calculate the composition of cationic and zwitterionic DDAO. So the presence of anionic surfactant at a concentration, such that micellization does not occur, does not affect the protonation behavior of DDAO surfactant considerably.

It is shown in Fig. 3.3 that the titration curve does not notably deviate from the theoretical titration curve ($pK_a = 4.9$), except at the very beginning and ending of the titration experiment. Figure 3.4 shows the monomer concentration of DDAO in protonated and deprotonated forms calculated from the titration experiment done for $1x10^{-4}$ M DDAO in the absence and presence of SDS below the mixed CMC. It can be seen that there is no significant effect of SDS on the concentrations of $DDAO^+$ and $DDAO^0$ in monomer form. This, again, verifies that premicellar aggregates of DDAO

and SDS are present at insignificant concentrations or they do not affect the protonation of DDAO.

3.4.3 Titration of Mixtures of DDAO and SDS Above the CMC

Mixed solutions of DDAO and SDS were prepared at concentrations above the mixed CMC with added 0.15 M NaCl. The experimental precipitation phase boundary of DDAO and SDS at 0.15 M NaCl was used as a guideline to select the concentration of the mixture that would be above the CMC and not form precipitate [27]. During the titration experiment, the solution was examined for any evidence of precipitation. The experiment was terminated if precipitation occurred. For the systems above the CMC, the overall degree of protonation of DDAO, z_{a^+}, was calculated directly from Eq. 3.44 by using pH readings and HCl concentrations during the titration. The mole fraction of $DDAO^+$ in both micellar and monomer phases were determined by applying the pseudophase separation model along with regular solution theory described previously. From a titration experiment, pH and concentration of HCl were recorded and input into Eqs. 3.17, 3.18, 3.21-3.24, 3.35-3.40, and 3.44 that were simultaneously solved to yield the monomer-micelle compositions of each surfactant species.

Figure 3.5 shows the degree of protonation of $3x10^{-3}$ M DDAO in the presence of $1x10^{-5}$ M SDS, where the total concentration is above the mixed CMC. As can be seen, the degree of protonation curve of DDAO in micelles almost coincides with the overall degree of protonation, corresponding to the fact that most of the DDAO is in the micellar form at this high concentration. The experimental

monomeric degree of protonation is the same as the theoretical degree of protonation if the pK_a is set at 4.9, indicating that the protonation of DDAO in monomer form is not affected by the presence of anionic surfactant.

The protonation of DDAO in micelles is higher than that in the monomer form at high pH (pH 5.0-8.0) because of the effect of the electrical potential at the surface of the micelle. The concentration of protons in the immediate vicinity of the micelle is higher due to the negatively charged sulfate head groups electrostatically attracting the cationic protons. This higher proton density than in the bulk solution promotes protonation of the micellar DDAO relative to DDAO monomer. As seen in Fig. 3.6, as the x_{a^+} increases (pH decreases), there is a higher fraction of $DDAO^+$ in the micelle than at higher pH that could shield the proton effect by screening the anionic SDS and also repel the proton by its same charge, causing pK_{aM} to decrease. Similar behavior is found in the pK_a shift in the titration of fatty acids solubilized in cationic, nonionic and anionic micelles. The pK_a shifts upwardly if the fatty acid is solubilized in micelles with other anionic surfactants due to high surface charge density [37].

Several titration experiments were carried out for the mixed DDAO-SDS system containing high mole ratio of SDS to DDAO. The overall protonation of DDAO is much higher than the calculated protonation in the monomer phase as seen in Fig. 3.7, which is a titration of 0.0001 M DDAO in the presence of 0.005 M SDS (SDS-rich system) and 0.15 M NaCl. The protonation of DDAO in micelles coincides with the overall protonation. The overall and micellar pK_a of these systems are considerably higher than pK_a of DDAO, which could imply that the high SDS fraction in micellar phases induces the protonation reaction. However, there is a

problem associated with the calculation of monomeric protonation of DDAO because of the very low concentration of DDAO in the monomer phase. The presence of high SDS concentration promotes the formation of mixed micelle with DDAO, so the mixed CMC is extremely low. The amount of DDAO monomer present is too low to obtain an accurate calculation.

In DDAO-alone system, the protonation of micellized DDAO deviates from monomer DDAO because of the interaction between $DDAO^+$ and $DDAO^0$. The value of pK_a is independent of the degree of protonation in the micellar phase, while the value of pK_{aM} depends on the degree of protonation in the micellar phase [25]. From Fig. 3.6, at DDAO-rich compositions, the pK_{aM} is not affected much by the presence of SDS. The pK_{aM} of DDAO in the DDAO-rich system remains approximately the same as the pK_{aM} of DDAO in the DDAO-alone system. Figure 3.8 shows that the monomer concentration of $DDAO^+$ is not affected by the SDS in the system of DDAO-rich composition. However, the monomer concentration of $DDAO^+$ deviates when the solution has high ratio of SDS to DDAO. For SDS-rich compositions, the overall value of pK_{aM} increases. The SDS-rich micelle could have a high negative value of surface potential that draws hydrogen ion and induces the protonation of DDAO. The deviation in the pK_{aM} of DDAO when SDS is present is due to the electrostatic effect as also observed by others. Tokiwa and Ohki found that the deviation of the protonation of DDAO in micelles is positive with anionic surfactant (sodium dodecylpolyoxyethylene sulfate) and negative with cationic surfactant (dodecylpyridinium chloride) [26].

3.5 REFERENCES

1. Porter MR (1994) Handbook of Surfactants, 2nd edn. Blackie Academic & Professional, London. pp. 258
2. Rosen MJ (2004) Surfactants and Interfacial Phenomena, 3rd edn. John Wiley & Sons, Hoboken, New Jersey. pp. 1
3. Herrmann KW (1962) Non-Ionic-Cationic Micellar Properties of Dimethyldodecylamine Oxide. J. Phys. Chem. 66: 295-300
4. Tokiwa F, Ohki K (1966) Potentiometric Titration of a Nonionic-Cationic Surfactant in Aqueous Solution. J. Phys. Chem. 70: 3437-3441
5. Ikeda S, Tsunoda M, Maeda H (1978) The Application of the Gibbs Adsorption Isotherm to Aqueous Solutions of a Nonionic-Cationic Surfactant. J. Colloid Interface Sci. 67: 336-348
6. Ikeda S, Tsunoda M, Maeda H (1979) The Effects of Ionization of Micelle Size of Dimethyldodecylamine Oxide. J. Colloid Interface Sci. 70: 448-455
7. Imae T, Ikeda S (1985) Formation of Rodlike Micelles of Dimethyloleylamine Oxide in Aqueous Solutions: Effects of Addition of Hydrochloric Acid and Sodium Chloride on the Micelle Size and the Intermicellar Interaction. J. Colloid Polym. Sci. 263: 756-766
8. Chang DL, Rosano HL, Woodward AE (1985) Carbon-13 NMR Study of the Effects of pH on Dodecyldimethylamine Oxide Solutions. Langmuir 1: 669-672

9. Rathman JF, Christian SD (1990) Determination of Surfactant Activities in Micellar Solutions of Dimethyldodecylamine Oxide. Langmuir 6: 391-395

10. Zimmerman JA, Schnaare RL (1999) Determination of Amine Oxide Micellar Activities in Nonswamping Electrolytes Solutions. Langmuir 15: 384-390

11. Mille M (1981) Effect of Nearest-Neighbor Interactions on Surface Titrations. J. Colloid Interface Sci. 81: 169-179

12. Maeda H (1988) Electric and Nonelectric Free Energy of Nonionic-Ionic Micelles. J. Phys. Chem. 92: 4490-4498

13. Maeda H (1995) A Simple Thermodynamic Analysis of the Stability of Ionic/Nonionic Mixed Micelles. J. Colloid Interface Sci. 172: 98-105

14. Maeda H (2003) A Thermodynamic Analysis of the Hydrogen Ion Titration of Micelles. J. Colloid Interface Sci. 263: 277-287

15. Lair V, Bouguerra S, Turmine M, Letellier P (2004) Thermodynamic Study of the Protonation of Dimethyldodecylamine N-Oxide Micelles in Aqueous Solution at 298 K. Establishment of a Theoretical Relationship Linking Critical Micelle Concentrations and pH. Langmuir 20: 8490-8495

16. Goldsipe A, Blankschtein D (2006) Molecular-Thermodynamic Theory of Micellization of pH-Sensitive Surfactants. Langmuir 22: 3547-3559

17. Kolp DG, Laughlin RG, Krause FP, Zimmerer RE (1963) Interaction of Dimethyldodecylamine Oxide with Sodium Dodecylbenzenesulfonate in Dilute Solution. J. Phys. Chem. 67: 51-55

18. Rosen MJ, Friedman D, Gross M (1964) A Surface Tension Study of the Interaction of Dimethyldodecylamine Oxide with Potassium Dodecanesulfonate in Dilute Aqueous Solution. J. Phys. Chem. 68: 3219-3225

19. Chang DL, Rosano HL (1984) Structure/Performance Relationships in Surfactants. In: Rosen MJ (ed) ACS Symposium Series 253. American Chemical Society, Washington DC. pp. 129

20. Imae T, Araki H, Ikeda S (1986) The Anomalous Behavior or Surface Tension of Aqueous Solutions of Dimethyloleylamine Oxide and its Multimolecular Adsorption on Aqueous Surfaces. Colloids Surf. 17: 207-219

21. Imae T, Araki H, Ikeda S (1986) The Absorption Spectra and the Micelle Species of Dimethyloleylamine Oxide in Aqueous Solutions. Colloids Surf. 17: 221-228

22. Abe M, Kato K, Ogino K (1989) Effects of Inorganic Electrolytes and of pH on Micelle Formation of Amphoteric-Anionic Mixed Surfactant Systems. J. Colloid Interface Sci. 127: 328-335

23. Weers JG, Rathman JF, Scheuing DR (1990) Structure/Performance Relationships in Long Chain Dimethylamine Oxide/Sodium Dodecylsulfate Surfactant Mixtures. Colloid Polym. Sci. 268: 832-846

24. Imae T, Kakitani M (1996) Electrokinetic Properties of Mixed Solutions of Dodecyldimethylamine Oxide and Sodium Dodecyl Sulfate: Specific Adsorption Effects of Small Ions. Colloid Polym. Sci. 274: 1170-1175

25. Goldsipe A, Blankschtein D (2006) Titration of Mixed Micelles Containing a pH-Sensitive Surfactant and Conventional (pH-insensitive) Surfactants: A Regular Solution Theory Modeling Approach. Langmuir 22: 9894-9904

26. Tokiwa F, Ohki K (1968) Effects of Small Ions and Long-Chain Alkyl Ions on the Potentiometric Behavior of Micelles of Dimethyldodecylamine Oxide. J. Colloid Interface Sci. 27: 247-252

27. Soontravanich S, Scamehorn JF, Harwell JH, Sabatini DA (2007) Interaction Between an Anionic and an Amphoteric Surfactant. Part II Precipitation. Submitted to J. Surfact. Deterg.

28. Davies CW (1962) Ion Association. Butterworths, London. pp. 41

29. Kanicky JR, Shah DO (2003) Effect of Premicellar Aggregation on the pK_a of Fatty Acid Soap Solutions. Langmuir 19: 2034-2038

30. Maeda H, Kakehashi R (2000) Effects of Protonation on the Thermodynamic Properties of Alkyl Dimethylamine Oxides. Adv. Colloid Interface Sci. 88: 275-293

31. Maeda H, Muroi S, Ishii M, Kakehashi R, Kaimoto H, Nakahara T, Motomura K (1995) Effects of Ionization on the Critical Micelle Concentration and the Surface Excess of Dodecyldimethylamine Oxide in Salt Solutions. J. Colloid Interface Sci. 175: 497-505

32. Holland PM, Rubingh DN (1983) Nonideal Multicomponent Mixed Micelle Model. J. Phys. Chem. 87: 1984-1990

33. Rubingh DN (1979) Mixed Micelle Solutions. In: Mittal KL (ed) Solution Chemistry of Surfactants. Plenum Press. pp. 337-354

34. Goloub TP, Pugh RJ, Zhmud BV (2000) Micellar Interactions in Nonionic/Ionic Mixed Surfactant Systems. J. Colloid Interface Sci. 229: 72-81

35. Tajima K, Nakamura A, Tsutsui T (1979) Surface Activity of Complex in Mixed Surfactant Solution. Bull. Chem. Soc. Jpn. 52: 2060-2063

36. Stellner KL, Amante JC, Scamehorn JF, Harwell JH (1987) Precipitation Phemomena in Mixtures of Anionic and Cationic Surfactants in Aqueous Solutions. J. Colloid Interface Sci. 123: 186-200

37. da Silva FLB, Bogren D, Soderman O, Akesson T, Jonsson B (2002) Titration of Fatty Acids Solubilized in Cationic, Nonionic, and Anionic Micelles. Theory and Experiment. J. Phys. Chem. B 106: 3515-3522

Table 3.1 Critical micelle concentration of DDAO in 0.15 M NaCl

pH	CMC (M)	Method
2	$1.3x10^{-3}$	Surface tension measurement
3	$1.3x10^{-3}$	Analysis from hydrogen ion titration
3.5	$1.1x10^{-3}$	Analysis from hydrogen ion titration
4	$9.2x10^{-4}$	Analysis from hydrogen ion titration
4.8	$7.37x10^{-4}$	Analysis from hydrogen ion titration
5	$6.5x10^{-4}$	Surface tension measurement
5	$7.5x10^{-4}$	Analysis from hydrogen ion titration
6.5	$1.1x10^{-3}$	Analysis from hydrogen ion titration
10	$1.2x10^{-3}$	Surface tension measurement

Table 3.2 Critical micelle concentration of mixed DDAO and SDS in 0.15 M NaCl

Ratio of DDAO to SDS	pH	CMC (M)
1:100	9	6.06×10^{-4}
1:10	9	2.75×10^{-4}
1:50	9	4.6×10^{-4}
100:1	3	1.2×10^{-4}
1:100	3	2.02×10^{-4}
1:50	3	1×10^{-4}

Table 3.3 Micellar interaction parameter

β_{a^+ds} ($DDAO^+$-SDS)	-12.8[a]
β_{a^0ds} ($DDAO^0$-SDS)	-6.61[a]
$\beta_{a^+a^0}$ ($DDAO^+$-$DDAO^0$)	-2.6[a]
$\beta_{a^+a^0}$ ($DDAO^+$-$DDAO^0$)	-2.0[b]

[a] Surface tension mesurement

[b] Analysis from titration curve

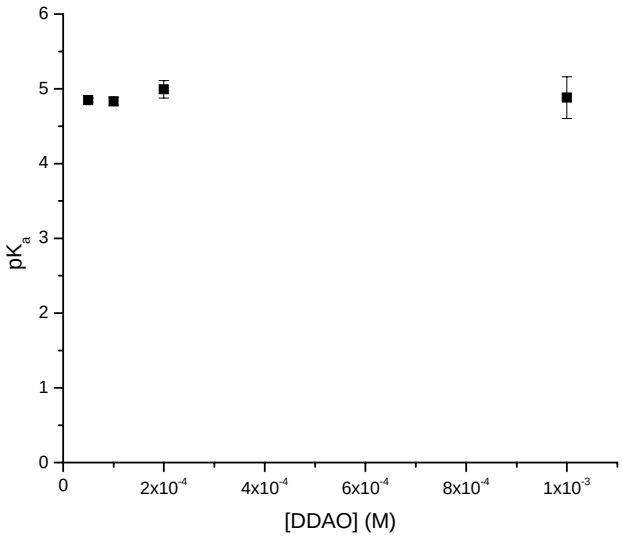

Fig. 3.1 Average pK_a of DDAO at concentrations below CMC

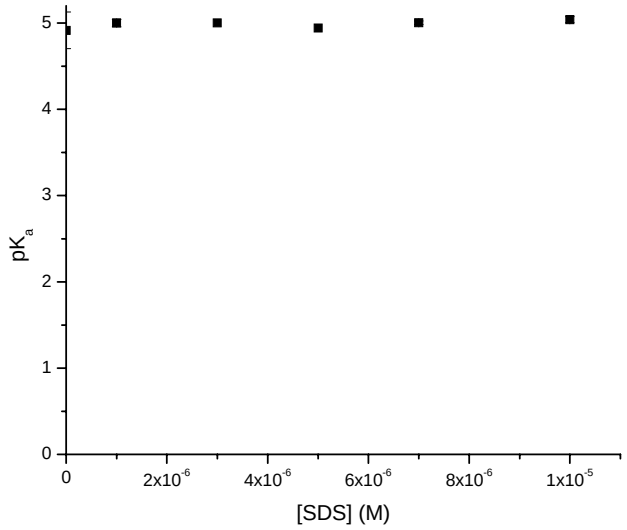

Fig. 3.2 The pK_a of DDAO in the presence of SDS below the mixed CMC at a DDAO concentration of $1x10^{-4}$ M in 0.15 M NaCl

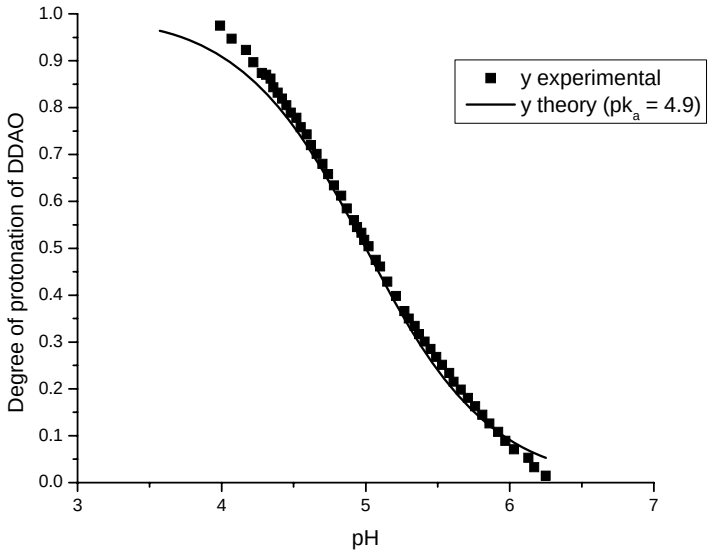

Fig. 3.3 Degree of protonation of $1x10^{-4}$ M DDAO with $1x10^{-6}$ M SDS in 0.15 M NaCl

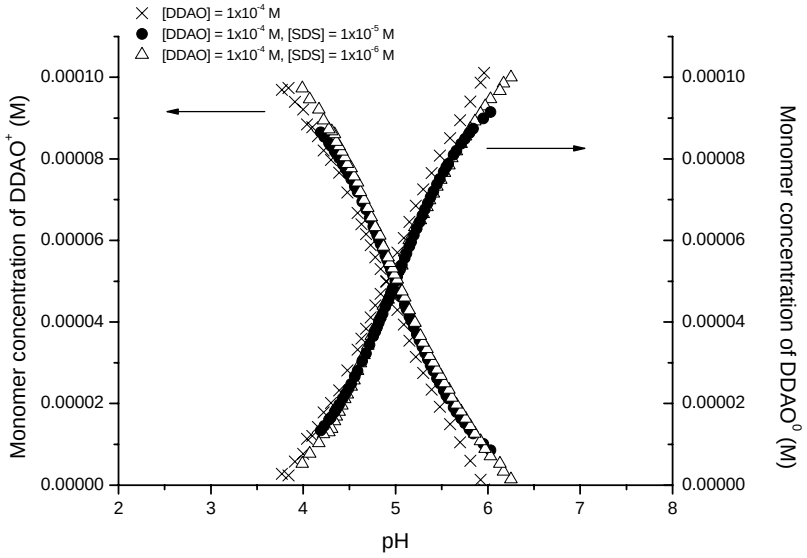

Fig. 3.4 Monomer concentration of $DDAO^+$ and $DDAO^0$ in $1x10^{-4}$ M DDAO in the absence and presence of SDS (concentrations are well below CMC)

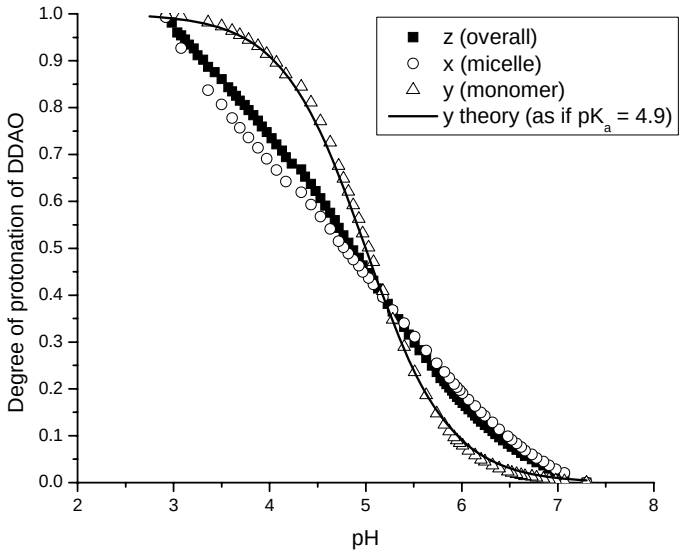

Fig. 3.5 Degree of protonation curve for the titration of $3x10^{-3}$ M DDAO with $1x10^{-5}$ M SDS and 0.15 M NaCl

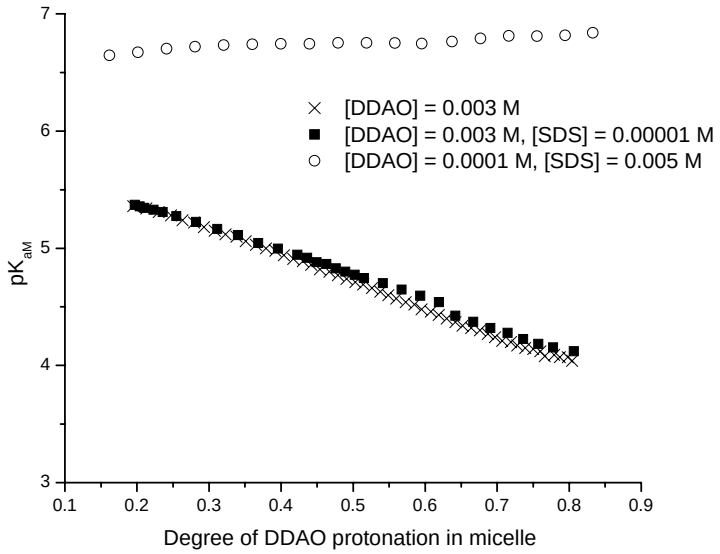

Fig. 3.6 Value of pK_{aM} as a function of degree of $DDAO^+$ protonation in micelle

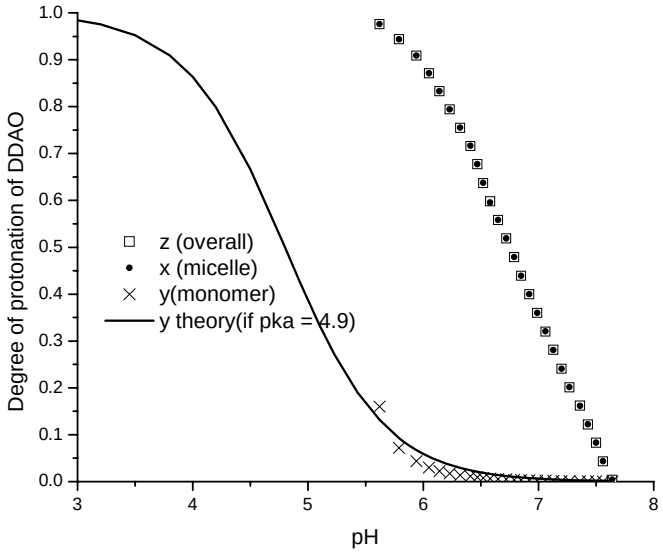

Fig. 3.7 Degree of protonation of $1x10^{-4}$ M DDAO with $5x10^{-3}$ M SDS (SDS-rich system) and 0.15 M NaCl

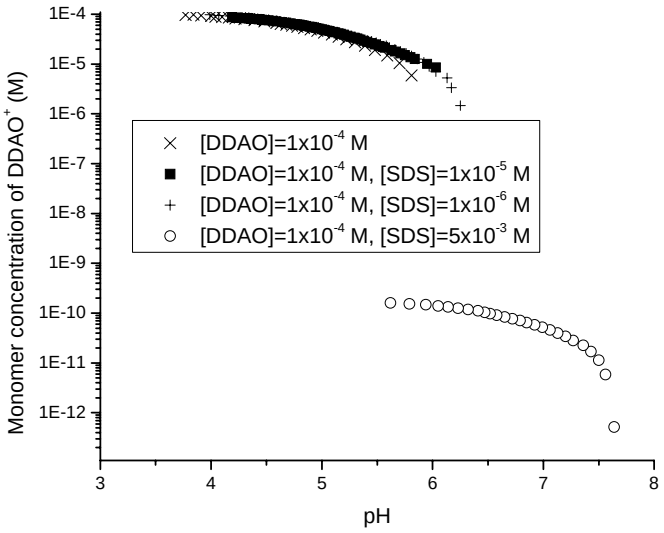

Fig. 3.8 The effect of SDS on the concentration of $DDAO^+$ in monomer phase

CHAPTER 4

Interaction Between an Anionic and an Amphoteric Surfactant.

Part II. Precipitation

Use of amphoteric and anionic surfactants is very common in practical formulations such as shampoos and hand dishwashing products. Precipitation of mixtures of dimethyldodecylamine oxide (DDAO) as an amphoteric surfactant and sodium dodecyl sulfate (SDS) as an anionic surfactant were studied here at different pH levels. The DDAO is a pH-sensitive surfactant and its protonation can be expressed in terms of a pK_a similar to an acid dissociation constant. The protonated form of DDAO carrying a positive charge precipitates with the oppositely charged SDS. Therefore, precipitation phase boundaries are pH dependent due to the varying degree of DDAO protonation. Use of regular solution theory and the pseudophase separation model to describe micellar mixing nonidealities, the precipitate solubility product, the protonation dissociation constant, a model to predict the precipitation phase boundary is presented here. The model agrees with experimental phase boundaries well at different pH levels.

4.1 INTRODUCTION

Surfactant precipitation is an important consideration in applications involving charged surfactants. Precipitation of surfactants can be desirable in some applications such as the recovery stage in surfactant-based separations. However, precipitation can also be detrimental in many applications including detergency, surfactant-based separation processes, and petroleum production using surfactants due to loss of surfactant activity. Ionic surfactants tend to precipitate out with oppositely charged simple ions or with surfactants with opposite charge. In formulation application, when a mixture of opposite charge surfactants is used (e.g. mixture of cationic and anionic surfactants), care must be taken to avoid precipitation. The precipitation of anionic surfactants with various monovalent and divalent cations such as Na^{+}, Ca^{2+}, Mg^{2+} has been extensively studied [1-28]. Precipitation of mixtures of anionic and cationic surfactants has been investigated as well [25, 28-31]. The ability to take advantage of synergistic behavior between oppositely charged surfactants is often limited by their tendency to precipitate. Models to predict the precipitation domains have also been successfully developed for both precipitation of anionic surfactants with metal ions and with cationic surfactants [20, 29, 30]. Those models apply the pseudophase separation model of micelle formation, which treats micelles as a separate thermodynamic phase in equilibrium with monomer, while regular solution theory was used to describe the nonideality in mixed micelle formation. With a known solubility product (K_{SP}) of the precipitating complex, a precipitation phase boundary can be predicted.

Mixed anionic and amphoteric surfactants are often used in formulations of liquid detergents and shampoos. In these formulations, anionic surfactant is added as a main surfactant for cleaning, while amphoteric surfactant is added to serve as a foam booster and for mildness. The mixture of these two surfactants shows strong interaction [32-34]; at certain pH levels, cationic form of amphoteric surfactant can precipitate with anionic surfactant. The ability to take advantage of synergistic behavior between oppositely charged surfactants is often limited by their tendency to precipitate.

In this present work, a model to predict the anionic-amphoteric surfactant precipitation phase boundary is developed and compared to experimental precipitation phase boundaries at different pH levels.

4.2 THEORY

The amphoteric amine oxide surfactant is a cationic surfactant due to a protonation at the amine oxide head group in acidic solution; it is a zwitterionic surfactant due to the net zero charge in the amine oxide head group under alkaline conditions [35]. Therefore, the solution properties of amine oxide surfactants strongly depend on pH [36-41]. The equilibrium between the cationic and zwitterionic surfactant in a solution of dimethyldodecylamine oxide (DDAO) can be expressed by a dissociation constant, K_a;

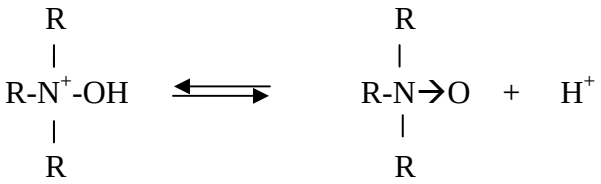

$$K_a = \frac{a_{H^+} a_{a^0}^m}{a_{a^+}^m} \qquad (4.1)$$

where a_{H^+}, $a_{a^0}^m$ and $a_{a^+}^m$ are the activities of the hydrogen ion, the zwitterionic ($DDAO^0$), and the protonated cationic amine oxide ($DDAO^+$) monomers, respectively. According to the previous paper in this series [42], the extended Debye-Huckel can be used to calculate the activity coefficient of charged ions in solution. The ionic strength is considered constant throughout the study since the swamping electrolyte approximation is always valid due to added salt (NaCl) at high concentration compared to ionic surfactant and acid or base concentration in the system.

$$\log \gamma_{\pm} = 0.5139 \,|\, n_i^{\,2} \,|\, \left\{ \frac{\sqrt{I}}{1+\sqrt{I}} - 0.3I \right\} \qquad (4.2)$$

where $\gamma_{\pm}$ is the average activity coefficient given by the extended Debye-Huckel equation outlined by Davies [43]; n_i is the valency number of charged species *i*. The ionic strength, *I*, is calculated as follow;

$$I = \sum 0.5 C_i (n_i)^2 \qquad (4.3)$$

where C_i is the molar concentration of charged species and the sum is overall ions present.

For the charged surfactants, where i represents ionic surfactants (*ds* for anionic dodecyl sulfate; a^+ for protonated DDAO):

$$\overline{f}_i^m = \gamma_{\pm} H_i C_i^m \qquad (4.4)$$

where $\overline{f}_i^m$ is the partial fugacity of surfactant i in monomer phase; H_i is the Henry's law constant, respectively; C_i^m is the monomer concentration of surfactant *i*. When a hypothetical infinite dilution standard state extrapolated to unit molarity (no added electrolyte) is chosen for the monomeric surfactant:

$$f_i^{o,m} = H_i (1M) \qquad (4.5)$$

where $f_i^{o.m}$ is a standard state fugacity of surfactant i in the monomer phase. By convention, activity coefficients are omitted from Eq. 4.5, even though at 1 M, ionic surfactant monomer concentration, from Eqs. 4.2 and 4.5, $\gamma_{\pm}$ can deviate from unity. Of course, the standard state is truly hypothetical since 1 M is far above the CMC of any surfactant, so monomer can't exist at this concentration. Rather, the infinite dilution standard state extrapolates the properties (e.g., partial fugacity) of the

component from infinitely dilute up to the arbitrary concentration or mole fraction of interest. The only reason 1 M is chosen to extrapolate to is that values of K_a (Eq. 4.1) and solubility product or K_{SP} use molarity units for concentration by convention for calculation and we will be consistent with accepted calculated values of these parameters.

The activity of charged surfactant *i* in monomer phase, a_i^m, is given by

$$a_i^m = \frac{\overline{f}_i^m}{f_i^{o,m}} \qquad (4.6)$$

By combining Eqs. 4.4-4.6,

$$a_i^m = \gamma_{\pm} C_i^m \qquad (4.7)$$

For the hydrogen ion, the partial fugacity of H^+, $\overline{f_{H^+}}$, is defined as:

$$\overline{f_{H^+}} = \gamma_{\pm} H_{H^+} C_{H^+} \qquad (4.8)$$

where H_{H^+} and C_{H^+} are the Henry's law constant and hydrogen ion concentration in the solution, respectively. Hydrogen ion in solution is also treated as an ideal dilute solution and its standard state is a hypothetical infinite dilution extrapolated to unit

molarity with no added electrolyte. The standard state fugacity of H^+, $f^o_{H^+}$, is written as:

$$f^o_{H^+} = H_{H^+}(1M) \qquad (4.9)$$

The activity of the hydrogen ion, a_{H^+}, is:

$$a_{H^+} = \frac{\overline{f}_{H^+}}{f^0_{H^+}} \qquad (4.10)$$

By combining Eqs. 4.8-4.10,

$$a_{H^+} = \gamma_{\pm} C_{H^+} \qquad (4.11)$$

For the uncharged amine oxide surfactant, $DDAO^0$, the partial fugacity of $DDAO^0$ in the monomer, $\overline{f}^m_{a^0}$, can be written as:

$$\overline{f}^m_{a^0} = H_{a^0} C^m_{a^o} \qquad (4.12)$$

where H_{a^0} and $C^m_{a^0}$ are the Henry's law constant and $DDAO^0$ concentration in the monomer phase. There is no activity coefficient in Eq. 4.12 since $DDAO^0$ has no net charge. With a hypothetical infinite dilution standard state extrapolated to unit

molarity solution, the standard state fugacity of $DDAO^0$ in monomer, $f_{a^0}^{o,m}$, is written as:

$$f_{a^0}^{0,m} = H_{a^0}(1M) \qquad (4.13)$$

The activity of $DDAO^0$, a_{a^0}, is:

$$a_{a^0} = \frac{\overline{f}_{a^0}^{m}}{f_{a^0}^{0,m}} \qquad (4.14)$$

By combining Eqs. 4.12-4.14,

$$a_{a^0} = C_{a^0}^{m} \qquad (4.15)$$

Substituting activities of $DDAO^+$, H^+, and $DDAO^0$ from Eqs. 4.7, 4.11, and 4.15 into Eq. 4.1:

$$K_a = \frac{C_{H^+} C_{a^0}^{m}}{C_{a^+}^{m}} \qquad (4.16)$$

where $C_{a^+}^{m}$ is $DDAO^+$ concentration in the monomer phase. Since the definition of activities of surfactant monomer and hydrogen ion has been defined with standard

state fugacities in a unit of molarity, the concentrations in Eq. 4.16 must also be in units of molarity as the activities are dimensionless and so is K_a. It is interesting to note that the activity coefficients cancel each other and do not appear in Eq. 4.16, so the specific correlation used for $\gamma_{\pm}$ does not affect K_a.

The mole fraction of the amine oxide monomer that is protonated is defined as y_{a^+};

$$y_{a^+} = \frac{C^m_{a^+}}{\left(C^m_{a^+} + C^m_{a^0}\right)} \qquad (4.17)$$

By combining Eqs. 4.16 and 4.17,

$$pK_a = pH + \log\frac{y_{a^+}}{1 - y_{a^+}} \qquad (4.18)$$

The pK_a of dodecyl dimethylamine oxide (DDAO) is around 4.9, which is a true thermodynamic pK_a [37, 38, 42, 44]. The pK_a indicates the dissociation of DDAO in monomer form so it is appropriate to use this value in Eqs. 4.17 and 4.18 to obtain the monomer concentration of $DDAO^+$ and $DDAO^0$ since only surfactant monomer can cause precipitation. Since the degree of dissociation of the DDAO is different in the mixed micelles than monomer, the apparent pK_a or the micellar pK_a (pK_{aM}) differs from the pK_a in Eq. 4.18. As discussed in detail in part I of this

series [42], in our model, this is accounted for by the modeling of nonideal mixing in the micelles above the CMC.

When a dilute aqueous solution contains anionic and amphoteric surfactants, it is in fact a ternary system consisting of anionic, cationic, and nonionic monomers. Anionic and cationic monomers can associate due to charge attraction and precipitate out if the solubility product is reached. Upon an increase in surfactant concentration, mixed micelles of these surfactants form. In this ternary system consisting of anionic and amphoteric surfactants, there are three simultaneous equilibrium, which must be satisfied: monomer-micelle, monomer-precipitate, and protonated-unprotonated amine oxide. The schematic equilibria are shown in Fig. 4.1.

Zwitterionic surfactant ($DDAO^0$) is present in monomer and micelle forms, while cationic ($DDAO^+$) and anionic surfactants exist in monomer, micelle, and precipitate. The counterions, which are excluded from the diagram, can bind to the micelle or stay unbound in bulk solution. Precipitation of anionic and cationic with their counterions is disregarded due to their very high K_{SP} when compared to K_{SP} of the anionic and cationic surfactant pairs under conditions used here (e.g. solid sodium dodecyl sulfate will not precipitate).

Precipitation of monomer is described by:

$$DS^-(aq) + DDAO^+(aq) \rightleftharpoons DS\text{-}DDAO(s)$$

where DS-DDAO represents the solid precipitate formed from a 1:1 stoichiometric ratio between dodecyl sulfate (DS^-) and protonated DDAO ($DDAO^+$). The activity based solubility product for this reaction can be expressed as,

$$K_{SP} = a_{ds}^{m} a_{a^+}^{m} \qquad (4.19)$$

where a_{ds}^{m} and $a_{a^+}^{m}$ are the activities of the SDS and $DDAO^+$ in the monomer phase. The activities of SDS and $DDAO^+$ in monomer form can be expressed according to Eq. 4.7 as;

$$a_{ds}^{m} = \gamma_{\pm} C_{ds}^{m} \qquad (4.20)$$

and $$a_{a^+}^{m} = \gamma_{\pm} C_{a^+}^{m} \qquad (4.21)$$

where C_{ds}^{m} is the monomer concentration of anionic SDS. Substitute Eqs. 4.20 and 4.21 into 4.19;

$$K_{SP} = C_{ds}^{m} C_{a+}^{m} \gamma_{\pm}^{2} \qquad (4.22)$$

All solutions studied here contained 0.15 M of NaCl as a swamping electrolyte so that the ionic strength and CMC of each single surfactant is assumed to be constant. The swamping electrolyte thus simplifies the model because the

concentration of counterions from added surfactant or acid and base in adjusting the pH is insignificant compared to the swamping NaCl.

If the swamping electrolyte approximation were not valid, it would be necessary to model the counterion binding on micelles (for example see [45, 46]) in order to estimate the unbound counterion concentrations which affect ionic surfactant CMC values [47, 48].

On a precipitation phase boundary, there is an infinitesimal amount of solid precipitate present, so all the surfactant is either present as monomer or as micelles. The solubility product equation requires the monomer concentration of precipitating surfactants from a material balance on each surfactant:

$$C_{ds} = C_{ds}^{m} + C_{ds}^{M} \qquad (4.23)$$

$$C_{a^+} = C_{a^+}^{m} + C_{a^+}^{M} \qquad (4.24)$$

$$C_{a^0} = C_{a^0}^{m} + C_{a^0}^{M} \qquad (4.25)$$

where C_{ds}, C_{a^+}, and C_{a^0} represent the total concentration of SDS, $DDAO^+$, and $DDAO^0$, respectively; C_{ds}^{M}, $C_{a^+}^{M}$, and $C_{a^0}^{M}$, are micellar concentration of SDS, $DDAO^+$, and $DDAO^0$, respectively. The total concentration of DDAO (C_a), which includes DDAO in monomer and micelle, in the solution can be written as;

$$C_a = C_{a^+} + C_{a^0} \qquad (4.26)$$

The pseudophase separation model is used to treat the monomer and micelle as separate thermodynamic phases, which are in equilibrium. The partial fugacities are then the same for each surfactant component in the monomer and micellar phases. The full detailed derivation is shown in the first paper of this series [42].

$$\bar{f}_i^m = \bar{f}_i^M \qquad (4.27)$$

where $\bar{f}_i^M$ is the partial fugacity of micellar surfactant *i*.

The partial fugacity of monomer surfactant is proportional to the surfactant monomer concentration with the activity coefficient given by the extended Debye-Huckel equation as shown in Eq. 4.2. For charged surfactant, SDS and $DDAO^+$,

$$\bar{f}_i^m = \gamma_{\pm} \mathrm{H}_i C_i^m = \gamma_{\pm} \mathrm{H}_i Y_i CMC_m \qquad (4.28)$$

where Y_i is the surfactant-only based mole fraction of monomeric surfactant *i* in the solution and CMC_m is the mixed CMC.

For surfactant in the micellar phase, the partial fugacity of surfactant *i*, $\bar{f}_i^M$, is described by,

$$\bar{f}_i^M = \gamma_i^M X_i f_i^{o,M} \qquad (4.29)$$

where $f_i^{o,M}$ is a standard state fugacity of surfactant *i* in the micellar phase, γ_i^M is the activity coefficient of surfactant *i* in the micelle, and X_i is the surfactant-only mole fraction of surfactant *i* in micellar form. The standard state in the micellar phase is a pure surfactant *i* micelle at the same temperature and electrolyte concentration as the mixture is at. This standard state micelle is in equilibrium with surfactant *i* monomer at a concentration equal to CMC_i, which is the CMC of pure surfactant *i*.

$$f_i^{o,M} = \gamma_{\pm} \mathrm{H}_i CMC_i \qquad (4.30)$$

So, $\bar{f}_i^M = \gamma_i^M X_i \gamma_{\pm} H_i CMC_i \qquad (4.31)$

Combining Eqs. 4.27, 4.28 and 4.31;

$$C_i^m = Y_i CMC_m = \gamma_i^M X_i CMC_i \qquad (4.32)$$

For uncharged surfactant, $DDAO^0$, $\gamma_{\pm}$ is omitted from the partial fugacity calculation. According to Eq. 4.12 the partial fugacity of $DDAO^0$ in monomer is,

$$\bar{f}_{a^0}^m = H_{a^0} C_{a^o}^m = H_{a^0} Y_{a^0} CMC_m \qquad (4.33)$$

where Y_{a^0} is the surfactant-only based mole fraction of $DDAO^0$ in the monomer phase.

For the fugacity of $DDAO^0$ in the micellar phase, $\bar{f}_{a^0}^{M}$, Eq. 4.29 is applied;

$$\bar{f}_{a^0}^{M} = \gamma_{a^0}^{M} X_{a^0} f_{a^0}^{o,M} \qquad (4.34)$$

where $\gamma_{a^0}^{M}$ is the activity coefficient of $DDAO^0$ in the micellar phase, X_{a^0} is the surfactant-only micellar mole fraction of $DDAO^0$, and $f_{a^0}^{o,M}$ is the standard state fugacity of $DDAO^0$ in the micellar phase.

The standard state of $DDAO^0$ in the micellar phase is a pure $DDAO^0$ micelle at the same temperature and electrolyte concentration as the mixture is at, which is in equilibrium with $DDAO^0$ monomer at a concentration equal to the CMC of pure $DDAO^0$. The standard state fugacity of $DDAO^0$ in the micellar phase, $f_{a^0}^{o,M}$, can be written as:

$$f_{a^0}^{o,M} = H_{a^o} CMC_{a^0} \qquad (4.35)$$

where CMC_{a^0} is the CMC of pure $DDAO^0$. Combining Eqs. 4.27, and 4.33-4.35,

$$C_{a^0}^{m} = Y_{a^0} CMC_m = \gamma_{a^0}^{M} X_{a^0} CMC_{a^0} \qquad (4.36)$$

The monomer and micellar compositions of SDS and $DDAO^+$ can be written according to Eq. 4.32.

$$C_{ds}^{m} = \gamma_{ds}^{M} X_{ds} CMC_{ds} \qquad (4.37)$$

$$C_{a^+}^{m} = \gamma_{a^+}^{M} X_{a^+} CMC_{a^+} \qquad (4.38)$$

where CMC_{a^+} and CMC_{ds} are the CMC of pure $DDAO^+$ and SDS, respectively.

In applying regular solution theory to three-component system, the pairwise interaction parameters with mixing rules for three component interactions are used [49]. These molecular interaction parameters can be obtained from independent experimental data CMC of each pure surfactant and binary mixed surfactant solution using well known procedures [50].

The model is intended to predict the concentration of DDAO that causes precipitation with specified concentrations of SDS and at a specific pH. If the CMC of each pure surfactant, pK_a, K_{SP} of $DDAO^+$-SDS, and the three binary molecular interaction parameters in the micellar phase are known, the concentration of DDAO causing precipitation at defined concentrations of SDS can be calculated by solving Eqs. 4.2, 4.3, 4.17, 4.18, 4.22-4.25, and 4.36-4.38 simultaneously. As will be seen, the shape of the precipitation phase boundary can yield two values of the DDAO concentration, both of which are physically possible, representing the two sides of the phase diagram.

4.3 EXPERIMENTAL

4.3.1 Materials

Sodium dodecyl sulfate (SDS) was obtained from Fisher Scientific (Fair Lawn, NJ) with purity greater than 99%. It was further purified by recrystallizing twice by water and methanol, respectively and dried under vacuum. N,N-Dimethyldodecyl amine N-oxide (DDAO), an amphoteric surfactant, was purchased from Sigma-Aldrich (St. Louis, MO) and was used as received. Sodium chloride (NaCl) (certified A.C.S.) was from Fisher Scientific (Fair Lawn, NJ) and was used as received. Sodium hydroxide (NaOH) and hydrochloric acid (HCl) from Fisher Scientific (Fair Lawn, NJ) were used to adjust the pH of the solutions. Double deionized water was used in all experiments.

4.3.2 Methods

4.3.2.1 Precipitation Phase Boundary

A series of samples was prepared by mixing stock solutions of surfactants. All solutions contained 0.15 M NaCl as a swamping electrolyte. The pH of the solutions was adjusted using standard solutions of HCl and NaOH. The pH was measured using an Accumet AR20 pH/Conductivity meter (Fisher Scientific). Dry nitrogen gas was supplied during pH adjustment to prevent acid formation from dissolved CO_2. The samples were first forced to precipitate at low temperature to avoid supersaturation and then kept in a temperature-controlled water bath at 30 ^{o}C while periodically

shaken to ensure equilibrium. Detection of the presence of crystals was made after at least 4 days of storage and observation continued for longer periods of time if needed. The presence of precipitate in the samples was detected visually by the reflection of light when a high-intensity beam of light was shone through the sample in a dark room. The initial surfactant composition was considered to be inside the precipitation phase boundary if the precipitate was observed after equilibration. The average of the two nearest concentrations on either side of the phase boundary of the surfactant being varied is the reported datum on the phase boundary.

4.4 RESULTS AND DISCUSSION

4.4.1 Determination of K_{SP} and Experimental Precipitation Phase Boundary

The solubility product, K_{SP}, can be obtained from the precipitation phase boundary measured in the absence of micelles or below the CMC at a low pH where essentially all the DDAO is protonated. A series of DDAO and SDS solutions at different concentrations with 0.15 M NaCl was made. The pH of the solution was adjusted to 3 in order to fully protonate the DDAO. The solutions were checked for precipitation and the data was plotted according to the procedure mentioned earlier. Equation 4.22 can be rearranged to give,

$$\log C_{a^+}^m = -\log C_{ds}^m + \log\left(\frac{K_{SP}}{\gamma_{\pm}^2}\right) \qquad (4.39)$$

where $C_{a^+}^m$ and C_{ds}^m are the total concentration of $DDAO^+$ and SDS under these conditions. If $\log C_{a^+}^m$ vs. $\log C_{ds}^m$ are plotted, the best fit of a line with a slope of -1, yields the K_{SP} according to Eq. 4.39 as shown in Fig. 4.2. The average K_{SP} is found to be 1.44 x 10^{-10} M^2. The K_{SP} for this system is comparable to the value of 2.24 x 10^{-10} M^2, which was obtained for the precipitation of SDS and dodecylpyridinium chloride (DPCl) in 0.15 M NaCl and at 30 ^oC [29].

The precipitation phase boundaries over a broad concentration range from pH 4.6 to 6.0 are shown in Fig. 4.3. There are three branches to each of the phase boundaries. At low concentrations of both surfactants, the system is below the CMC as can be confirmed by calculating the minimum concentration of one surfactant at a given concentration of the second surfactant to form micelles using the equations in the theory section. This calculated surfactant concentration is above that on the precipitation phase boundary for the linear region of the boundary on the lower left side in Fig. 4.3; i.e., precipitation occurs before micelles can form. As the SDS concentration increases, eventually the calculated DDAO to form micelles equals that to cause precipitation and at higher SDS concentrations, micelles and precipitate simultaneously exist along the anionic-micelle enriched branch in Fig. 4.3. At high DDAO concentrations, in analogy, there is the cationic-micelle enriched branch shown in Fig. 4.3. This shape of the precipitation phase boundary is typical of anionic-cationic surfactant systems [29, 51, 52] and anionic-cationic-nonionic surfactant systems [30]. In Fig. 4.3, the precipitation phase boundary shrinks as pH increases.

4.4.2 Precipitation Phase Boundary Model and Comparison to Data

Parameters used in the model to predict the precipitation phase boundary in the system of SDS and DDAO at various pH are summarized in Table 4.1. The K_{SP} was obtained from this study as already discussed while all other parameters were obtained from the first paper in this series [42] which addressed protonation and monomer-micelle equilibrium. In that paper, it was shown that premicellar aggregation (e.g., ion-pair formation) is insignificant in this system, so that phenomenon does not need to be included in the model.

Predicted precipitation phase boundaries are shown in Fig. 4.4 and compared with experimental precipitation phase boundaries obtained experimentally in Figs. 4.5-4.7 at different pH levels. In Fig. 4.4, the predicted precipitation phase is larger as pH decreases as also qualitatively seen in Fig. 4.3 for experimental phase diagrams. As pH increases, the fraction of DDAO which is protonated decreases. As a result, below the CMC, the precipitation region decreases both theoretically and experimentally (Fig. 4.4 and 4.3, respectively). Above the CMC, the decreased degree of protonation with increasing pH reduces the synergism or negative degree of ideality of mixing for micelle formation as indicated by the zwitterionic DDAO having a less negative β (-6.61) compared to the cationic DDAO β (-12.88) with the SDS (see Table 4.1). This results in higher monomer concentrations of the surfactants $DDAO^+$ and SDS than for more nonideal mixed micelles, thereby enhancing the tendency to precipitate. These two offsetting tendencies with increasing pH help explain why the cationic-rich micelle branch of the precipitation phase diagram shows little pH dependence theoretically or experimentally in Figs. 4.4 and 4.3. In

fact, the micelle nonideality effect is greater than the protonation of monomer effect at the highest DDAO concentrations studied accounting for the slightly enlarged precipitation phase boundary at the lowest pH on the cationic-enriched micelle arm of the curve in Fig. 4.4.

In general, there is only slight deviation in the predicted precipitation phase boundary from the experimental precipitation phase boundary (Figs. 4.5-4.7). Deviation in the predicted phase boundary from the experimental precipitation phase boundary is also reported in the system SDS and dodecylpyridinum chloride (DPCl) [29, 30]. In their work, most of the deviation was observed in the anionic-rich region of the precipitation phase boundary and the formation of coacervate was proposed as a cause of deviation [29]. However, in this same system with added nonionic surfactant, Shiau et al. (1994) proposed that the deviation is rather a formation of a stable dispersion of microcrystals since the deviation was observed without coacervation. It has been found that SDS can adsorb onto precipitate particles and the dispersion can be destabilized by adding electrolyte to suppress the electrical double layer and hence reduce the electrostatic repulsion between particles [30, 53]. In our system, coacervate formation has not been observed. In addition, the slight deviation observed in this study is found only in the amphoteric-rich region as can be seen in Figs. 4.5-4.7 so the stable dispersion because of adsorbed SDS onto microcrystals is evidently not the cause of the deviation found here. The model predicts precipitation phase boundary well in SDS-rich region. At high ratio of zwitterionic surfactant, the protonated amine oxide can have a very strong interaction with anionic SDS resulting in less monomer to precipitate out so it is hard to experimentally determine the

existence of precipitate in those solutions, so the measured phase boundary is less accurate in this region.

The reason that pH levels below 4.6 or above 6.0 where not modeled here is that the numerous equation required simultaneous solution exhibited severe convergence problems outside this range. The pH range covered corresponded to monomer degree of protonation varying from 7.4 % to 66.6 %, so the essential features of the model results are described. We believe that there is not a problem with the existence of a physically reasonable phase boundary at extreme pH levels, just a numerical solution limitation. This model could be extended to include additional surfactant components, multiple precipitating species, a non-swamping electrolyte, etc. in a straightforward fashion.

4.5 REFERENCES

1. Miyamoto S (1960) The Effect of Metallic Ions on Surface Chemical Phenomena. III. Solubility of Various Metal Dodecyl Sulfates in Water. Bull. Chem. Soc. Jpn. 33: 371-375
2. Hato M, Shinoda K (1973) Krafft Points of Calcium and Sodium Dodecylpoly(oxyethylene) Sulfates and Their Mixtures. J. Phys. Chem. 77: 378-381
3. Clarke DE, Lee RS, Robb ID (1976) Precipitation of Calcium Salts of Surfactants. Faraday Disc. Chem. Soc. 61: 165-74
4. Shinoda K, Tsuyoshi H (1977) Ionic Surfactants Applicable in the Presence of Multivalent Cations. Physicochemical Properties. J. Phys. Chem. 81: 1842-1845
5. Bozic J, Krznaric I, Kallay N (1979) Precipitation and Micellization of Silver, Copper, and Lanthanum Dodecyl Sulfates in Aqueous Media. Colloid Polym. Sci. 257: 201-205
6. Lee RS, Robb ID (1979) Precipitation of Calcium Surfactants. Part 2. J. Chem. Soc. Faraday Trans. 1 75: 2116-2125
7. Peacock JM, Matijevic E (1980) Precipitation of Alkylbenzene Sulfonates with Metal Ions. J. Colloid Interface Sci. 77: 548-554
8. Celik MS, Manev ED, Somasundaran P (1982) Sulfonate Precipitation-Redissolution-Reprecipitation in Inorganic Electrolytes. AIChE Symp. Ser. 78: 86-96

9. Chiu Y (1982) Relationship of Oil Recovery Activity to Surfactant Aggregate Size in Petroleum Sulfonate Solutions. In: Mittal KL (ed) Solution Behav. Surfactants: Theor. Appl. Aspects, [Proc. Int. Symp.]. Plenum Press, New York. pp. 1415-1440

10. Baviere M, Bazin B, Aude R (1983) Calcium Effect on the Solubility of Sodium Dodecyl Sulfate in Sodium Chloride Solutions. J. Colloid Interface Sci. 92: 580-583

11. Chou SI, Bae JH (1983) Surfactant Precipitation and Redissolution in Brine. J. Colloid Interface Sci. 96: 192-203

12. Gerbacia WEE (1983) Calcium Dodecyl Sulfate Precipitation from Solutions containing Sodium Chloride. J. Colloid Interface Sci. 93: 556-559

13. Somasundaran P, Ananthapadmanabhan KP, Celik MS, Manev ED (1984) A Thermodynamic Model of Redissolution of Calcium Sulfonate Precipitates in Sodium Chloride Solutions. Soc. Pet. Eng. J. 24: 667-676

14. Cox MF, Matheson KL (1985) Interactions between Linear Alkylbenzenesulfonates and Water Hardness Ions. II. Reducing Hardness Sensitivity by the Addition of Micelle Promotion Agents. J. Am. Oil Chem. Soc. 62: 1396-1399

15. Kallay N, Pastuovic M, Matijevic E (1985) Solubility and Enthalpy of Precipitation of Magnesium, Calcium, Strontium, and Barium Dodecyl Sulfates. J. Colloid Interface Sci. 106: 452-458

16. Matheson KL, Cox MF, Smith DL (1985) Interactions between Linear Alkylbenzene Sulfonates and Water Hardness Ions. I. Effect of Calcium Ion

on Surfactant Solubility and Implications for Detergency Performance. J. Am. Oil Chem. Soc. 62: 1391-1396

17. Matheson KL (1985) Detergency Performance Comparison between LAS and ABS using Calcium Sulfonate Precipitation Boundary Diagrams. J. Am. Oil Chem. Soc. 62: 1269-1274

18. Noik C, Baviere M, Defives D (1987) Anionic Surfactant Precipitation in Hard Water. J. Colloid Interface Sci. 115: 36-45

19. Fan XJ, Stenius P, Kallay N, Matijevic E (1988) Precipitation of Surfactant Salts II. The Effect of Nonionic Surfactants on Precipitation of Calcium Dodecyl Sulfate. J. Colloid Interface Sci. 121: 571-578

20. Stellner KL, Scamehorn JF (1989) Hardness Tolerance of Anionic Surfactant Solutions. I. Anionic Surfactant with Added Monovalent Electrolyte. Langmuir 5: 70-77

21. Stellner KL, Scamehorn JF (1989) Hardness Tolerance of Anionic Surfactant Solutions. 2. Effect of Added Nonionic Surfactant. Langmuir 5: 77-84

22. Rodriguez CH, Chintanasathien C, Scamehorn JF, Saiwan C, Chavadej S (1998) Precipitation in Solutions containing Mixtures of Synthetic Anionic Surfactant and Soap. I. Effect of Sodium Octanoate on Hardness Tolerance of Sodium Dodecyl Sulfate. J. Surfact. Deterg. 1: 321-328

23. Burckett St Laurent J, Connor D, Cripe T, Kott K, Scheibel J, Stidham R, Reilman R (2000) Improved Alkyl Benzene Surfactants: Molecular Design and Solution Physical Chemical Properties. In: 5th World Surfactants

Congress, CESIO 2000: Proceedings. Milan, Italy. Federchimica Assobase-P.I.T.I.O. pp. 716

24. Kott KL, Gederle TW, Baillely, Scheibel JJ, Lawson RJ (2001) Proceedings of New Horizons: Detergents for the New Millennium. AOCS Press, Champaign, Illinois. Ch. 11

25. Rodriguez CH, Lowery LH, Scamehorn JF, Harwell JH (2001) Kinetics of Precipitation of Surfactants. I. Anionic Surfactants with Calcium and with Cationic Surfactants. J. Surfact. Deterg. 4: 1-14

26. Rodriguez CH, Scamehorn JF (2001) Kinetics of Precipitation of Surfactants. II. Anionic Surfactant Mixtures. J. Surfact. Deterg. 4: 15-26

27. Rodriguez CH, Yuan WL, Scamehorn JF, O'Rear EA (2002) Kinetics of Precipitation of Surfactants. III. Atomic Force Microscopy of Precipitate Crystals. J. Surfact. Deterg. 5: 269-280

28. Scamehorn JF, Harwell JH (2004) Precipitation of Surfactant Mixtures. In: Abe M, Scamehorn JF (eds) Mixed Surfactant Systems 2nd edn. Marcel Dekker, New York. pp. 601-655

29. Stellner KL, Amante JC, Scamehorn JF, Harwell JH (1987) Precipitation Phemomena in Mixtures of Anionic and Cationic Surfactants in Aqueous Solutions. J. Colloid Interface Sci. 123: 186-200

30. Shaiu BJ, Harwell JH, Scamehorn JF (1994) Precipitation of Mixtures of Anionic and Cationic Surfactants III. Effects of Added Nonionic Surfactant. J. Colloid Interface Sci. 167: 332-345

31. Mehreteab A (1999) Anionic-Cationic Surfactant Mixtures. In: Broze G Handbook of Detergents, Part A: Properties. Marcel Dekker. pp. 133-155

32. Kolp DG, Laughlin RG, Krause FP, Zimmerer RE (1963) Interaction of Dimethyldodecylamine Oxide with Sodium Dodecylbenzenesulfonate in Dilute Solution. J. Phys. Chem. 67: 51-55

33. Rosen MJ, Friedman D, Gross M (1964) A Surface Tension Study of the Interaction of Dimethyldodecylamine Oxide with Potassium Dodecanesulfonate in Dilute Aqueous Solution. J. Phys. Chem. 68: 3219-3225

34. Tsujii K, Okahashi K, Takeuchi T (1982) Addition-Compound Formation between Anionic and Zwitterionic Surfactants in Water. J. Phys. Chem. 86: 1437-1441

35. Porter MR (1994) Handbook of Surfactants, 2nd edn. Blackie Academic & Professional, London. pp. 258

36. Herrmann KW (1962) Non-Ionic-Cationic Micellar Properties of Dimethyldodecylamine Oxide. J. Phys. Chem. 66: 295-300

37. Tokiwa F, Ohki K (1966) Potentiometric Titration of a Nonionic-Cationic Surfactant in Aqueous Solution. J. Phys. Chem. 70: 3437-3441

38. Ikeda S, Tsunoda M, Maeda H (1978) The Application of the Gibbs Adsorption Isotherm to Aqueous Solutions of a Nonionic-Cationic Surfactant. J. Colloid Interface Sci. 67: 336-348

39. Ikeda S, Tsunoda M, Maeda H (1979) The Effects of Ionization of Micelle Size of Dimethyldodecylamine Oxide. J. Colloid Interface Sci. 70: 448-455

40. Imae T, Ikeda S (1985) Formation of Rodlike Micelles of Dimethyloleylamine Oxide in Aqueous Solutions: Effects of Addition of Hydrochloric Acid and Sodium Chloride on the Micelle Size and the Intermicellar Interaction. J. Colloid Polym. Sci. 263: 756-766

41. Chang DL, Rosano HL, Woodward AE (1985) Carbon-13 NMR Study of the Effects of pH on Dodecyldimethylamine Oxide Solutions. Langmuir 1: 669-672

42. Soontravanich S, Scamehorn JF, Harwell JH, Sabatini DA (2007) Interaction Between an Anionic and an Amphoteric Surfactant. Part I Monomer-Micelle Equilibrium. Submitted to J. Surfact. Deterg.

43. Davies CW (1962) Ion Association. Butterworths, London. pp. 41

44. Rathman JF, Christian SD (1990) Determination of Surfactant Activities in Micellar Solutions of Dimethyldodecylamine Oxide. Langmuir 6: 391-395

45. Rathman JF, Scamehorn JF (1984) Counterion Binding on Mixed Micelles. J. Phys. Chem 88: 5807-5816

46. Hall DG, Price TJ (1984) Electrochemical Studies of Micellar-Counterion Interactions in Mixtures of Ionic and Non-ionic Surfactants. J. Chem. Soc. Faraday Trans. 1. 80: 1193-1199

47. Stellner KL, Scamehorn JF (1986) Surfactant Precipitation in Aqueous Solutions Containing Mixtures of Anionic and Nonionic Surfactants. JAOCS 63: 566-574

48. Scamehorn JF (1986) Phenomena in Mixed Surfactant Systems. In: Scamehorn JF (ed) ACS Symp. Ser. 311. ACS, Washington. pp. 1

49. Holland PM, Rubingh DN (1983) Nonideal Multicomponent Mixed Micelle Model. J. Phys. Chem. 87: 1984-1990

50. Rosen MJ (2004) Surfactants and Interfacial Phenomena, 3rd edn. John Wiley & Sons, Hoboken, New Jersey. pp.379

51. Amante JC, Scamehorn JF, Harwell JH (1991) Precipitation of Mixtures of Anionic and Cationic Surfactants. II. Effect of Surfactant Structure, Temperature, and pH. J. Colloid Interface Sci. 144: 243-253

52. Doan T, Acosta E, Scamehorn JF, Sabatini DA (2003) Formulating Middle-Phase Microemulstions Using Mixed Anionic and Cationic Surfactant Systems. J. Surfact. Deterg. 6: 215-224

53. Nemeth R, Matijevic E (1971) Precipitation and Electron Microscopy of Calcium Oleate and Barium Oleate Sols. Kolloid Z. Z. Polym. 245: 497-507

Table 4.1 Summary of the parameters used in the model

Parameters	Value	Reference
K_{SP}	1.44×10^{-10} M^2	This work
β_{a^+ds}	-12.88	[42]
β_{a^0ds}	-6.61	[42]
$\beta_{a^+a^0}$	-2.6	[42]
CMC_{a^+}	1.3×10^{-3} M	[42]
CMC_{a^0}	1.2×10^{-3} M	[42]
CMC_{ds}	9×10^{-4} M	[42]

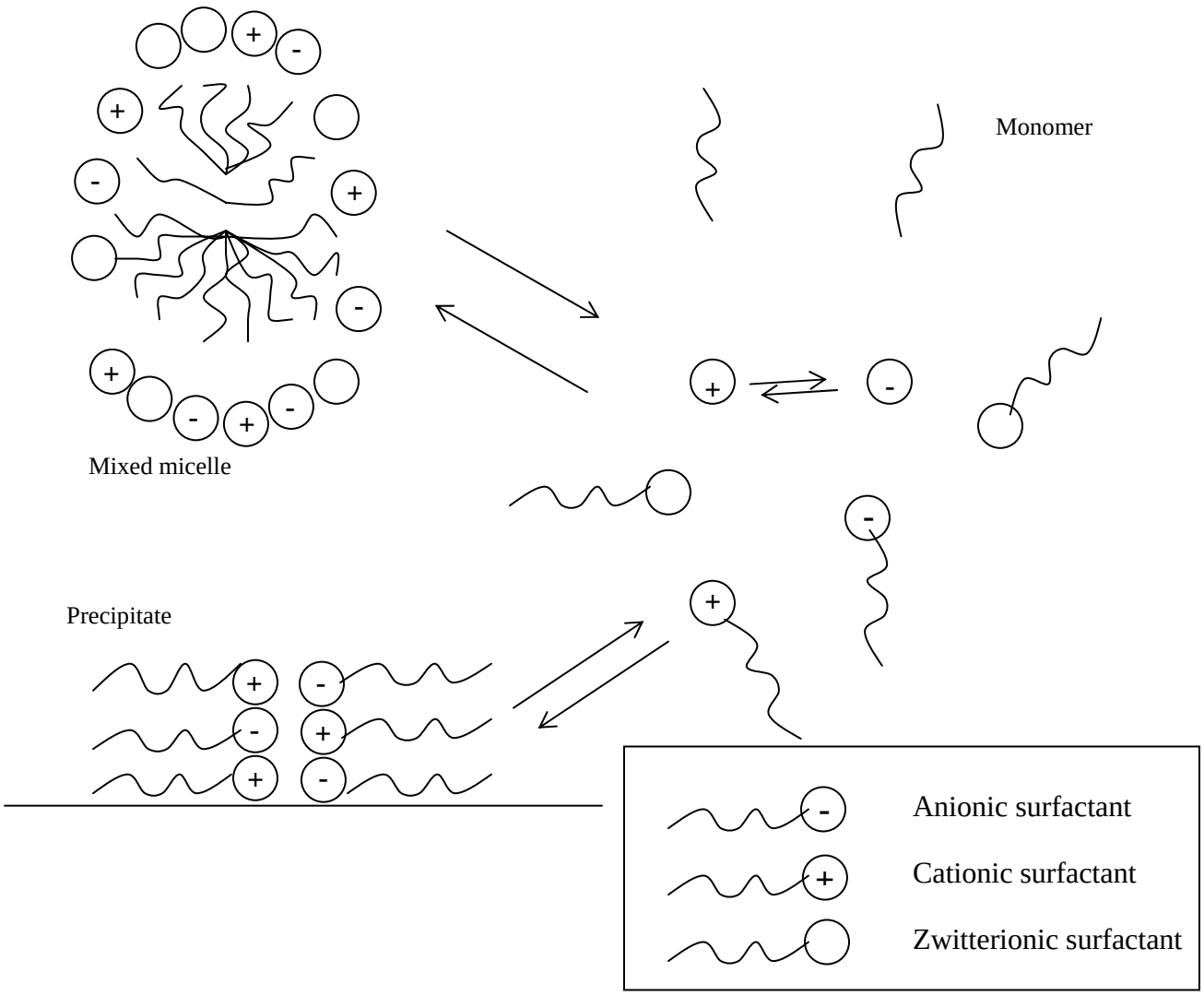

Fig. 4.1 Schematic of equilibria in anionic/amphoteric surfactant system

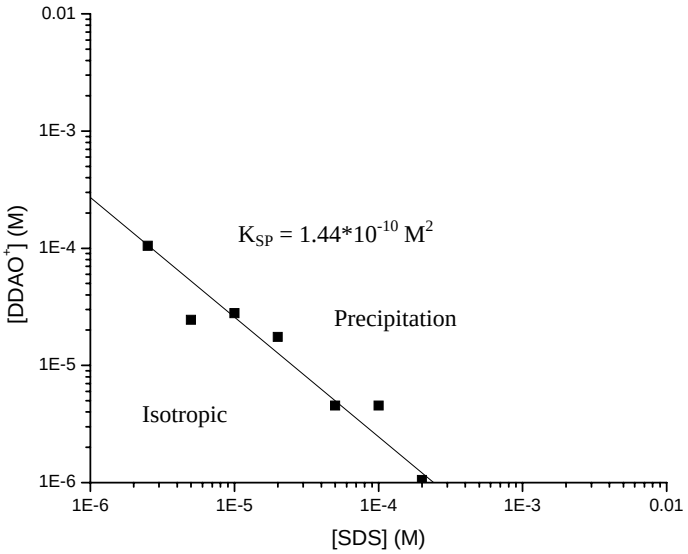

Fig. 4.2 Experimental precipitation phase boundary below the CMC at pH 3 used to obtain the K_{SP}

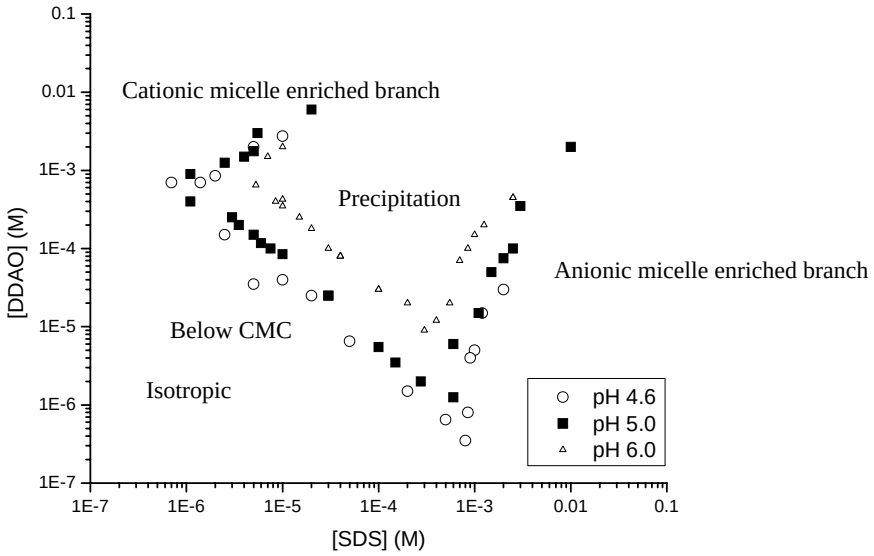

Fig. 4.3 Experimental precipitation phase boundaries in solutions of SDS and DDAO at different pH levels

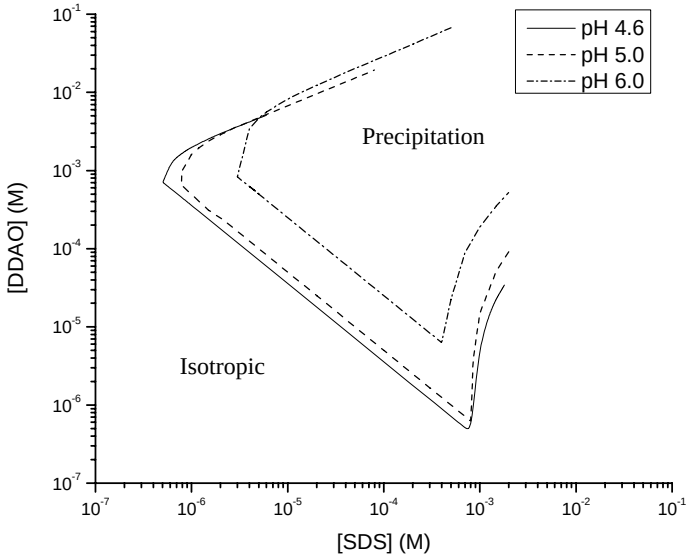

Fig. 4.4 Predicted precipitation phase boundary for SDS/DDAO at different pH levels

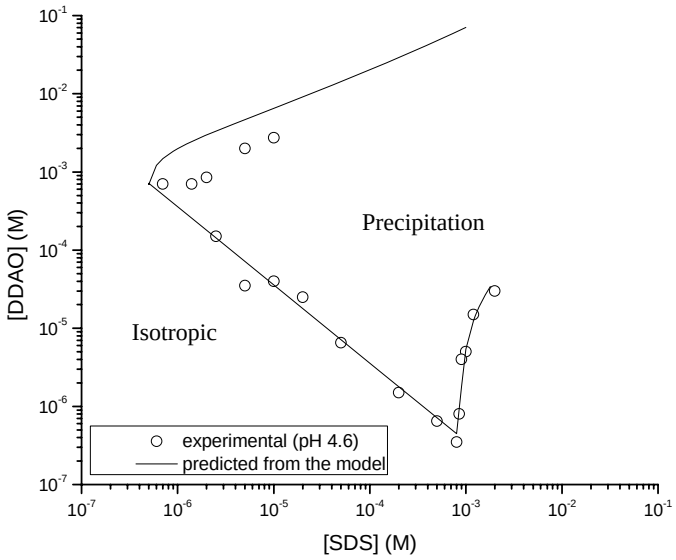

Fig. 4.5 Comparison of predicted and experimental precipitation phase boundary at pH 4.6

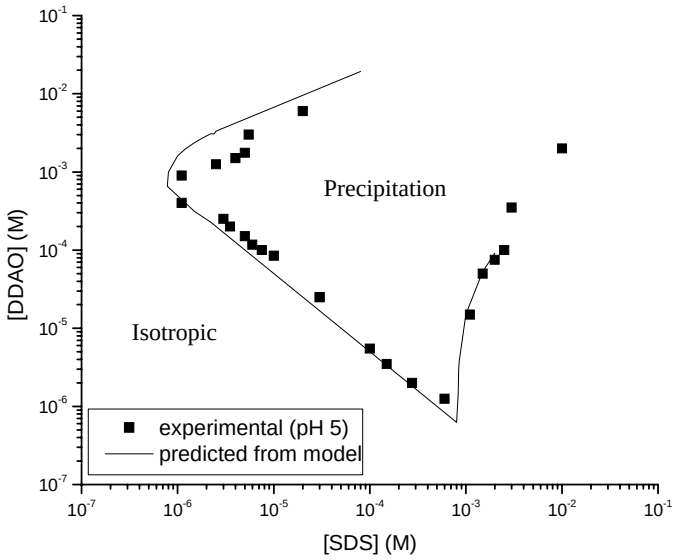

Fig. 4.6 Comparison of predicted and experimental precipitation phase boundary at pH 5

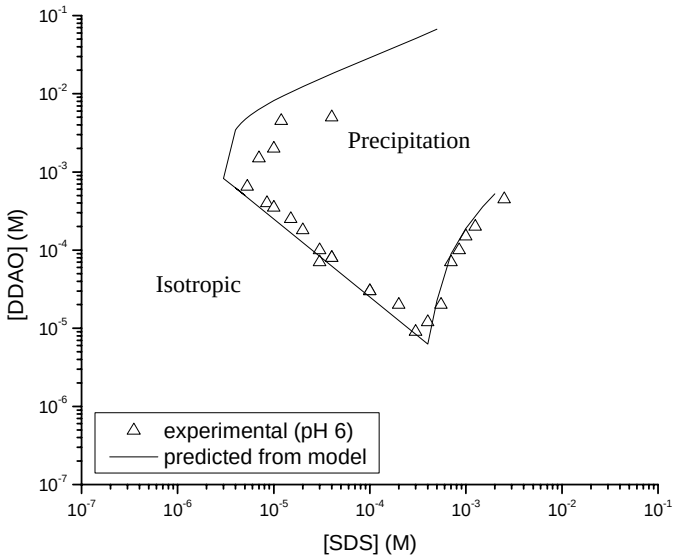

Fig 4.7 Comparison of predicted and experimental precipitation phase boundary at pH 6

CHAPTER 5

Dissolution Study of Salt of Long Chain Fatty Acids (Soap Scum) in Surfactant Solutions. Part I. Equilibrium Dissolution

Dissolution of calcium salt of a long chain fatty acid or soap scum is a major challenge for hard surface cleaners since soap scum forms when soap is exposed to hard water and has very low water solubility. Some common formulations contain micelle-forming surfactants as well as chelants for hardness cations in aqueous solutions, but the mechanism by which they dissolve soap scum is not well understood. In this paper, the equilibrium solubility of calcium octadecanoate (calcium stearate or $Ca(C_{18})_2$) was measured as a function of pH as well as chelating agent (ethylenediaminetetraacetate disodium salt or Na_2EDTA) and surfactant concentrations. Anionic, nonionic, and amphoteric surfactants were studied. The highest soap scum solubilities were observed at high pH with an amphoteric surfactant. Under this condition, the chelant effectively binds calcium and the stearate anion forms mixed micelles well with the amphoteric surfactant, which is in zwitterionic form at high pH. In the second part of this series, we address the kinetics of soap scum dissolution.

5.1 INTRODUCTION

Soap scum is the calcium or magnesium salt of a long chain fatty acid. Many personal care products consist of soaps, which are salts of carboxylic acids or fatty acids. Soaps are unstable in hard water containing metal ions, especially calcium and magnesium, because soaps form insoluble precipitates with those metal ions. Insoluble soap scum creates the well-known stain in the bathroom (e.g., ring around the bathtub). There have been extensive efforts to formulate bathroom cleaners and other hard surface cleaners to remove soap scum stains. Requirements for good formulation generally include effective, rapid removal of the scum with little or no mechanical force involved. One common approach in hard surface cleaners used for soap scum removal involves an aqueous solution of a chelant for calcium or magnesium complexation with a micelle-forming surfactant. Simultaneous chelation of calcium and mixed micellization of the fatty acid with the added water-soluble surfactant are hypothesized to be responsible for soap scum dissolution.

The relationship between the structure of different surfactants and performance of the equilibrium dissolution of soap scum in the solution containing chelating agent and the effect of solution pH are main focuses in this study. The solution pH can have an effect on both the effectiveness of the chelating reaction and the structure of the fatty acid due to protonation [1]. Generally, the solubility of soap decreases or the Krafft temperature increases as its alkyl chain length increases [2]. Mixture of soaps are more soluble than pure soaps [2].

Calcium stearate ($Ca(C_{18})_2$), $[CH_3(CH_2)_{16}CO_2]_2Ca$ or the calcium salt of octadecanoic acid, was used as a model soap scum in this study (Fig. 5.1). Actual soap scum can be a mixture of other metal salts (e.g., magnesium) of other fatty acids such as palmitic acid. Calcium stearate is normally considered "insoluble" in water, alcohol, and ether but soluble in mineral oils and hot pyridine. The solubility of calcium stearate is only about 0.04 g/L of water at 15 ^oC [3]. Long chain fatty acid salts are weak ionizable surfactants [4] with the charge varying with pH. Figure 5.1 shows the possible forms of $Ca(C_{18})_2$ existing in aqueous solution at different pH levels. Calcium stearate has a pK_a of 4.5 [5]. So, at low pH (e.g., 2), the stearate anion protonates and forms nearly insoluble stearic acid. The solubility of stearic acid is only 0.003g/L of water at 20 ^oC [6]. At higher pH level, calcium cannot dissociate so the $Ca(C_{18})_2$ remains mainly insoluble. At intermediate pH level, protonation is only partial so there is a mixture of stearate anion and stearic acid, both of which have low solubility. So, without some way to remove the calcium from the stearate or some aggregates like micelles to increase the solubility of the stearate anion or stearic acid in solution, $Ca(C_{18})_2$ is nearly insoluble throughout a wide pH range.

The solubilities of either the nonionic stearic acid at low pH and the $Ca(C_{18})_2$ at high pH are so low that micelles do not form; i.e., as surfactant concentration increases, the solubility limit is reached before a CMC is reached. One strategy of increasing the solubility of $Ca(C_{18})_2$ at any pH is to add a "micelle promoting agent" [7], which forms micelles with which the protonated stearic acid or stearate anion can co-micellize. This is a common general strategy in increasing the solubility of surfactants. Since the tendency to co-micellize or form mixed micelles will depend on

the charge of the added surfactant, we will study added anionic, nonionic, and amphoteric surfactants here.

A chelating agent is sometimes added into cleaning products to prevent precipitation of active ingredients with metal ions naturally found in the hard water by forming a water soluble complex with the metal ions. In the system studied here, the chelating agent was added to complex with and promote the dissociation of calcium ion from the solid calcium stearate so the dissociated stearate anion can form micelles. There are several types of chelating agents or complexing agents such as phosphates and aminocarboxylates (e.g., ethylenediaminetetraacetate or EDTA) [8]. Ethylenediaminetetraacetate disodium salt, Na_2EDTA, (molecular structure shown in Fig. 5.1) was used here. It is a common complexing agent, which has four main active sites that can form a water-soluble complex with metal ions. One molecule of Na_2EDTA can chelate one molecule of calcium ion stoichiometrically [9]. The effectiveness in metal complex formation depends on the equilibrium constants or stability constants of the ligand with the metal. There are five possible forms of EDTA in the absence of calcium depending on pH (H_4Y, which has four ionizable hydrogens, H_3Y^-, H_2Y^{2-}, HY^{3-}, and Y^{4-}) and there are 2 forms (HY^{3-} and Y^{4-}) which can form complexes with calcium ions [9]. At high pH, the major species found is Y^4, which is the most effective form of EDTA in chelating calcium. The molecule of EDTA in acidic solution is less effective than in a basic solution due to protonation of active sites on the EDTA.

At high pH, as calcium is removed from solid $Ca(C_{18})_2$, the stearate anion solubility increases to the point where all the solid dissolves, or it forms micelles, or

forms precipitate with some other counterions (e.g., Na^+) in solution in the absence of a co-surfactant acting as a micelle promoting agent. The presence of a co-surfactant forming micelles further improves solubility synergistically with the chelant. At a low enough pH, the protonation reaction should cause complete dissolution of the solid calcium stearate to nearly insoluble protonated fatty acid which can co-micellize (but doesn't have enough hydrophilicity in the nonionic head group to form micelles independently). So at low enough pH, the chelant shouldn't have any effect on the equilibrium solubility of $Ca(C_{18})_2$.

5.2 EXPERIMENTAL

5.2.1 Materials

Sodium dodecyl sulfate (SDS) (99+% purity), obtained from Fisher Scientific (Fair Lawn, NJ), was further purified by recrystallization from water and then from methanol, followed by drying under a vacuum at 30 ^oC. Octyl polyglycoside (C_8APG) was obtained from Akzo Nobel and used as received. Disodium ethylenediaminetetraacetate (Na_2EDTA) (100% purity) are obtained from Fisher Scientific and used without further purification. Stearic acid (99 % purity), obtained from Alfa Aesar (Heysham, Lancaster), was used without further purification. Calcium hydroxide (99.995% purity) was obtained from Sigma-Aldrich (St. Louis, MO). Absolute ethyl alcohol (100% purity) was obtained from AAPER (Shelbyville, KY). Acetone (A.C.S. grade) was obtained from Fisher Scientific. Dimethyldodecylamine oxide (DDAO) was obtained from Stepan and used without

further purification. The NaOH and HCl were from Fisher Scientific (Fair Lawn, NJ) and were used as received to adjust the solution pH. Water was double deionized.

5.2.2 Methods

Calcium stearate, calcium salt of stearic acid, was prepared from stearic acid. Stearic acid was first dissolved in ethanol and then reacted with a clear solution of calcium hydroxide. The precipitate was filtered and rinsed with water, ethanol and acetone to remove excess calcium ion and unreacted stearic acid. Finally, the precipitate was dried in a vacuum oven at 30 ^{o}C.

The equilibrium solubility of calcium stearate in anionic, nonionic, and amphoteric surfactants was measured at 25 ^{o}C. A series of surfactant solution was prepared at pH 4-11 using HCl and NaOH solutions. Sodium dodecyl sulfate (SDS) was used as an anionic surfactant. Octyl polyglycoside was used as a nonionic surfactant. Dimethyldodecylamine oxide (DDAO) was used as an amphoteric surfactant. An excess amount of $Ca(C_{18})_2$ was added into a mixed solution with other surfactants and Na_2EDTA at the pH of interest. The $Ca(C_{18})_2$ was forced to dissolve by heating it up to above 70 ^{o}C or until most of $Ca(C_{18})_2$ was dissolved. Then it was equilibrated at the temperature of interest (25 ^{o}C) in a temperature-controlled water bath. The solution was allowed to equilibrate for at least 1 week with routine shaking to ensure that equilibrium was reached. The solution was filtered using a 0.22-micron Durapore hydrophilic membrane. Then the supernatant was analyzed for the concentration of $Ca(C_{18})_2$ by a gas chromatography (GC) (Varian 3300), using an SPB 20 column (Supelco) with an FID detector following derivatization. Calcium

stearate was derivatized into methyl stearate by using a derivatizing agent, BF_3-methanol (Alltech, Deerfield, IL). The derivatized solution was diluted by hexane before being analyzed by GC.

5.3 RESULTS AND DISCUSSION

5.3.1 Chelant-Only Systems

The equilibrium solubility of $Ca(C_{18})_2$ was measured in solutions of different types of surfactants with and without chelating agent (Na_2EDTA) at 25 ^oC and at varying pH. Figure 5.2 shows the equilibrium solubility of $Ca(C_{18})_2$ in 0.1 M SDS, 0.1 M Na_2EDTA, and a solution of 0.1 M SDS/0.1 M Na_2EDTA as a function of pH. Figure 5.3 shows the equilibrium solubility of $Ca(C_{18})_2$ in 0.1 M DDAO, 0.1 M Na_2EDTA, and a solution of 0.1 M DDAO/0.1 M Na_2EDTA as a function of pH. From both Figs. 5.2 and 5.3, the Na_2EDTA alone has no significant effect on $Ca(C_{18})_2$ solubility at any pH studied. Neither the protonated nonionic stearic acid (low pH) or the stearate anionic can attain a high enough solubility to form micelles without co-surfactant, even if free calcium is largely complexed. There is competition for calcium between the Na_2EDTA and the precipitated $Ca(C_{18})_2$ and the extremely low K_{SP} of the latter maintains the solid $Ca(C_{18})_2$ even at very low free calcium concentrations in the presence of the chelant at high pH where the Na_2EDTA is most effective. At the lowest pH studied here (pH 4), the protonated form of the fatty acid and the solid $Ca(C_{18})_2$ will both be present. We did not attempt to ascertain the

fraction of the solid present in either form since the focus of this study is the solubility of the stearate or stearic acid, neither of which was significant without co-surfactants. Table 5.1 summarizes the possible forms of $Ca(C_{18})_2$ and chelant Na_2EDTA that could be found at different pH levels. The stearic acid could form due to low pH by the protonaton of stearate anion. The Na_2EDTA will also be protonated into less effective chelant forms at low pH. At intermediate pH, calcium is released by the protonation of $Ca(C_{18})_2$ and also is complexed with chelant to some level, but not very high as the chelant is not its most effective form. The other molecules formed from $Ca(C_{18})_2$ are stearic acid and stearate anion. At higher pH, even though the calcium is complexed effectively, the dissolution of $Ca(C_{18})_2$ is still considered very low since the stearate anion has limited solubility and at the temperature of study (25 ^{o}C), it cannot form micelles alone to increase its solubility.

5.3.2 Surfactant-Only Systems

The SDS and DDAO are present at least an order of magnitude above their CMC, so almost all these surfactants are present as micelles. As shown in Figs. 5.2 and 5.3, in the absence of chelating agent, both SDS and DDAO increased the solubility of $Ca(C_{18})_2$ slightly, with DDAO causing higher solubility than SDS at all pH levels. The SDS effect had little pH dependence except at pH below 5 where solubility of $Ca(C_{18})_2$ increased. The DDAO caused a monotonic increase in solubility in $Ca(C_{18})_2$ with decreasing pH, exhibiting an order of magnitude greater solubility at pH of 4 compared to SDS. At high pH (pH 7-11), the solubility of $Ca(C_{18})_2$ in DDAO is approximately 5 times higher than that in SDS.

The charge on the stearate/stearic acid molecule becomes less negative (high fraction of protonated or nonionic surfactant) as pH decreases as already discussed with a pK_a around 4.5. The effective pK_a can alter upon incorporation of the stearate into mixed micelles depending on the charge of the co-surfactant, increasing when co-micellizing with an anionic surfactant like SDS [10].

The DDAO is an amphoteric surfactant, which can exist in the form of a cationic or a zwitterionic surfactant depending on the solution pH as shown by the protonation reaction:

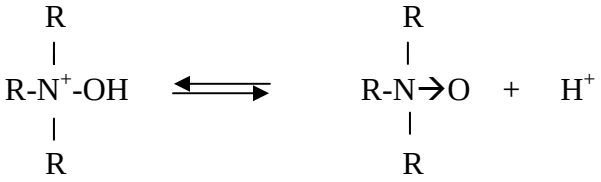

The pK_a of DDAO monomer is reported at about 5 [11], but the effective pK_a can be much higher in micelle form, even higher when co-micellized with an anionic surfactant [11]. Since 0.1 M DDAO is about two orders of magnitude above the CMC, the effective pK_a is that in micellar form. At the pH = pK_a, half of the surfactant is in cationic form and half in zwitterionic form. At pH below the pK_a, the cationic form dominates and at pH above the pK_a, the zwitterionic form dominates. In addition to protonation of the stearate and the DDAO, the effectiveness of complexation of Na_2EDTA varies with pH as previously discussed, with higher pH being more effective.

In explaining the pH effects on $Ca(C_{18})_2$ dissolution, three effects dominate as pH decreases; protonated nonionic stearic acid/anionic stearate anion ratio increases; cationic DDAO/zwitterionic DDAO ratio increases; and complexation of calcium by Na_2EDTA decreases. The effect of micellar composition on the effective pK_a of the stearate is probably a secondary effect in explaining trends. Charge repulsion of the head groups when anionic stearate is incorporated into an SDS micelle would inhibit co-micellization of stearate with SDS, so the increase in solubility of $Ca(C_{18})_2$ at pH below 5 in a chelant-free SDS solution is due to a higher fraction of the fatty acid being in nonionic, protonated form. The highest synergism in mixed micellization is for a cationic/anionic surfactant mixture [12], explaining why the highest solubility in a chelant-free surfactant system is DDAO at low pH where it is below its pK_a and primarily in cationic form, co-micellizing with anionic stearate and (less synergistically) with protonated stearic acid. The synergism between a zwitterionic and an anionic surfactant is between that of an anionic/anionic and a cationic/anionic surfactant mixture [12], explaining why the solubility of $Ca(C_{18})_2$ at high pH (where the DDAO is primarily zwitterionic) is greater than that for SDS, but less than that of DDAO at low pH in the absence of chelant. Table 5.1 shows the ionic form of possible formed components and degree of interaction in micellar solutions of anionic, amphoteric, and nonionic surfactants in equilibrium with solid soap scum at low, intermediate, and high pH, respectively.

At low pH, the main soap scum component that forms mixed micelles with the adeed soluble surfactant is nonionic stearic acid. The formation of mixed micelles is expected to be most effective in either cationic (DDAO at low pH) or anionic

surfactant micelles since cation/nonionic or anionic/nonionic surfactant synergism is present.

At intermediate pH, stearic acid and stearate anion form mixed micelles with added surfactant. The DDAO is composed of both cationic and zwitterionic surfactants. Even though the formation of mixed micelle when DDAO is used can be enhanced due to the mixed cationic (DDAO) and anionic (stearate) surfactants, the solubility of $Ca(C_{18})_2$ is lower than at low pH because stearate solubility is so low in equilibrium with $Ca(C_{18})_2$ when no calcium is complexed and less protonated stearic acid is formed than at low pH.

At high pH, the soap scum mostly remains as an undissolved solid precipitate since the solubility of soap scum is very low. Even if there is any stearate anion, there is still an electrostatic repulsion between stearate and in SDS in micelles so the solubility of $Ca(C_{18})_2$ is low. The DDAO is in completely zwitterionic form and would form micelles synergistically with stearate, but stearate solubility is so low in equilibrium with $Ca(C_{18})_2$ with no chelation.

5.3.3 Surfactant-Chelant Systems

In the presence of Na_2EDTA, the highest solubility is with DDAO at high pH, where it is several orders of magnitude greater than in the chelant-free system. The solubility increases monotonically with pH, the opposite trend than for the chelant-free system. At a pH below about 5, the presence of the chelant does not significantly increase solubility of $Ca(C_{18})_2$. So as long as there are zwitterionic or cationic micelles with which the stearate can co-micellize, the complexation of calcium by a

chelant is crucial to improving solubility of the $Ca(C_{18})_2$ and the increasing effectiveness of complexation of calcium by Na_2EDTA at high pH dominates pH effects, leading to maximum solubility at high pH.

For the SDS system, the synergism for the chelant/surfactant mixture increases as pH decreases in contrast to DDAO. Here, the more efficient co-micellization of the nonionic, protonated stearic acid into the anionic SDS micelles relative to co-micellization of anionic stearate is more important than the decrease in complexation effectiveness of the chelant as pH decreases. However, it is important to note that the maximum solubility of $Ca(C_{18})_2$ in the SDS/chelant system is over an order of magnitude less than for the DDAO/chelant system, so lack of effectiveness of chelation at low pH greatly inhibits freeing of the stearic acid/stearate molecule from the solid $Ca(C_{18})_2$ to permit them to co-micellize.

More limited studies were carried out using the nonionic surfactant C_8APG compared to SDS and DDAO as shown in Figs. 5.4 and 5.5 for the C_8APG/chelant system (chelant-free C_8APG was not studied). The solubility of $Ca(C_{18})_2$ in the C_8APG system shows increasing solubility of $Ca(C_{18})_2$ with increasing pH as with the DDAO system, although at high pH where maximum solubility is observed, total solubility is about a factor of 5 less for C_8APG than DDAO. Since anionic/nonionic mixed micelles are less synergistic than anionic/zwitterionic mixed micelles, the stearate/C_8APG synergism is less than the stearate/DDAO at these high pH conditions, explaining this surprising large amphoteric surfactant effectiveness. Aiding this performance difference is that the DDAO has much larger hydrophobe than the C_8APG, forming micelles which co-micellize more effectively. Similarly, at

low pH, the SDS system shows higher $Ca(C_{18})_2$ solubility than the C_8APG system, explainable by the greater synergism of the nonionic/anionic mixed micelles composed of protonated nonionic stearic acid/SDS compared to the nonionic/nonionic protonated stearic acid/C_8APG mixed micelles. Table 5.1 shows the molecular structure of $Ca(C_{18})_2$ and the tendency for mixed micelle formation when $Ca(C_{18})_2$ is dissolved in a micellar solution with chelant (Na_2EDTA) at varying pH, in which the explanation of the effects of pH on the chelation, release of calcium, surfactant structure, and formation of mixed micelles is already discussed above.

5.4 REFERENCES

1. Pandit NK, Strykowski JM (1989) Effect of pH and Temperature on the Solubility of a Surface Active Carboxylic Acid. J. Pharm. Sci 78: 767-770
2. de Mul MNG, Davis HT, Evans DF, Bhave AV, Wagner JR (2000) Solution Phase Behavior and Solid Phase Structure of Long-Chain Sodium Soap Mixtures. Langmuir 16: 8276-8284
3. National Organic Standards Board Technical Advisory Panel (TAP) Review, http://www.ams.usda.gov/nop/NationalList/TAPReviews/CalciumStearate2.pdf. [cited June 2007]
4. Kanicky JR, Shah DO (2003) Effects of Premicellar Aggregation on the pK_a of Fatty Acid Soap Solutions. Langmuir 19: 2034-2038
5. Sukhija PS, Palmquist DL (1990) Dissociation of Calcium Soaps of Long-Chain Fatty Acids in Rumen Fluid. J. Dairy Sci. 73: 1784-1787
6. Bagby MO (1993) Carboxylic Acids (Survey). In: Kirk-Othmer Encyclopedia of Chemical Technology Vol 5. John Wiley & Sons, New York. pp. 147-168
7. Scamehorn JF, Harwell JH (2004) Precipitation of Surfactant Mixtures. In: Abe M, Scamehorn JF Mixed Surfactant Systems. 2nd edn. Marcel Dekker, New York. pp. 601-655
8. Tai LHT (2000) Formulating Detergents and Personal Care Products A Complete Guide to Product Development. AOCS Press, Champaign, Illinois. pp. 56

9. Martell AE, Motekaitis RJ (1992) Determination and Use of Stability Constants. 2nd edn. VCH Publishers, Inc., New York. pp. 7

10. Rodriguez CH, Chintanasathien C, Scamehorn JF, Saiwan C, Chavadej S (1998) Precipitation in Solutions Containing Mixtures of Synthetic Anionic Surfactant and Soap. I. Effect of Sodium Octanoate on Hardness Tolerance of Sodium Dodecyl Sulfate. J. Surfact. Deterg. 1: 321-328

11. Soontravanich S, Scamehorn JF, Harwell JH, Sabatini DA (2007) Interaction Between an Anionic and an Amphoteric Surfactant. Part I. Monomer-Micelle Equilibrium. Submitted to J. Surfact. Deterg.

12. Rosen MJ (2004) Surfactants and Interfacial Phenomena. 3rd edn. John Wiley & Sons, Hoboken, New Jersey. pp. 379

Table 5.1 Forms of soap scum, DDAO, ability of Na_2EDTA to complex calcium, and solubility of $Ca(C_{18})_2$ in surfactant/chelant system at different pH levels

pH	Dominant Form of Soap Scum	Dominant Charge on DDAO	Ability of Na_2EDTA to Complex Calcium	Solubility of $Ca(C_{18})_2$ in Surfactant/Chelant System		
				SDS	DDAO	C_8APG
Low	Protonated Stearic Acid (Nonionic)	Cationic	Low	Medium	Low	Low
Intermediate	Protonated Stearic Acid (Nonionic) and Stearate (Anionic)	Cationic and Zwitterionic	Medium	Low	High	Medium
High	Stearate (Anionic)	Zwitterionic	High	Low	Very High	High

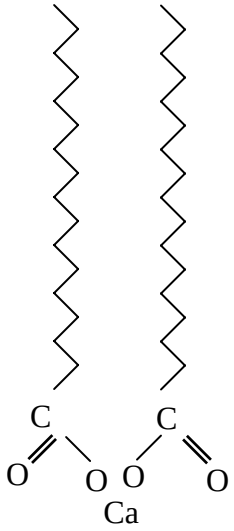

Soap scum or $Ca(C_{18})_2$ (s)

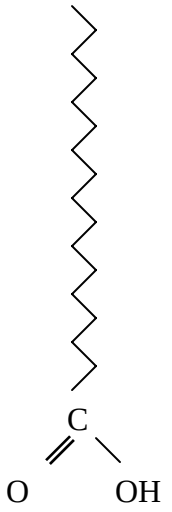

Stearic acid (s)

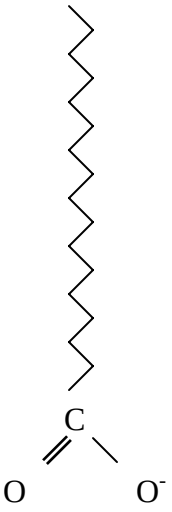

Stearate anion (aq)

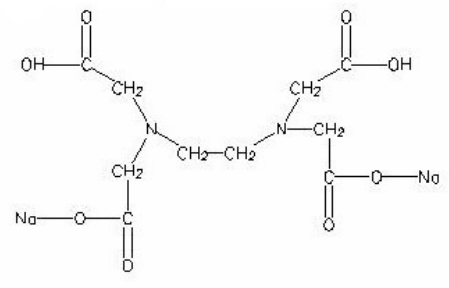

Na_2EDTA

Fig. 5.1 Molecular structure of soap scum or $Ca(C_{18})_2$, stearic acid, stearate anion, and Na_2EDTA

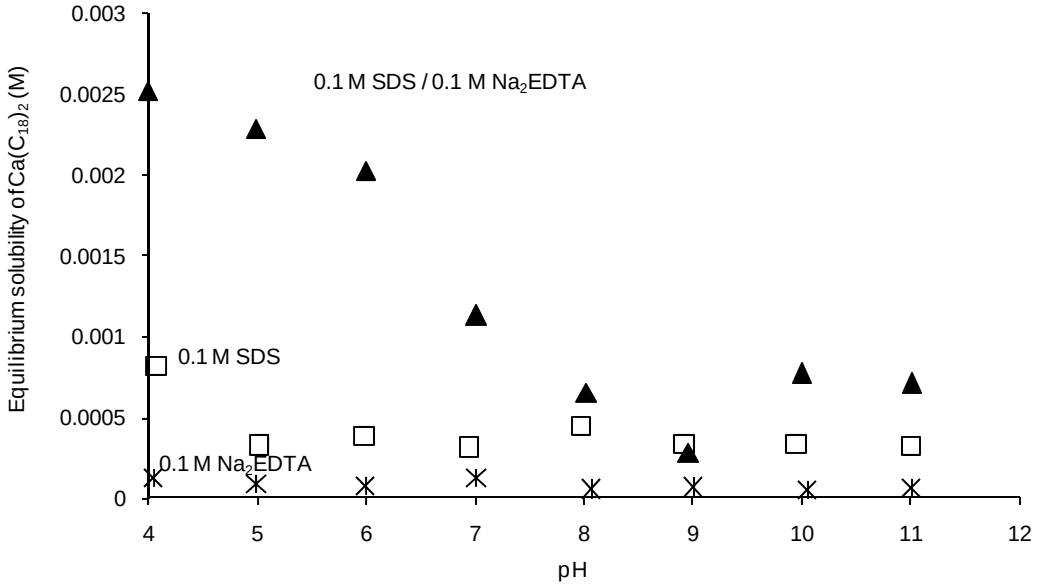

Fig. 5.2 Equilibrium solubility of $Ca(C_{18})_2$ in SDS/Na_2EDTA solutions

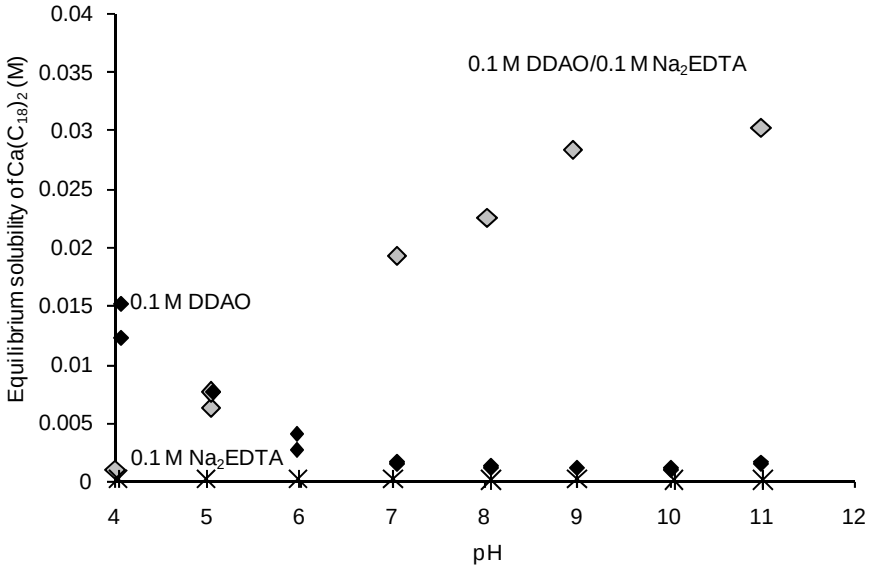

Fig. 5.3 Equilibrium solubility of $Ca(C_{18})_2$ in DDAO/Na_2EDTA solutions

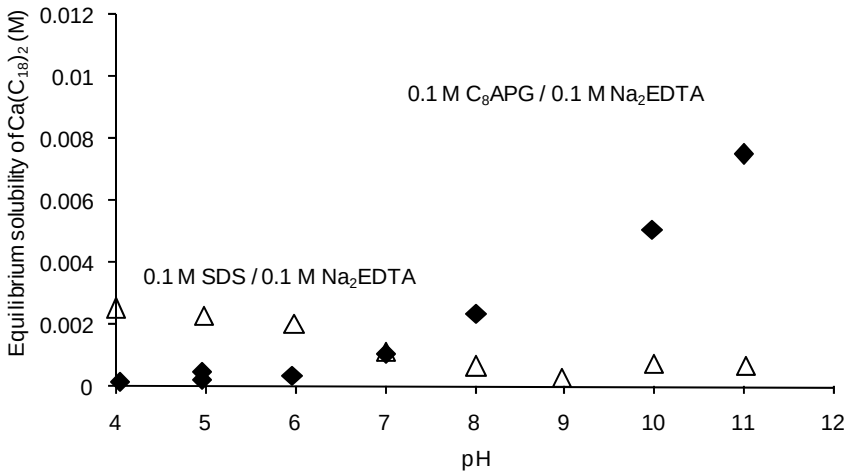

Fig. 5.4 Equilibrium solubility of $Ca(C_{18})_2$ in solutions of 0.1 M of SDS/0.1 M Na_2EDTA and 0.1 M C_8APG/0.1 M Na_2EDTA

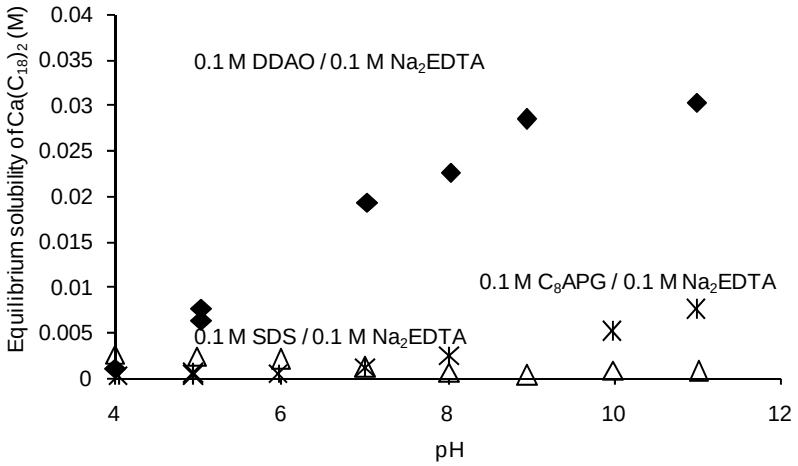

Fig. 5.5 Equilibrium solubility of $Ca(C_{18})_2$ in solutions of 0.1 M SDS/0.1 M Na_2EDTA, 0.1 M C_8APG/0.1 M Na_2EDTA, and 0.1 M DDAO/0.1 M Na_2EDTA

CHAPTER 6

Dissolution Study of Salt of Long Chain Fatty Acids (Soap Scum) in Surfactant Solutions. Part II. Kinetics of Dissolution

A study of the dissolution kinetics of soap scum, calcium octadecanoate ($Ca(C_{18})_2$), by aqueous solutions containing three different types of surfactants; dimethyldodecylamine oxide (DDAO), sodium dodecyl sulfate (SDS), and octyl polyglycoside (C_8APG) in the presence of a chelating agent, disodium ethylenediaminetetraacetate (Na_2EDTA) was carried out by measuring the rate of dissolution of $Ca(C_{18})_2$ using a flow cell apparatus. The resulting rate of dissolution corresponds well with the equilibrium solubility obtained in the part I of this series even though the dissolution is rate-limited (far from equilibrium). High rates of $Ca(C_{18})_2$ dissolution are achieved in solutions of zwitterionic DDAO or nonionic C_8APG with Na_2EDTA at high pH. From rate analysis, the $Ca(C_{18})_2$ dissolution was found to be surface-reaction limited, rather than limited by processes in solution. The wettability of dissolving solution on a soap scum disc was analyzed from the dynamic contact angle of a sessile drop and wettability is good enough to not limit the rate of dissolution for the systems studied.

6.1 INTRODUCTION

Soap scum or calcium salts of long chain fatty acids are often found in the bathroom and are considered unpleasant. Several hard surface cleaning products designed to remove soap scum and other undesirable deposits, such as calcium carbonate, are available with various formulations and ranges of pH. The main ingredients of hard surface cleaning detergents are surfactants, chelants, and solvents. We will only consider aqueous systems here.

The first part of this series [1] measured the equilibrium solubility of calcium stearate of $Ca(C_{18})_2$ in surfactant/chelant solution as a function of pH. It was found that both complexation of calcium by the chelant and formation of mixed micelles between stearic acid/stearate anion and added surfactants are important in order to obtain high solubility of $Ca(C_{18})_2$. For the systems studied, the highest equilibrium solubility was obtained when an amphoteric surfactant, dimethyldodecylamine oxide (DDAO), with chelant, disodium ethylenediaminetetraacetate (Na_2EDTA), was used at high pH. The high pH solution promotes both the dissociation of calcium from a molecule of $Ca(C_{18})_2$ through the chelation reaction and the formation of mixed micelles between the zwitterionic DDAO and the stearate anion [1].

Rapid dissolution is a crucial characteristic of a consumer hard surface cleaner. In this present work, the kinetics of dissolution of soap scum was measured in a flow cell apparatus. The ability of the dissolving solution to wet the hydrophobic surface of soap scum is expected to affect the kinetics of dissolution. Therefore, the

dynamic contact angle of the surfactant/chelant solutions on the solid soap scum was also measured in this work to aid in interpreting the dissolution kinetics.

6.1.1 Kinetic Analysis

A first order reaction rate is used to model the dissolution kinetics:

$$-r = \frac{dM}{dt} = -kM \qquad (6.1)$$

Integrating Eq. 6.1 gives

$$\ln\left(\frac{M}{M_0}\right) = -kt \qquad (6.2)$$

where r is the rate of $Ca(C_{18})_2$ dissolution, k is the apparent rate constant of dissolution (min^{-1}), and M_0 and M are the initial mass of $Ca(C_{18})_2$ and the remaining undissolved $Ca(C_{18})_2$ at time t, respectively. The value of k can be obtained from a slope of a plot of $\ln\left(\frac{M}{M_0}\right)$ vs. t.

Chan et al. [2] proposed a theory of solubilization kinetics in a micellar solution based on results from a rotating disc experiment as follows,

1. Surfactant molecules diffuse to the surface
2. Surfactant molecules adsorb on the surface of the solubilizate
3. Mixed micelle is formed between surfactant and solubilizate

4. Mixed micelle diffuses away into the bulk solution

The dissolution of lauric, palmitic, and stearic acid in sodium dodecyl sulfate (SDS) solutions in a rotating disk configuration was studied and it was found that the desorption of micelles and their diffusions are the rate-limiting steps [2, 3].

Kralchevsky et al. [4] summarized that there are three major solubilization mechanisms important in determining the kinetics of solubilization in micellar solutions.

1. Penetration mechanism

The requirement for formation of mixed micelles or solubilization of mostly solid solubilizates with a micellar solution is the ability of the surfactant solution to penetrate into the oily phase and the formation of a liquid crystalline phase at the interface [5-9].

2. Direct Solubilization

Oil molecules dissolve into the aqueous phase and then they are subsequently solubilized by surfactant micelles. This mechanism applies to oils which have an adequately large solubility in water [10-13].

3. Micelle Adsorption

It is adsorption of a micellar solution at the oil-water interface and surface reaction (an uptake of oil by surfactant). This mechanism applies to oil that has low solubility in water [2, 3, 10, 12, 14-17].

According to the mechanisms mentioned above, the solubilization of solid $Ca(C_{18})_2$ would require a good contact between the dissolving solution and solid $Ca(C_{18})_2$. The $Ca(C_{18})_2$ dissolution steps that are likely to occur in a solution of

surfactant/chelant are proposed below. These are adapted from the previous work by Chan et al. [2].

1. Diffusion of a mixture of surfactant and chelating agent from bulk fluid to the surface of $Ca(C_{18})_2$
2. Adsorption of surfactant and chelant and wetting on the solid $Ca(C_{18})_2$
3. Penetration of solution and reaction of solution with $Ca(C_{18})_2$
    a. Chelating reaction
    b. Formation of mixed micelle with stearic acid/stearate anion at the surface
4. Desorption of mixed micelle containing stearic acid/stearate anion from the surface
5. Diffusion of mixed micelle into the bulk fluid

6.1.2 Wettability

Generally, wetting is the displacement from a surface of one fluid by another and a wetting agent is a substance that increases the ability of aqueous solution to wet or spread on the surface [18]. In this context, wetting refers to the displacement of a surfactant solution on to a soap scum substrate.

Wetting of a dissolving solution on a soap scum substrate is a necessary step for the surface reaction leading to the dissolution of soap scum. The hydrophobic nature of the soap scum surface is a factor making aqueous based cleaning more difficult. Surfactant has been known for its ability to promote the wetting of aqueous solution on to a nonpolar (low-energy) surface by reducing the surface tension of a

liquid [18]. Luner et al. [19] found that there is a correlation between dissolution of a hydrophobic drug powder and wettability by surfactant solutions. In a similar way, the wettability was found to influence the dissolution of hydrophobic drugs by bile salts or other surfactants independent of solubility [19-22].

One method to evaluate the wetting ability or wettability is to measure the contact angle of a sessile drop on the substrate as illustrated in Fig. 6.1. The contact angle is defined as the angle between the substrate and the droplet and measured on macroscopic, smooth, nonporous, planar substrates. A direct measurement of contact angle can be done using an angle goniometer or image photography [18, 23]. Young's equation [18] shows the relationship between the contact angle and the interfacial tension of the three interfaces which intersect at the droplet perimeter at equilibrium.

$$\cos\theta = \frac{\gamma_{SV} - \gamma_{SL}}{\gamma_{LV}} \qquad (6.3)$$

where θ is the contact angle, and γ_{SV}, γ_{SL}, and γ_{LV} are the interfacial tension for the solid-vapor, solid-liquid, and liquid-vapor interfaces, respectively. The lower the contact angle, the better the wetting of that solution.

6.2 EXPERIMENTAL

6.2.1 Materials

Sodium dodecyl sulfate (SDS) (99+% purity), obtained from Fisher Scientific (Fair Lawn, NJ), was further purified by recrystallization from water and then from

methanol, followed by drying under a vacuum at 30 ^{o}C. Dimethyldodecylamine oxide (DDAO) was obtained from Stepan and used without further purification. Octyl polyglycoside (C_8APG) was obtained from Akzo Nobel and used as received. Disodium ethylenediaminetetraacetate (Na_2EDTA) (100% purity) was obtained from Fisher Scientific and used without further purification. Stearic acid (99 % purity), obtained from Alfa Aesar (Heysham, Lancaster), was used without further purification. Sodium stearate (> 99% purity) was obtained from Sigma-Aldrich and used as received. Calcium hydroxide (99.995% purity) was obtained from Sigma-Aldrich (St. Louis, MO). Absolute ethyl alcohol (100% purity) was obtained from AAPER (Shelbyville, KY). Acetone (A.C.S. grade) and methanol (A.C.S. grade) were obtained from Fisher Scientific. Double deionized water was used in all experiments.

6.2.2 Sample Preparation

Calcium stearate ($Ca(C_{18})_2$), calcium salt of stearic acid, was prepared from stearic acid. Stearic acid was first dissolved in ethanol or methanol and then mixed with an excess concentration of a clear solution of calcium hydroxide. The precipitate was filtered and rinsed with water, ethanol, and acetone to remove excess calcium ion and unreacted stearic acid. Finally, the precipitate was dried in a vacuum oven at 30 ^{o}C.

6.2.3 Methods

6.2.3.1 Kinetics of Dissolution

The rate of $Ca(C_{18})_2$ dissolution was evaluated using a differential reactor (a flow cell reactor), shown in Fig. 6.2. The flow cell was modified from the differential flow cell apparatus used in the study of asphaltene dissolution [24]. An aqueous solution containing a mixture of surfactant and chelating agent was injected through the reactor at a constant flow rate controlled by a peristaltic pump. A reactor flow cell is made from a 25-mm Millipore Teflon filter holder. A 0.0100 gm sample of $Ca(C_{18})_2$ was placed between two 0.22-micron Durapore hydrophilic membranes. The flow cell and tubing system were immersed in the temperature-controlled water bath, which was set at a temperature of 25 ^{o}C. The amount of dissolved $Ca(C_{18})_2$ was quantified by measuring the weight loss.

Percentage of $Ca(C_{18})_2$ dissolved = [(Initial mass of $Ca(C_{18})_2$ - Unreacted mass of $Ca(C_{18})_2$)/Initial mass of $Ca(C_{18})_2$] x 100 %

6.2.3.2 Preparation of Solid Surface for Contact Angle Measurement

A smooth surface of $Ca(C_{18})_2$ substrate was made by lightly pressing the $Ca(C_{18})_2$ powder against a glass sl]ide.

6.2.3.3 Contact Angle Measurement

An automated drop tensiometer (Tracker 100, IT-Concept, Saint-Clément-les-Places, France) was used to measure the dynamic contact angle of solutions of interest on solid soap scum. A sessile drop was created by injecting a solution from a

micro syringe on the solid substrate. A digital video image of the drop was captured and the contact angle on both sides of the drop was calculated in real-time, based on the axisymmetric drop shape analysis. The data were taken at one second intervals. The reported contact angle value is a grand average of the left and right angles from all the runs. The temperature was maintained at 25 ^{o}C.

6.3 RESULTS AND DISCUSSION

6.3.1 Kinetics of Dissolution

Figures 6.3, 6.4 and 6.5 show the dissolution of $Ca(C_{18})_2$ at varying pH levels in solutions of 0.1 M SDS/0.1 M Na_2EDTA, 0.1 M DDAO/0.1 M Na_2EDTA, and 0.1 M C_8APG/0.1 M Na_2EDTA, respectively, as a function of time with their calculated initial rate constants (k). Figures 6.6-6.8 plot the same data with the three different solution compositions compared at constant pH at 4, 7, and 11, respectively, with their calculated initial rate constants. The temperature was maintained at 25 ^{o}C for all experiments. The solid lines plotted in Figs 6.3-6.5 and 6.6-6.8 are the theoretical dissolution rate of $Ca(C_{18})_2$ calculated from the k values. All systems show an increase in dissolution of $Ca(C_{18})_2$ with time, asymptotically approaching 100 % for the systems with the fastest kinetics over the 30-minute observation time. Increasing pH causes an increasing dissolution at all times for DDAO and C_8APG, but decreasing dissolution for SDS (Figs. 6.3, 6.4 and 6.5), consistent with the trends of equilibrium solubility [1]. However, even at a pH of 4, the dissolution was low for SDS (maximum of 40 % at 30 minutes) and about the same for DDAO and SDS, with

C_8APG showing about half the percentage dissolved compared to DDAO and SDS at all times (Fig. 6.6). The highest rate of dissolution was for DDAO and C_8APG at pH 11, which show nearly quantitative removal at 30 minutes (Fig. 6.8). At pH 11, SDS causes little dissolution (3% at 30 minutes). At pH 7, the order of effectiveness is DDAO> C_8APG>SDS (Fig. 6.7).

Table 6.1 and Fig. 6.9 show the equilibrium solubility [1] of $Ca(C_{18})_2$ and the fraction of the $Ca(C_{18})_2$ dissolved after 10 minutes in the flow experiments from Figs. 6.3, 6.4, and 6.5 for the three surfactants and three pH levels used in this study at the same surfactant and chelant concentrations. Even though DDAO has both the highest solubility and the highest dissolution of $Ca(C_{18})_2$ at its best pH (11), at a given $Ca(C_{18})_2$ solubility, the order of dissolution effectiveness is C_8APG, DDAO, then SDS from Fig. 6.9. So, the nonionic surfactant is the most synergistic in improving the rate of dissolution of $Ca(C_{18})_2$ for a given thermodynamic driving force for dissolution (the solubility), followed by the cationic surfactant (DDAO at pH 4 where solubilities are comparable), followed by the anionic surfactant. At this pH, the stearate is protonated to form the nonionic stearic acid [1].

The highest dissolutions for pH 11 at a given time with DDAO or C_8APG are driven by high $Ca(C_{18})_2$ solubility and moderate solubility/rapid kinetics, respectively. From the solubility study of $Ca(C_{18})_2$ as Part I of this series [1], the high solubility of pH 11 is due to the chelant most effectively complexing calcium at that pH and the anionic stearate anion co-micellizing with the zwitterionic DDAO, and to lesser extent, the nonionic C_8APG.

Figures 6.10 and 6.11 compare the dissolution of $Ca(C_{18})_2$ at different flowrates of 0.5 and 1 mL/min in a 0.1 M SDS/0.1 M Na_2EDTA solution at pH 4 and 11, respectively, with their calculated initial rate constants. Figures 6.12-6.14 compare the dissolution of $Ca(C_{18})_2$ at different flowrates of 0.5 and 1 mL/min in a 0.1 M DDAO/0.1 M Na_2EDTA solution at pH 4, 7 and 11, respectively, with their calculated initial rate constants. The solid lines in Figs. 6.10-6.14 represent the theoretical dissolution rate of $Ca(C_{18})_2$ based on the experimental k values. The dissolution curves for the same surfactant/chelant system and pH level show no significant different when compared at flow rates of 0.5 and 1 mL/min. These results indicate that the dissolution of $Ca(C_{18})_2$ is independent of the mass transfer effects in the bulk solution adjacent to the solid surface of soap scum since the time for dissolution of a specified fraction of the $Ca(C_{18})_2$ would be halved by doubling the flow rate if the dissolution were equilibrium-limited, the independence if rate of dissolution on flow rate proves that the dissolution is not equilibrium limited.

Only the dissolution data from the first 10 minutes of the experiment is used to obtain the values of k, so it is referred to as an "initial rate constant". The initial rate constants for each systems were calculated from a slope of a plot of $\ln(M/M_0)$ vs. time (Eq. 6.2). From Figs 6.3-6.8 and 6.10-6.14, the first order kinetic expression describes the rate of $Ca(C_{18})_2$ dissolution quite well (R^2 no lower than 0.98 for any systems). The theoretical rate of dissolution calculated from k is also shown along with the experimental rate of dissolution and there is a good agreement between experimental and theoretical dissolution except in some systems at longer dissolution time. The kinetic rate constant (k) is a convenient single parameter useful in

comparing the rate of dissolution in different systems. The trends already discussed can be deduced from the values of k in Tables 6.2-6.4 (e.g., Table 6.4 clearly shows the rate of dissolution increases with increasing pH for the C_8APG system). Small changes in the rate of dissolution data can substantially affect the best fit value of k. For example, from Fig. 6.10, the rate of dissolution data at flow rates of 0.5 mL/min and 1.0 mL/min are indistinguishable (error bars overlap), but k = 0.0239 min^{-1} and 0.0250 min^{-1}, respectively.

Table 6.5 shows the duration of time for the systems of 0.1 M surfactant/0.1 M chelant at 1 mL/min to dissolve 100% of $Ca(C_{18})_2$ initially placed (0.01 gm) if the system were to reach equilibrium instantaneously from equilibrium solubility data from [1]. It is clearly shown that all the systems are far from equilibrium. For example, for 0.1 M DDAO/0.1 M Na_2EDTA, it would require 30 seconds to completely dissolved 0.01 gm of $Ca(C_{18})_2$, but at 10-minute reaction time, only 65 % of $Ca(C_{18})_2$ is dissolved. This confirms the conclusion that the dissolution is rate-limited, not equilibrium-limited deduced from flow rate effects.

The first order reaction assumes that the rate of dissolution is proportional to the amount of solid soap scum remaining. Since we have shown that the surface reaction is the rate limiting step in dissolution, this would imply that the area of solid available to be contacted by the solution is proportional to the mass of solid remaining as the solid shrinks with dissolution. This might be a characteristic of the shape of the disk used in our flow cell apparatus so the general applicability of the first order kinetics is not known.

6.3.2 Wettability

Figures 6.15 and 6.16 show the dynamic contact angle of $Ca(C_{18})_2$ of 0.1 M SDS/0.1 M Na_2EDTA and 0.1 M DDAO/0.1 M Na_2EDTA on the smooth surface of solid $Ca(C_{18})_2$. The contact angle of a water droplet on a surface is very high at about 120^o, indicating how hydrophobic the $Ca(C_{18})_2$ is. The surfactant concentration used was much higher than the CMC so all of three surfactants have very low γ_{LV} at around 30 mN/m. The γ_{SV} would be the same for all solution systems but γ_{SL} could vary from system to system since γ_{SL} depends on the adsorption of the dissolved surfactant on the surface of $Ca(C_{18})_2$ [25, 26]. The solution system that has higher interaction with the $Ca(C_{18})_2$ (lower γ_{SL}) could produce a lower contact angle. According to Young's equation, it has to be noted here that the flat surface of the $Ca(C_{18})_2$ used here is not non-porous and not inert to the wetting solution. When the surfactant/chelant is in contact with the surface, it completely wets and/or penetrates the surface so an equilibrium contact angle does not exist. Therefore, we measured the dynamic contact angle at a short period of contact time (< 300 seconds) since eventually, the droplet would become flat and the contact angle disappears.

The dynamic contact angles shown in Figs 6.15 and 6.16 are low, even for systems with slow dissolution (e.g., SDS at pH 11). The fast dissolving DDAO solutions have a higher contact angle than the slow dissolving SDS solutions. So, the dissolution rate is not limited by the rate of wetting. At pH 11 for the 0.1 M SDS/0.1 M Na_2EDTA solution, where no dissolution was observed, the contact angle is low but the rate of change in contact angle is very low compared to the other faster dissolving systems that the contact angle keeps decreasing at a higher rate. Since the

dissolution rate is limited by a surface reaction, these results support the intriguing possibility that a high rate of change of contact angle may correlate to a fast surface reaction.

6.3.3 Mechanism Determining Rate of Dissolution

The systems studied here are quite far from equilibrium when comparing the rate of dissolution and equilibrium solubility and the transfer of surfactant/chelant from bulk solution to the surface of $Ca(C_{18})_2$ is not a rate determining step. Even though higher dissolution corresponds to higher equilibrium solubility as depicted in Fig. 6.9, the equilibrium solubility as a thermodynamic driving force cannot be used to explain the dissolution kinetics. Also supporting this concept is that at the same solubility, the different surfactant systems exhibit different rates of dissolution. For example, the solubility of $Ca(C_{18})_2$ in 0.1 M C_8APG/0.1 M Na_2EDTA is lower than 0.1 M DDAO/0.1 M Na_2EDTA at pH 11, but the dissolution of $Ca(C_{18})_2$ in both system can attain the same level of dissolution when compared at 10-minute reaction time. So, correlation between solubility and dissolution rate is not cause and effect. However, it is reasonable to hypothesize that a faster surface reaction between the soap scum and surfactant/ligand increases with increasing equilibrium solubility. The same mechanisms responsible for solution solubility of $Ca(C_{18})_2$ (chelation of calcium by ligand and mixed aggregate formation by the added surfactant and stearate) can also be occurring at the soap scum surface in a surface reaction. The contact angle data shows that all the systems studied here can wet the surface quite well so wettability at the soap scum does not limit the dissolution rate. A higher rate of

contact angle change correlates with a faster dissolution rate, supporting a surface interaction or reaction as important in determining dissolution kinetics. According to the $Ca(C_{18})_2$ dissolution steps proposed earlier, the rate limiting steps could be steps 2-4, which are adsorption of surfactant/chelant, penetration of solution, and desorption of mixed micelle containing stearic acid/stearate anion away from surfaces.

6.4 REFERENCES

1. Soontravanich S, Lopez HE, Scamehorn JF, Sabatini DA, Scheuing DR (2007) Dissolution Study of Salt of Long Chain Fatty Acids (Soap Scum) in Surfactant Solutions. Part I Equilibrium Dissolution. Submitted to J. Surfact. Deterg.
2. Chan AF, Evans DF, Cussler EL (1976) Explaining Solubilization Kinetics. AIChE Journal 22: 1006-1012
3. Shaeiwitz JA, Chan AF, Cussler EL, Evans DF (1981) The Mechanism of Solubilization in Detergent Solutions. J. Colloid Interface Sci. 84: 47-56
4. Kralchevsky PA, Denkov ND, Todorov PD, Marinov GS, Broze G, Mehreteab A (2002) Kinetics of Triglyceride Solubilization by Micellar Solutions of Nonionic Surfactant and Triblock Copolymer: 2. Theoretical Model. Langmuir 18: 7887-7895
5. Lawrence ASC (1958) Solubility in Soap Solutions. Disc. Faraday Soc. 25: 51-58
6. Lawrence ASC, Bingham A, Capper CB, Hume K, (1964) The Penetration of Water and Aqueous Soap Solutions into Fatty Substances Containing One or Two Polar Groups. J. Phys. Chem. 68: 3470-3476
7. Stowe L, Shaeiwitz JA (1982) Liquid Solubilization Dynamics: Oleic Acid in Bile Salt. J. Colloid Interface Sci. 90: 495-508

8. Raterman KT, Shaeiwitz JA (1984) Liquid Solubilization Dynamics, II Flux Enhancement by Interface Gel Formation. J. Colloid Interface Sci. 98: 394-405

9. Lim J -C, Miller CA (1991) Dynamic Behavior and Detergency in Systems Containing Nonionic Surfactants and Mixtures of Polar and Nonpolar Oils. Langmuir 7: 2021-2027

10. Carroll BJ (1981) The Kinetics of Solubilization of Nonpolar Oils by Nonionic Surfactant Solutions. J. Colloid Interface Sci. 79: 126-135

11. Kabalnov A, Weers J (1996) Kinetics of Mass Transfer in Micellar Systems: Surfactant Adsorption, Solubilization Kinetics, and Ripening. Langmuir 12: 3442-3448

12. Weiss J, Coupland JN, Brathwaite D, McClements DJ (1997) Influence of Molecular Structure of Hydrocarbon Emulsion Droplets on Their Solubilization in Nonionic Surfactant Micelles. Colloids. Surf. A 121: 53-60

13. Todorov PD, Kralchevsky PA, Denkov ND, Broze G, Mehreteab A (2002) Kinetics of Solubilization of n-Decane and Benzene by Micellar Solutions of Sodium Dodecyl Sulfate. J. Colloid Interface Sci. 245: 371-382

14. Huang C, Evans DF, Cussler EL (1981) Linoleic Acid Solubilization with a Spinning Liquid Disc. J. Colloid Interface Sci. 82: 499-506

15. Plucinski P, Nitsch W, (1993) Kinetics of Interfacial Phenylalanine Solubilization in a Liquid/Liquid Microemulsion System. J. Phys. Chem. 97: 8983-8988

16. Chen BH, Miller CA, Garrett PR (1997) Rates of Solubilization Triolein into Nonionic Surfactant Solutions. Colloids. Surf. A 128: 129-143

17. Chen BH, Miller CA, Garrett PR, (1998) Rates of Solubilization of Triolein/Fatty Acid Mixtures by Nonionic Surfactant Solutions. Langmuir 14: 31-41

18. Rosen MJ (2004) Surfactants and Interfacial Phenomena. 3rd edn. John Wiley & Sons, Inc., Hoboken, New Jersey. pp 243

19. Luner PE, Babu SR, Mehta SC (1996) Wettability of a Hydrophobic Drug by Surfactant Solutions. Int. J. Pharm. 128: 29-44

20. Weintraub H, Gibaldi M (1969) Physiological Surface Active Agents and Drug Absorption. IV. Effect of Premicellar Concentrations of Surfactants on Dissolution Rate. J. Pharm. Sci. 58: 1368-1372

21. Efentakis E, Fell JT (1981) The Wetting and Dissolution Rates of Aspirin Powder in Surfactant Solutions. Acta Pharm. Technol. 27: 33-35

22. Bakatselou V, Oppenheim RC, Dressman JB (1991) Solubilization and Wetting Effects of Bile Salts on the Dissolution of Steroids. Pharm. Res. 8: 1461-1469

23. Adamson AW, Gast AP (1997) Physical Chemistry of Surfaces. 6th edn. John Wiley & Sons, New York, pp. 362

24. Nalwaya V, Tantayakom V, Piumsomboon P, Fogler S (1999) Studies on Asphaltenes through Analysis of Polar Fractions. Ind. Eng. Chem. Res. 38: 964-972

25. Balasuwatthi P, Dechabumphen N, Saiwan C, Scamehorn, JF (2004) Contact Angle of Surfactant Solutions on Precipitated Surfactant Surfaces. II. Effects of Surfactant Structure, Presence of a Subsaturated Surfactant, pH, and Counterion/Surfactant Ratio. J. Surfact. Deterg. 7: 31-40

26. Luepakdeesakoon B, Saiwan C, Scamehorn, JF (2006) Contact Angle of Surfactant Solutions on Precipitated Surfactant Surfaces. III. Effects of Subsaturated Anionic and Nonionic Surfactants and NaCl. J. Surfact. Deterg. 9: 125-136

Table 6.1 Equilibrium solubility and dissolution of $Ca(C_{18})_2$ in surfactant/chelant systems

0.1 M Surfactant/0.1 M Chelant	pH	Equilibrium solubility of $Ca(C_{18})_2$ (M)	Dissolution of $Ca(C_{18})_2$ at a flowrate of 1 mL/min at 10 minutes (%)
SDS/Na_2EDTA	4	0.0025	22
	7	0.0011	15
	11	0.0007	0
DDAO/Na_2EDTA	4	0.0001	26
	7	0.0192	66
	11	0.03	65
C_8APG/Na_2EDTA	4	0.0001	7
	7	0.005	55
	11	0.0075	64

Table 6.2 Kinetic rate constants of the dissolution of $Ca(C_{18})_2$ by a solution of 0.1 M SDS/0.1 M Na_2EDTA

	Reaction rate constant (min^{-1})	
Flowrate	0.5 mL/min	1 mL/min
pH 4	0.0239	0.0250
pH 7	0.0177	0.0179

Table 6.3 Kinetic rate constants of the dissolution of $Ca(C_{18})_2$ by a solution of 0.1 M DDAO/0.1 M Na_2EDTA

	Reaction rate constant (min^{-1})	
Flowrate	0.5 mL/min	1 mL/min
pH 4	0.0168	0.0220
pH 7	0.1262	0.1134
pH 11	0.1234	0.1151

Table 6.4 Kinetic rate constants of the dissolution of $Ca(C_{18})_2$ by a solution of 0.1 M C_8APG/0.1 M Na_2EDTA

	Reaction rate constant (min^{-1}) at a flowrate of 1 mL/min
pH 4	0.0070
pH 7	0.0917
pH 11	0.1287

Table 6.5 The duration of time for the solutions of 1 mL/min of 0.1 M surfactant/0.1 M chelant to completely dissolve 0.0100 gm of $Ca(C_{18})_2$ in a flow cell experiment if the system were at equilibrium

0.1 M surfactant/0.1 M chelant	pH	Time to dissolve 100 % (min)	Dissolution at 10 minutes (%)
SDS/Na_2EDTA	4	6.5	22
	7	14.6	15
	11	23.2	0
DDAO/Na_2EDTA	4	16.8	26
	7	0.9	66
	11	0.5	65
C_8APG/Na_2EDTA	4	106.9	7
	7	15.3	55

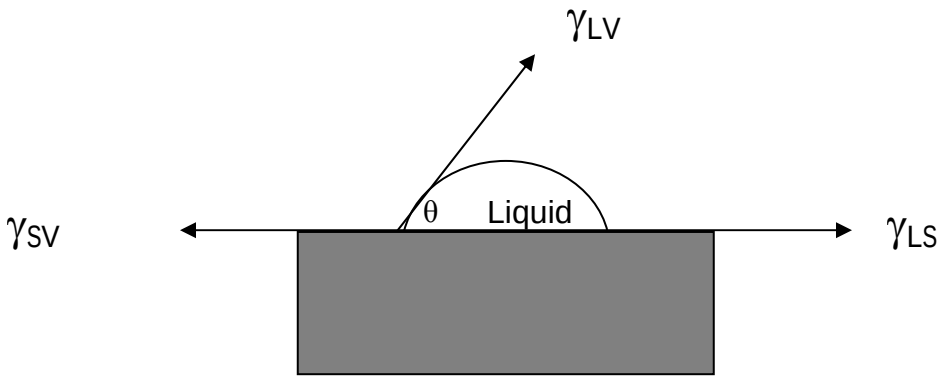

Fig. 6.1 Illustration of contact angle and interfacial tensions of the three interfaces affecting the drop shape on the substrate

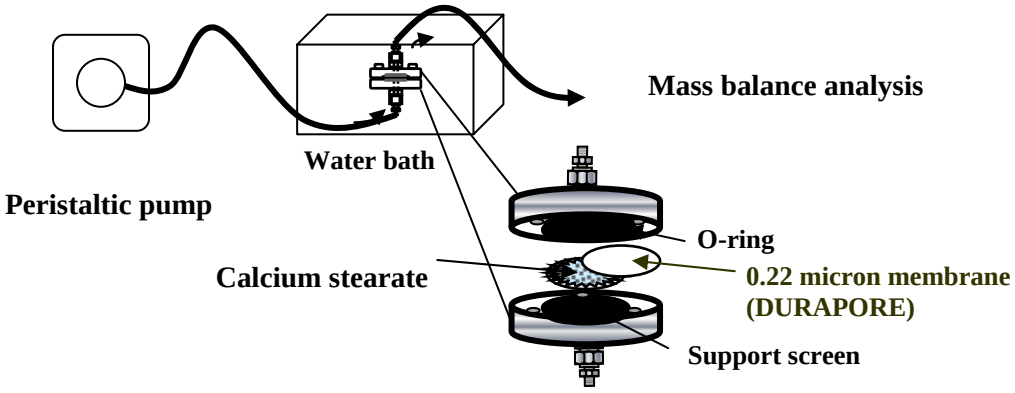

Fig. 6.2 Schematic illustration of the flow cell apparatus

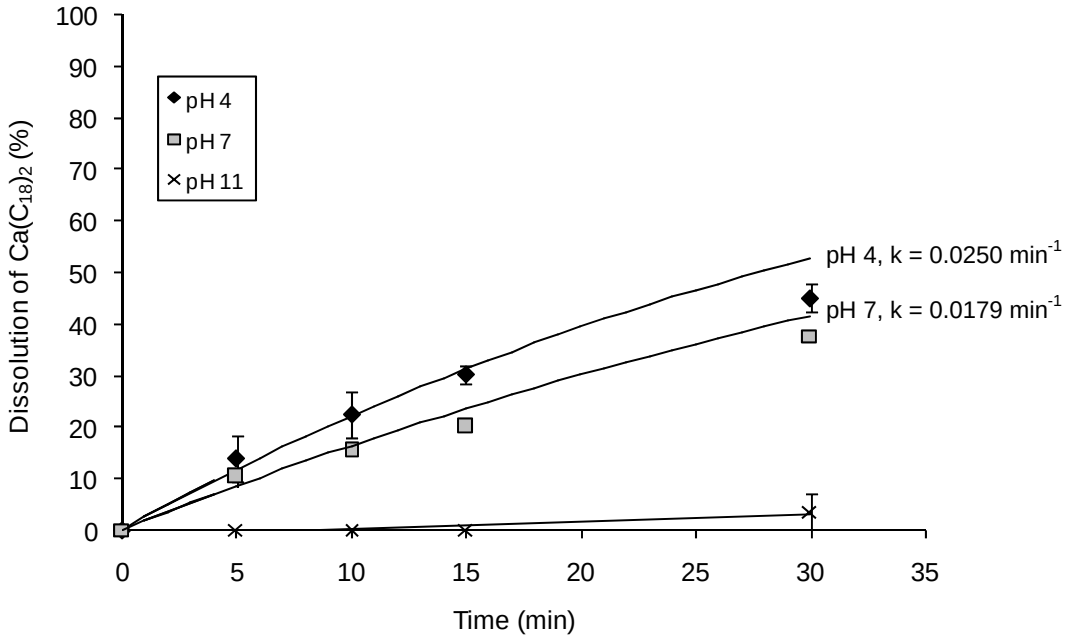

Fig. 6.3 Dissolution of $Ca(C_{18})_2$ in a solution of 0.1 M SDS/0.1 M Na_2EDTA at a flowrate of 1 mL/min

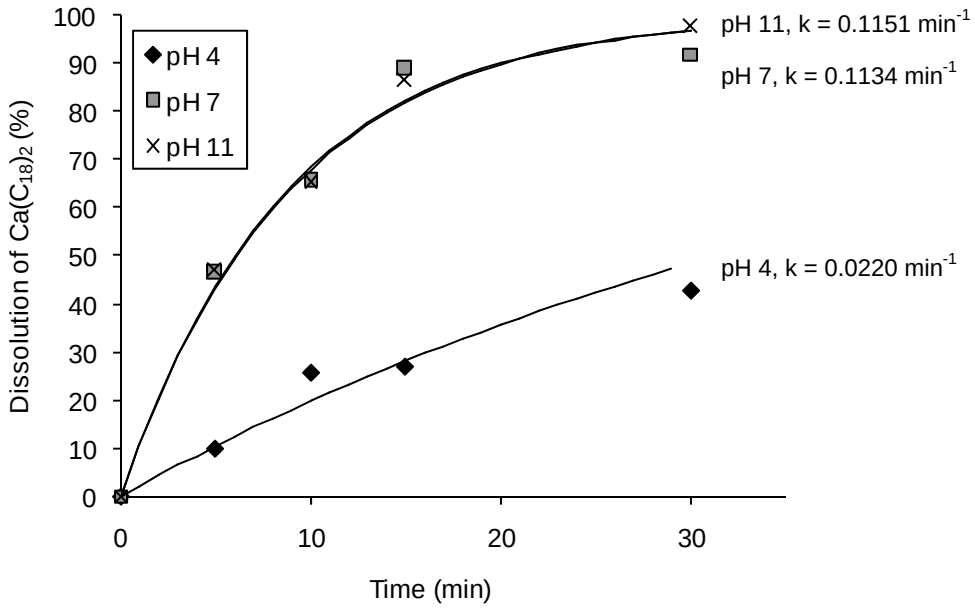

Fig. 6.4 Dissolution of $Ca(C_{18})_2$ in a solution of 0.1 M DDAO/0.1 M Na_2EDTA at a flowrate of 1 mL/min

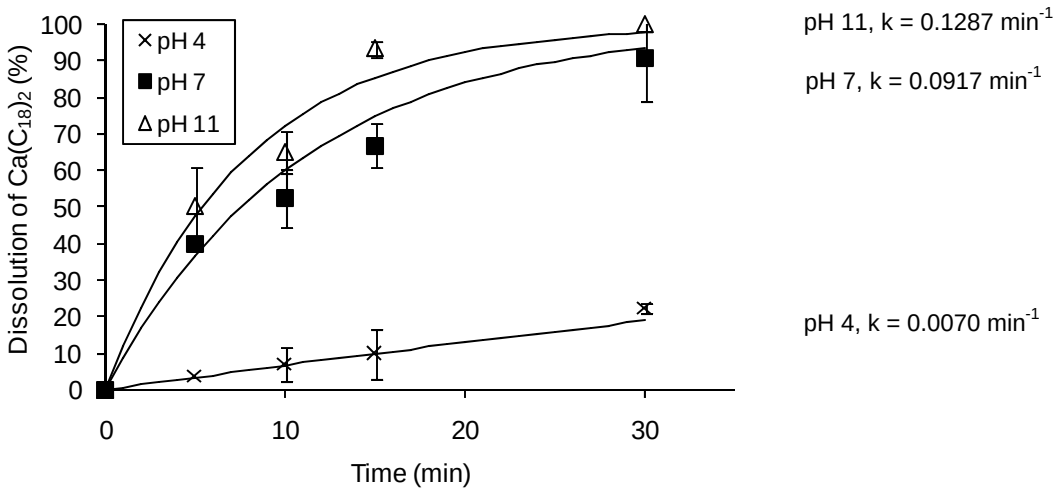

Fig. 6.5 Dissolution of $Ca(C_{18})_2$ in a solution of 0.1 M C_8APG/0.1 M Na_2EDTA at a flowrate of 1 mL/min

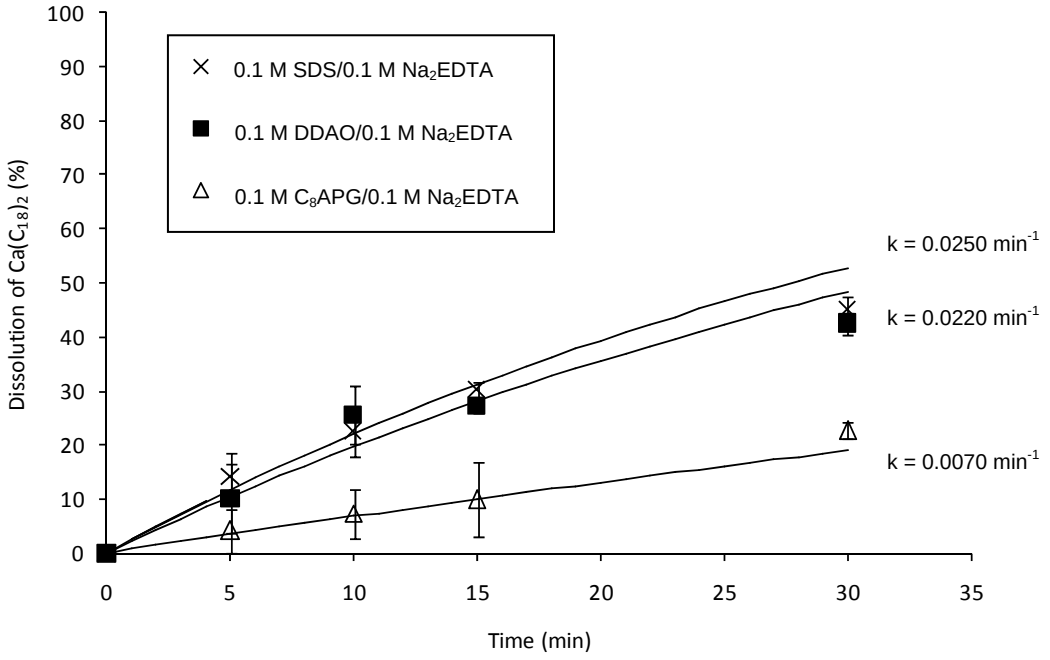

Fig. 6.6 Dissolution of $Ca(C_{18})_2$ in different surfactant/chelant systems at pH 4 and a flowrate of 1 mL/min

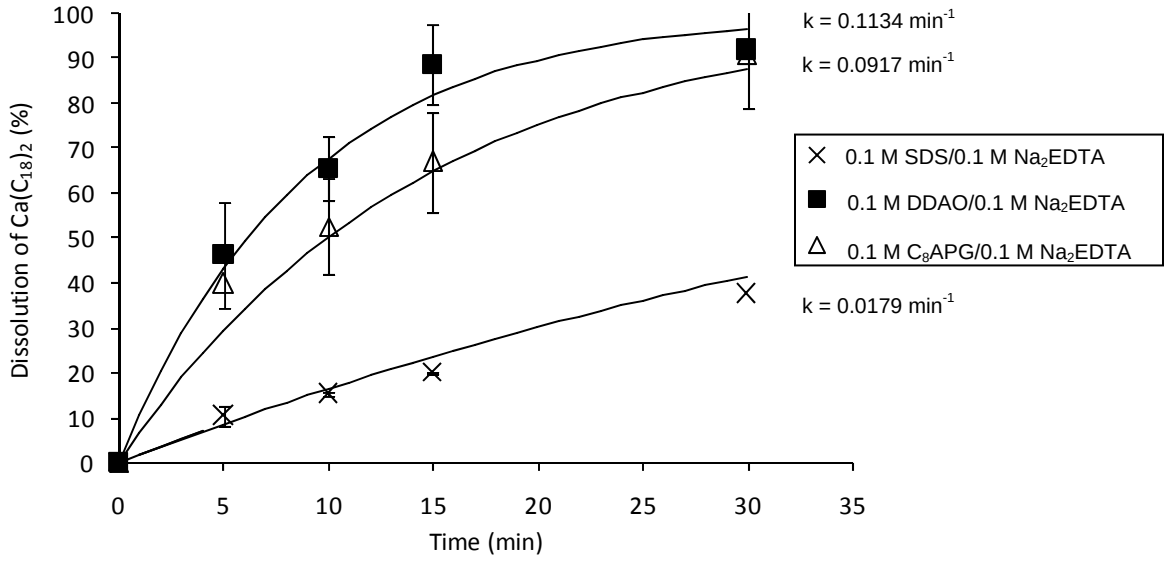

Fig. 6.7 Dissolution of $Ca(C_{18})_2$ in different surfactant/chelant systems at pH 7 at a flowrate of 1 mL/min

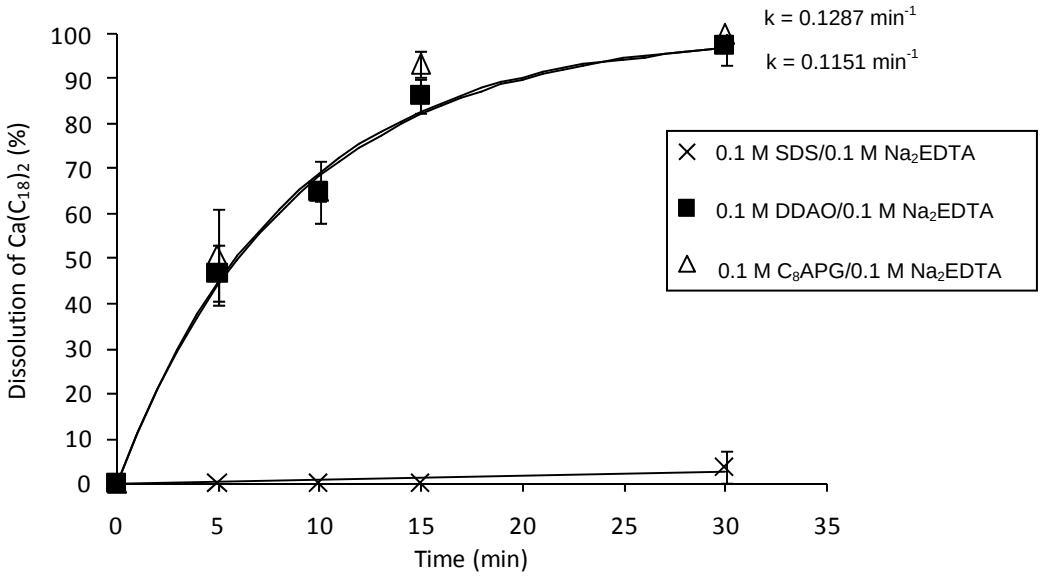

Fig. 6.8 Dissolution of $Ca(C_{18})_2$ in different surfactant/chelant systems at pH 11 at a flowrate of 1 mL/min

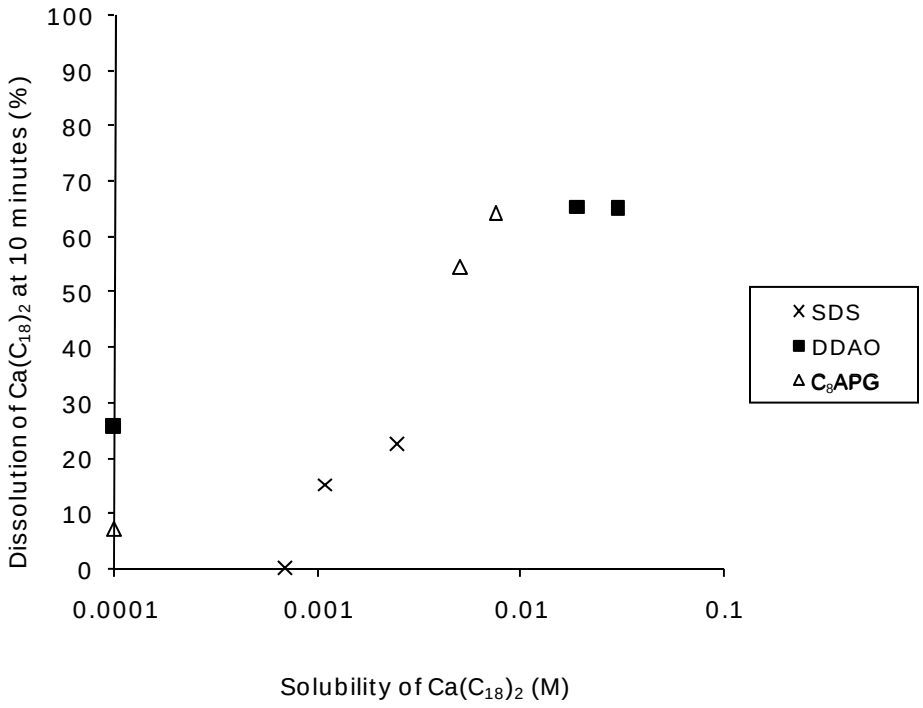

Fig. 6.9 Comparison of equilibrium solubility and dissolution of $Ca(C_{18})_2$ at 10 minutes (flowrate 1 mL/min) in 0.1 M surfactant/0.1 M Na_2EDTA

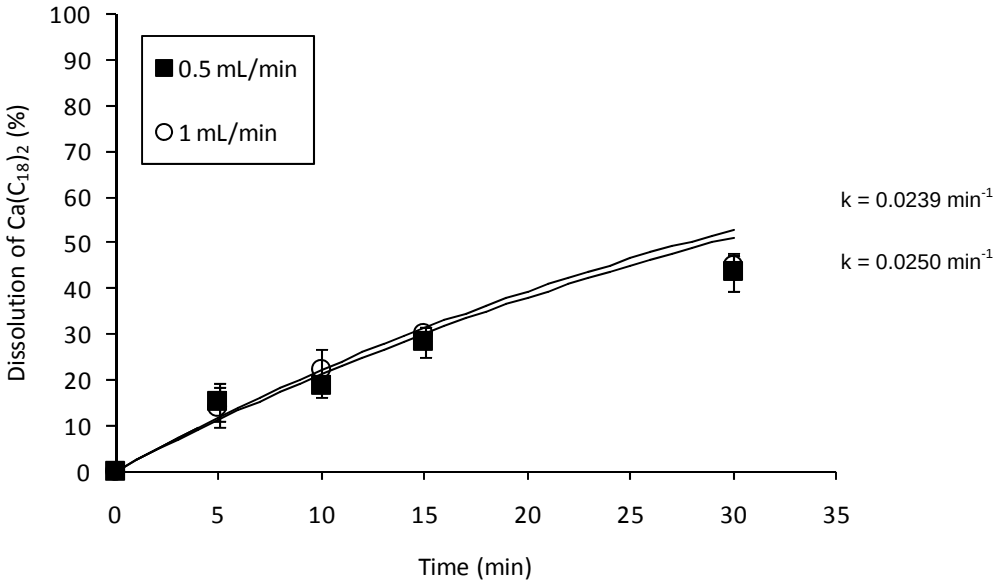

Fig. 6.10 Dissolution of $Ca(C_{18})_2$ by 0.1 M SDS/0.1 M Na_2EDTA at flowrates of 0.5 and 1 mL/min and pH of 4

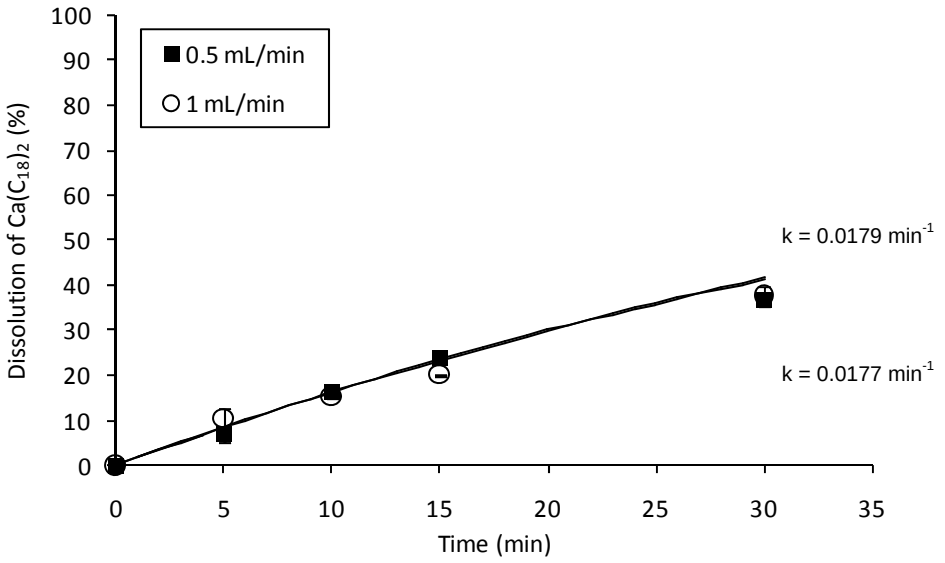

Fig. 6.11 Comparison of dissolution of $Ca(C_{18})_2$ by 0.1 M SDS/0.1 M Na_2EDTA at flowrates of 0.5 and 1 mL/min and pH of 7

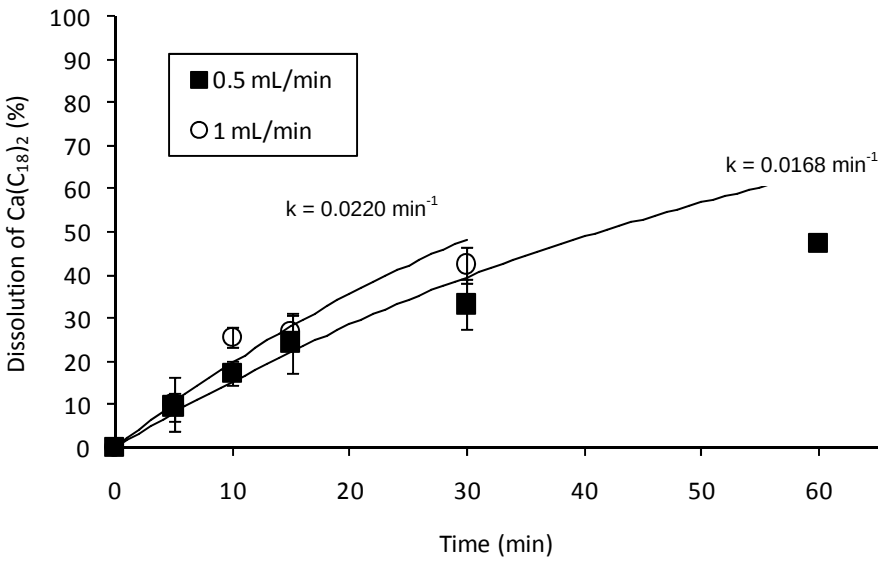

Fig. 6.12 Dissolution of $Ca(C_{18})_2$ by 0.1 M DDAO/0.1 M Na_2EDTA at flowrates of 0.5 and 1 mL/min at pH of 4

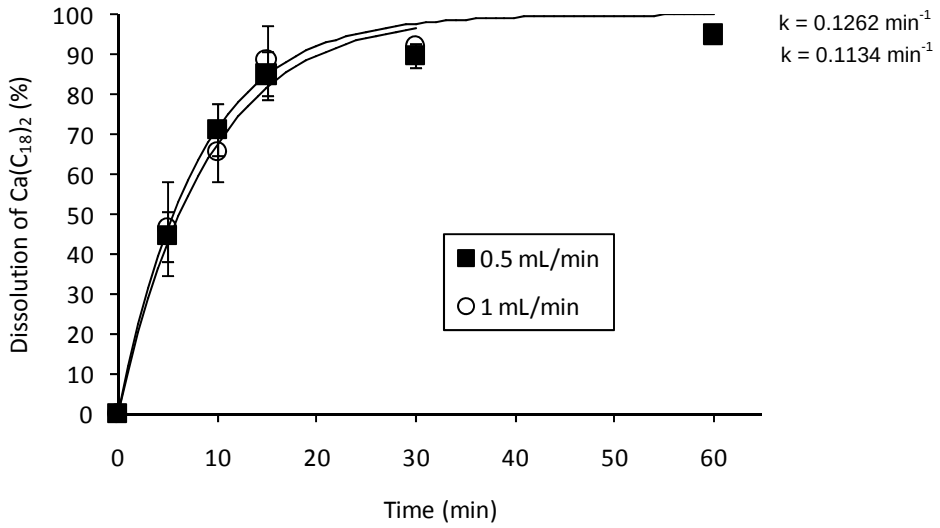

Fig. 6.13 Dissolution of $Ca(C_{18})_2$ by 0.1 M DDAO/0.1 M Na_2EDTA at flowrates of 0.5 and 1 mL/min at pH of 7

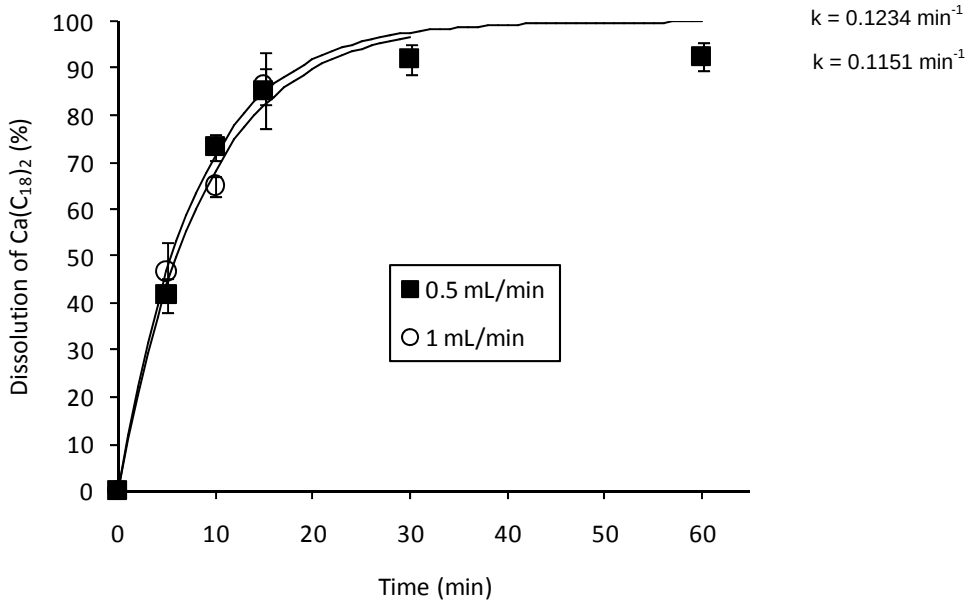

Fig. 6.14 Dissolution of $Ca(C_{18})_2$ by 0.1 M DDAO/0.1 M Na_2EDTA at flowrates of 0.5 and 1 mL/min at pH of 11

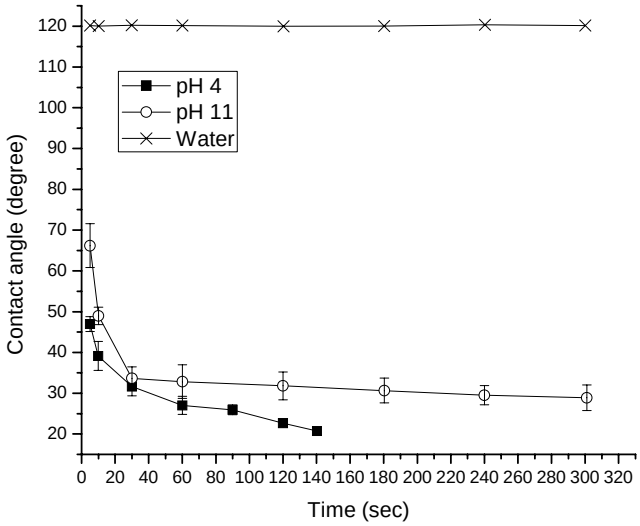

Fig. 6.15 Dynamic contact angle of a solution of 0.1 M SDS/0.1 M Na_2EDTA at pH 4 and 11 compared with water on solid $Ca(C_{18})_2$

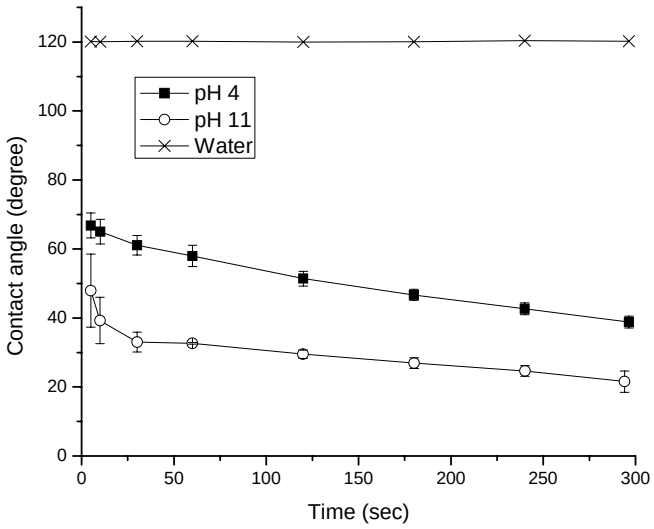

Fig. 6.16 Dynamic contact angle of a solution of 0.1 M DDAO/0.1 M Na_2EDTA at pH 4 and 11 compared with water on solid $Ca(C_{18})_2$